DOKUZ EYLÜL UNIVERSITY

GRADUATE SCHOOL OF NATURAL AND APPLIED SCIENCES

DETERMINATION OF COMPOSITE PRESSURE VESSELS UNDER VARIOUS LOADINGS

by

Eşref YAYLAĞAN

May, 2010

İZMİR

DETERMINATION OF COMPOSITE PRESSURE VESSELS UNDER VARIOUS LOADINGS

A Thesis Submitted to the
Graduate School of Natural and Applied Sciences of Dokuz Eylül University
In Partial Fulfillment of the Requirements for the Degree of Master of Science
in Mechanical Engineering, Mechanics Program

by
Eşref YAYLAĞAN

May, 2010
İZMİR

M.Sc THESIS EXAMINATION RESULT FORM

We have read the thesis entitled **"DETERMINATION OF COMPOSITE PRESSURE VESSELS UNDER VARIOUS LOADINGS"** completed by **EŞREF YAYLAĞAN** under supervision of **PROF. DR. ONUR SAYMAN** and we certify that in our opinion it is fully adequate, in scope and in quality, as a thesis for the degree of Master of Science.

Prof. Dr. Onur SAYMAN

Supervisor

(Jury Member)

(Jury Member)

Prof. Dr. Mustafa SABUNCU
Director

ACKNOWLEDGMENTS

The financial supporting of this project by TÜBİTAK (The Scientific and Technological Research Council of Turkey) under Project number 104M424 is greatly appreciated.

First of all, I would like to thank my supervisor, Prof. Dr. Onur SAYMAN, for his support and guidance throughout this study.

I would also like to thank Tolga DOĞAN for his help and guidance during the numerical and experimental phase of the study.

I would like to thank Murat SARI , research assistant Mehmet Emin DENİZ for their help during experimental phase of the study.

I also wish to express my thanks to my other colleagues who helped me in this thesis.

I would also like to thank Dokuz Eylül Machine Tools Laboratory and Artipol Poliüretan Kauçuk İmalat İthalat İhracat San.ve Tic. Ltd. Şti. for their help during manufacturing test apparatus.

Finally, I would like to thank my parents for their loving support throughout my education.

Eşref YAYLAĞAN

DETERMINATION OF COMPOSITE PRESSURE VESSELS UNDER VARIOUS LOADINGS

ABSTRACT

In this study, optimal angle-ply orientations of antisymmetric $[\theta/-\theta]_{2a}$ composite pressure vessels with a plastic liner designed for maximum first-ply failure and burst pressure, were investigated at $2^{\circ}C$, $25^{\circ}C$, $60^{\circ}C$ and $80^{\circ}C$ temperatures. The cylindrical section of composite pressure vessels is conducted. A finite element method and experimental approaches are studied to verify optimum winding angles. Glass reinforced plastic (GRP) pipes are made of E-glass epoxy and a plastic liner in them and tested close-ended condition. For this study, a PLC controlled hydraulic pressure testing machine has been used. Study deals with the influences of winding angle and environment temperature on filament-wound composite pressure vessels with a liner. An elastic solution procedure based on the Lekhnitskii's theory was developed in order to predict the first-ply failure of the pressure vessels. To compare the first-ply failure of layers in a simple form with the experimental results, The Tsai-Wu failure criterion and maximum stress theories were applied. The solution was presented and discussed for various orientation angles at different temperatures. Test specimens have four layers, which have various orientation angles. The layers were oriented antisymmetrically for, $[45^{o}/\text{-}45^{o}]_{2a}$, $[55^{o}/\text{-}55^{o}]_{2a}$, $[60^{o}/\text{-}60^{o}]_{2a}$, $[75^{o}/\text{-}75^{o}]_{2a}$ and $[88^{o}/\text{-}88^{o}]_{2a}$ orientations. Analytical and experimental solutions were compared with the finite element solutions, in which commercial software ANSYS 10.0 was utilized, and close results were obtained between them. The optimum winding angle for the composite pressure vessel with a liner analysis with the internal pressure loading case was obtained as $[55^{\circ}]$ for laminates.

Keywords: Composite pressure vessels, filament winding, finite element analysis, internal pressure, temperature

DEĞİŞİK YÜKLER ALTINDA KOMPOZİT BASINÇLI KAPLARIN BELİRLENMESİ

ÖZ

Bu çalışmada, antisimetrik $[\theta/-\theta]_{2a}$ şeklindeki tabakalı, ince cidarlı, içten plastik linerli kompozit basınçlı tüpün, 2 ^{o} C, 25 ^{o} C, 60 ^{o} C and 80 ^{o} C sıcaklıklardaki ilk katman hasarı ve maksimum patlama basıncı için en uygun tabaka-açı oryantasyonları araştırıldı. Kompozit basınçlı tüplerin silindirik kısmına değinilmiştir. Sonlu elemanlar metodu ve deneysel çalışmalarla en uygun sarım açısı bulunmaya çalışılmıştır. E-cam/epoksi CTP borular içlerinde liner plastik bir malzemeyle üretilmiş ve kapalı uçlu iç statik basınç testleri uygulanmıştır. Bu çalışma için PLC kontrollü hidrolik basınç test cihazı kullanılmıştır. Çalışmada içten liner plastik malzemeli, filaman sarımlı kompozit tüpler üzerindeki sarım açılarının ve değişen ortam sıcaklıklarının etkileri ele alınmıştır. Kompozit tüpte oluşan ilk katman hasarını belirlemek için nümerik çözüm yöntemi Lekhnitskii teorisi kullanılarak geliştirilmiştir. Bu yöntemle hasar basıncı aynı ısı etkisi ile değişik açı oryantasyonlarında hesaplanmıştır. Tsai-Wu hasar kriteri ve maksimum gerilme teorisinden elde edilen analitik sonuçlarla, deneyler sonucu tabakalarda oluşan hasarı meydana getiren basınç değerleri karşılaştırılmıştır. Sonuçlar, çeşitli sarım açıları için hesaplanıp, yorumlanmıştır. Test numuneleri en içte plastik liner malzemeli, diğer dış katmanlarda da dört tabakalı ve $[45^{o}/\text{-}45^{o}]_{2a}$, $[55^{o}/\text{-}55^{o}]_{2a}$, $[60^{o}/\text{-}60^{o}]_{2a}$, $[75^{o}/\text{-}75^{o}]_{2a}$ and $[88^{o}/\text{-}88^{o}]_{2a}$ açı oryantasyonlarında ele alınmıştır. Kompozit malzeme olarak E-cam epoksi seçilmiş ve bu malzemenin termal ve mekanik özellikleri hesaplamalarda kullanılmıştır. Bazı nümerik sonuçlar sonlu elemanlar programı ANSYS 10.0 sonuçları ile karşılaştırılmış ve yakın değerler elde edilmiştir. Nümerik sonuçlarda ısı etkisinin patlama basıncı üzerinde fazla bir etkisi olmadığı gözlenmiştir. İçten basınca maruz helisel açıda sarımlı kompozit tüplerde en uygun sarım açısının 55^{o} civarında olduğu tespit edilmiştir.

Anahtar sözcükler: Kompozit basınçlı tüpler, filaman sargı, sonlu elemanlar analizi, iç basınç, sıcaklık

CONTENTS

Page

CHAPTER ONE

INTRODUCTION

1.1 Development of Composite Pressure Vessels

Pressure vessels have long been manufactured by filament winding. They appear to be simple structures, but pressure vessels are among the most difficult to design. Filament-wound composite pressure vessels have found widespread use not only for military use but also for civilian applications. This technology previously developed for the military's internal use was adapted to civilian purpose and following this, extended to the commercial market. Applications include breathing device, such as self-contained breathing apparatuses used by fire-fighters and other emergency personnel, scuba tanks for divers, oxygen cylinders for medical and aviation cylinders for emergency slide inflation, opening doors or lowering of landing gear, mountaineering expedition equipment, paintball gas cylinders, etc. A potential widespread application for composite pressure vessels is the automotive industry. Intensions for reducing emissions leads the conversion to Compressed Natural Gas (CNG) fuelled vehicles worldwide. The main aim of the industry here is the attempt to replace fuel oils with natural gas or hydrogen as the energy supply in vehicles for air quality improvements and reduce global warming. The successful application of these fuels in vehicles may be achieved by fuel cells in concert with hydrogen gas storage technologies. One of the missing milestones here is the inadequasy of the vehicle range between refuelling stops. Other important parameters in these applications are weight, volume and cost of the containment vessel.

Filament-wound composite pressure vessels developed from high strength and high modulus to density ratio materials offer significant weight savings over conventional all-metal pressure vessels for the containment of high pressure gases and fluids. The structural efficiency of pressure vessels is defined as:

$$e = \frac{P_b V}{W}$$

P_b = Burst pressure
where : V = Contained volume
W = Vessel weight

The structural efficiencies of all-metal pressure vessels change from 7.6×10^6 to 15.2×10^6 mm, while filament wound composite vessels have efficiencies in the range from 20.3×10^6 to 30.5×10^6 mm. This can be stated as the structural efficiencies of composite pressure vessels are better than all-metal pressure vessels of similar volume and pressure.

Composite vessels with very high burst pressures (70-100 Mpa) are in service today in the aerospace industry . Vessels with burst pressure between 200 – 400 Mpa have been under investigation and such containment levels were achieved in the late 1970's through mid 1980's. Further researches must be made for the design of advanced ultra-high pressure composite vessels.

A maximum pressure of 35 Mpa is permitted under current regulations, 21 Mpa is a standard vehicle refuelling system's nominal output pressure for civilian applications. Higher pressures are not yet approved for use on public roads or commercial aircraft. This implies a great need for advancement in composite pressure vessel technology.

For their broad application in the transportation industry, the pressure containtment limits of thin walled composite vessels are still inadequate. Further research for the development of thick-walled designs is required in order to hold ultra-high pressure fuel gases safely. It is found that stress decline rapidly through the wall thickness. At first glance changes in the orientation angles of wound fibers appears to be able to change the distribution of stress through the wall thickness, but practical research has shown that the effects are limited. Optimization of stress distributions through a variation of geometry is considered in the design stages of pressure vessels. It is also found that stress distributions through the thickness in pressure vessels appear to be not sensitive to geometry modifications. As has been

pointed out earlier, the current ultra high pressure vessels are low in structural efficiency. There also exists a fundamental lack of confidence in the ability to understand and predict their behaviours for real life cases as the analysis results and experimental results are not always exactly the same. In addition, in some cases these results may differ much more than the expected values as new parameters show up in most new designs.

Most of finite element analyses on composite pressure vessels are based on shell elements which are generated using the classical lamination theory. The results should be good when the internal pressures are not very high and ratio of diameter to wall thickness is greater than 15. Some FEA tools like ANSYS provide a thick shell element to reflect the influence of shear stress in the radial direction and capture the transverse shear deformation.

1.2 Structure of Composite Pressure Vessels

Cylindrical composite pressure vessels mostly consists of a metallic/plastic internal liner, a filament wound and a composite outer shell as shown in Fig. 1.1. The metal/plastic liner is needed to prevent leakage, while some of the metal liners also provide strength to share internal pressure load. For composite pressure vessels, a big portion of the applied load is carried by the strong outer layers made from filament wound composite material, and this design of the outer filament wound composite material is mostly the main parameter for the amount of pressure that can be present in the container.

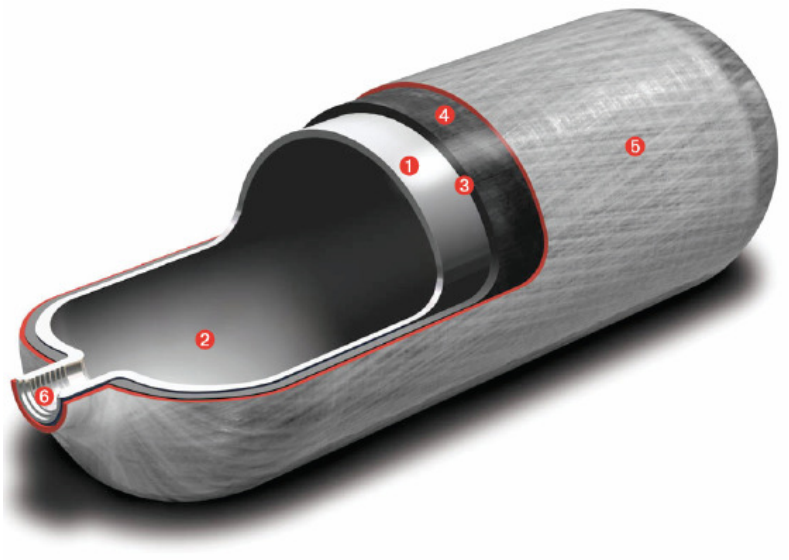

Figure 1.1 Example of filament wound composite pressure vessels.

1- Thin plastic liner / Ultra thin-walled aluminium liner
2- Protexal smooth, inert, corrosion resistant internal finish
3- Insulating layer
4- High - performance carbon - fiber overwrap in epoxy resin matrix.
5- High - strength fibreglass-reinforced plastic (FRP) protective layer with smooth gel coat.
6- Precision – machined thread

1.3 Properties of Composite Pressure Vessels

Composite pressure vessels should make full usage of the extremely high tensile strength and high elastic modulus of the fibers from which they are made. Theories of laminated composite materials for evaluating these properties are relatively well established for modulus, and to a lesser extent for strength. Generally, there are two approaches to modelling composite material behaviours:

1) Micromechanics where interaction of constituent materials is examined in detail as part of the definition of the behaviour of heterogeneous composite material

2) Macromechanics where the material is assumed homogeneous and the effect of the constituents are detected only as averaged properties.

CHAPTER TWO
LITERATURE REVIEW

From the literature review; it was found that most of design and analysis of composite pressure vessels are based on thin-walled vessels. As pointed out earlier, when the ratio of the outside diameter to inside diameter is larger than 1.1, the vessel should be considered thick-walled. Only a few researchers have considered the effect of wall thickness.

The solution of composite cylinders is based on the Lekhnitskii's theory (1981). He investigated the plane strain case or the generalized plane strain cases. Roy and Tsai (1988) proposed a simple and efficient design method for thick composite cylinders; the stress analysis is based on 3-dimensional elasticity by considering the cylinder in the state of generalized plane strain for both open-ended (pipes) and closed-ended (pressure vessel).

Sayman (2005) studied analysis of multi-layered composite cylinders under hygrothermal loading. Mackerle (2002) gives a bibliographical review of finite element methods applied for the analysis of pressure vessel structures and piping from the theoretical as well as practical points of view. Xia et al. (2001) studied multi-layered filament-wound composite pipes under internal pressure. Xia et al. (2001) presented an exact solution for multi-layered filament-wound composite pipes with resin core under pure bending. Rao and Sinha (2004) studied the effects of temperature and moisture on the free vibration and transient response of multidirectional composites. A three-dimensional finite element analysis is developed for the solution.

Önder et al. (2007) studied the determination of burst failure pressures of composite pressure vessels by using finite element and analytical methods. They also investigated the comparison of filament winding angles of composite pressure vessels at different temperatures. Kam et al. (1997) and Chang (2000) investigated

the first-ply failure in composite pressure vessels by using acoustic emission technique. They obtained close results between FEM and experimental methods.

Azzam et al. (1996) studied the comparison between the analytical and experimental failure behaviour of a proposed design for the filament-wound composite pressure vessels. This comparison has shown close results between the theoretical and experimental analysis.

Parnas and Katırcı (2002) discussed the design of fiber-reinforced composite pressure vessels under various loading conditions based on a linear elasticity solution of the thick-walled multilayered filament wound cylindrical shell. A cylindrical having number of sublayers, each of which is cylindrically orthotropic, is treated as in the state of plane strain.

Roy et. al. (1992) studied the design of thick multi-layered composite spherical pressure vessels based on a 3-D linear elastic solution. They found that the Tsai-Wu failure criterion is suitable for strength analysis. One of the important discoveries of Roy's research is that hybrid spheres made from two materials presented an opportunity to increase the burst pressure.

Adali et. al. (1995) gave another method on the optimization of multi-layered composite pressure vessels using an exact elasticity solution. A three dimensional theory for anisotropic thick composite cylinders subjected to axis symmetrical loading conditions was derived. The three dimensional interactive Tsai-Wu failure criterion was employed to predict the maximum burst pressure. The optimization of pressure vessels show that the stacking sequence can be employed effectively to maximum burst pressure. However Adali's results weren't compared to experimental testing and the stiffness degradation wasn't considered during analysis.

The effect of surface cracks on strength has been investigated theoretically and experimentally for glass/epoxy filament wound pipes, by Tarakçioğlu et al (2000). They were investigated theoretically and experimentally as the effect of surface

cracks on strength in glass/epoxy filament wound pipes which were exposed to open ended internal pressure.

Mirza et al. (2001) investigated the composite vessels under concentrated moments applied at discrete lug positions by finite element method. Jacquemin and Vautrin (2002) examined the moisture concentration and the hygrothermal internal stress fields for evaluating the durability of thick composite pipes submitted to cyclic environmental condition. Sun et al. (1999) calculated the stresses and bursting pressure of filament wound solid-rocket motor cases which are a kind of composite pressure vessel; maximum stress failure criteria and stiffness-degradation model were introduced to the failure analysis. Hwang et al. (2003) manufactured composite pressure vessels made by continuous winding of fibrous tapes reinforced in longitudinal and transverse directions and proposed for commercial applications instead of traditional isotensoid vessels. Sonnen et al. (2004) studied computerized calculation of composite laminates and structures.

Literature reveals that:

- Most of the finite element analyses of composite pressure vessels are based on elastic constitutive relations and traditional thin-walled laminated shell theory.
- Optimization of composite pressure vessels is done by changing the parameters of the composite materials including filament winding angle, lamination sequence, and material.
- A Tsai-Wu failure criterion is regarded to be one of the best theories at predicting failure in composite material.

The present research focuses on:

- Determination of first and final failure pressures of composite pressure vessels by using a finite element method.
- Optimization of composite pressure vessels

- Comparison of filament winding angles of composite pressure vessels
- Observation of different temperature effects on composite pressure vessels
- Comparison of theoretical results with experimental

CHAPTER THREE

ENGINEERING MATERIALS

3.1 Conventional Engineering Materials

There are more than 50,000 materials available to engineers for the design and manufacturing of products for various applications. These materials range from ordinary materials (e.g., copper, cast iron, brass), which have been available for several hundred years, to the more recently developed, advanced materials (e.g., composites, ceramics, and high-performance steels). Due to this wide variety of materials, today's engineers are in a big challenge for the right selection of a material and its manufacturing process for an application. It is difficult to study all these materials individually; therefore, a broad classification is necessary for simplification and characterization.

These materials, depending on their major characteristics (e.g., stiffness, strength, density, and melting temperature), can be broadly divided into four main categories: (1) metals, (2) plastics, (3) ceramics, and (4) composites. Each class contains large number of materials with a range of properties which to some extent results in an overlap of properties with other classes. For example, most common ceramic materials such as silicon carbide (SiC) and alumina (Al_2O_3) have densities in the range 3.2 to 3.5 g/cc and overlap with the densities of common metals such as iron (7.8 g/cc), copper (6.8 g/cc), and aluminum (2.7 g/cc). Table 3.1 presents the properties of some selected materials in each class in terms of density (specific weight), stiffness, strength, and maximum continuous use temperature. The maximum operating temperature in metals does not degrade the material the way it degrades the plastics and composites. Metals generally tend to temper and age at high temperatures as the microstructure of the metals alters significantly at these temperatures. Due to mentioned microstructural changes, modulus and strength values generally drop. The maximum temperatures cited in Table 3.1 are the temperatures at which the materials retain their strength and stiffness values to at least 90% of the original values shown in the table.

Table 3.1 Typical properties of some engineering materials.

Material	Density (ρ) (g/cm^3)	Tensile Modulus (E) (GPa)	Tensile Strength (σ) (GPa)	Specific Modulus (E/ρ)	Specific Strength (G/ρ)	Max. Service Temp. (°C)
Metals						
Cast iron, grade 20	7.8	100	0.14	14.3	0.02	230-300
Steel, AISI 1045 hot rolled	7.8	205	0.57	26.3	0.073	500-650
Aluminum 2024-T4	2.7	73	0.45	27	0.17	150-250
Aluminum 6061-T6	2.7	69	0.27	25.5	0.10	150-250
Plastics						
Nylon 6/6	1.15	2.9	0.082	2.52	0.071	75-100
Polypropylene	0.9	1.4	0.083	1.55	0.037	50-80
Epoxy	1.25	3.5	0.069	2.8	0.055	80-215
Phenolic	1.35	3.0	0.006	2.22	0.004	70-120
Ceramics						
Alumina	3.8	350	0.17	92.1	0.045	1425-1540
MgO	3.6	205	0.06	56.9	0.017	900-1000
Short fiber composites						
Glass-filled epoxy (35%)	1.9	25	0.30	8.26	0.16	80-200
Glass-filled polyester (35%)	2.00	15.7	0.13	7.25	0.065	80-125
Glass-filled nylon (35%)	1.62	14.5	0.20	8.95	0.12	75-110
Glass-filled nylon (60%)	1.95	21.8	0.29	11.18	0.149	80-215
Unidirectional composites						
S-glass/epoxy (45%)	1.81	39.5	0.87	21.8	0.48	80-215
Carbon/epoxy (61%)	1.59	142	1.73	89.3	1.08	80-215
Kevlar/epoxy (53%)	1.35	63.6	1.1	47.1	0.81	80-215

3.1.1 Metals

Metals have long been the dominating materials in the past for structural applications. They provide the largest design and processing history to the engineers. The common metals are iron, aluminum, copper, magnesium, zinc, lead, nickel, and titanium. In structural applications, alloys are more frequently used than pure metals. Alloys are formed by mixing different materials, sometimes including non-metallic elements. Alloys offer better properties than pure metals. For example, cast iron is brittle and easy to corrode, but the addition of less than 1% carbon in iron makes it tougher, and the addition of chromium makes it corrosion resistant. Through the principle of alloying, thousands of new metals are created.

Metals are, in general, heavy as compared to plastics and composites. Only aluminum, magnesium, and beryllium provide densities close to plastics. Steel is 4 to 7 times heavier than plastic materials; aluminum is 1.2 to 2 times heavier than plastics. Metals generally require several machining operations to obtain the final product. Depending upon the final geometry of the design, the machining operations are planned carefully, and sometimes, if sheet metal usage is involved (especially in defence/aerospace industry), the process for the final geometry causes the material properties change significantly from their original values.

Metals have high stiffness, strength, thermal stability, and thermal and electrical conductivity. Due to their higher temperature or fatigue resistance than plastics, they can be used for applications with higher service temperature or higher life-cyle requirements.

3.1.2 Plastics

Plastics have become the most common engineering materials over the past decade. In the past 5 years, the production of plastics on a volume basis has exceeded steel production. Due to their light weight, easy processability, and corrosion resistance, plastics are widely used for automobile parts, aerospace components and consumer goods. Plastics can be purchased in the form of sheets, rods, bars, powders, pellets, and granules. With the help of a manufacturing process, plastics can be formed into near-net-shape or net-shape parts. They can provide high surface finish and therefore eliminate several machining operations. This feature provides the production of low-cost parts.

Plastics are not used for high-temperature applications because of their poor thermal stability. In general, the operating temperature for plastics is less than 100°C. Some plastics can take service temperature in the range of 100 to 200°C without a significant decrease in the performance. Plastics have lower melting temperatures than metals and therefore they are easy to process.

3.1.3 Ceramics

Ceramics have strong covalent bonds and therefore provide great thermal stability and hardness. They are the most rigid of all materials. The major distinguishing characteristic of ceramics as compared to metals is that they possess almost no ductility. They fail in brittle fashion. Ceramics have the highest melting points of engineering materials. They are generally used for high-temperature and high-wear applications and are resistant to most forms of chemical attack. Ceramics cannot be processed by common metallurgical techniques and require high-temperature equipment for fabrication. Due to their high hardness, ceramics are difficult to machine and therefore require net-shape forming to final shape. Ceramics require expensive cutting tools, such as carbide and diamond tools.

3.1.4 Composites

Composite materials have been utilized to solve technological problems for a long time but only in the 1960s did these materials start capturing the attention of industries with the introduction of polymeric-based composites. Since then, composite materials have become common engineering materials and are designed and manufactured for various applications including automotive components, sporting goods, aerospace parts, consumer goods, and in the marine and oil industries. The growth in composite usage also came about because of increased awareness regarding product performance and increased competition in the global market for lightweight components. Among all materials, composite materials have the potential to replace widely used steel and aluminium, and many times with better performance. Replacing steel components with composite components can save 60 to 80 % in component weight, and 20 to 50 % weight by replacing aluminium parts. Today, it appears that composites are the materials of choice for many engineering applications. Also, it is observed that with the successful designs of new suitable composite components, all the past metal components will be replaced by these new creations.

3.2 Introduction to Composites

A composite material is made by combining two or more materials to give a unique combination of properties. The above definition is more general and can include metals alloys, plastic co-polymers, minerals, and wood. Fiber-reinforced composite materials differ from the above materials in that the constituent materials are different at the molecular level and are mechanically separable. In bulk form, the constituent materials work together but remain in their original forms. The final properties of composite materials are better than constituent material properties in a way to achieve the needed directional properties (longitudinal, long transverse, short-transverse).

The concept of composites was not invented by human beings; in fact it is found in nature. An example is wood, which is a composite of cellulose fibers in a matrix of natural glue called lignin. The shell of invertebrates, such as snails and oysters, is an example of a composite. Such shells are stronger and tougher than man-made advanced composites. Scientists have found that the fibers taken from a spider's web are stronger than synthetic fibers. In India, Greece, and other countries, husks or straws mixed with clay have been used to build houses for several hundred years. Mixing husk or sawdust in a clay is an example of a particulate composite and mixing straws in clay is an example of a short fiber composite. These reinforcements are done to improve structural performance.

The main concept of a composite is that it contains matrix materials. Typically, composite material is formed by reinforcing fibers in a matrix resin as shown in Figure 3.1. The reinforcements can be fibers, particulates, or whiskers, and the matrix materials can be metals, plastics, or ceramics.

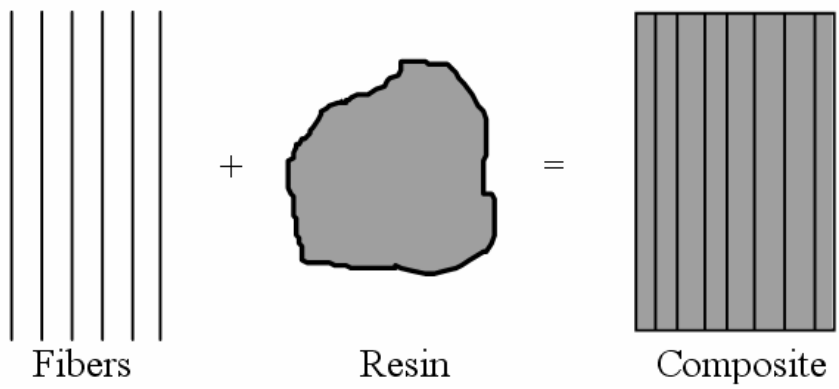

Figure 3.1 Formation of a composite material using fibers and resin.

The reinforcements can be made from polymers, ceramics, and metals. The fibers can be continuous, long, or short. Composites made with a polymer matrix have become more common and are widely used in various industries. The main focus here is the composite material in which the matrix material is polymer-based resin. They can be thermoset or thermoplastic resins. The reinforcing fiber or fabric provides strength and stiffness to the composite, whereas the matrix gives rigidity and environmental resistance. Reinforcing fibers are found in different forms, from long continuous fibers and woven fabric to short chopped fibers and matrix. Each configuration results in different properties. The way the fibers are laid in the composites has a strong effect on the properties. All of the above combinations or only one form can be used in a composite. The important thing to remember about composites is that the fiber carries the load and its strength is greatest along the axis of the fiber. Long continuous fibers in the direction of the loading result in a composite with properties far exceeding the matrix resin itself. The same material chopped into short lengths yields lower properties than continuous fibers, as illustrated in Figure 3.2. Depending on the type of application (structural or non-structural) and manufacturing method, the fiber form is selected. For structural applications, continuous fibers or long fibers are recommended; whereas for non-structural applications, short fibers are recommended. Injection and compression molding utilize short fibers, whereas filament winding, pultrusion, and roll wrapping use continuous fibers.

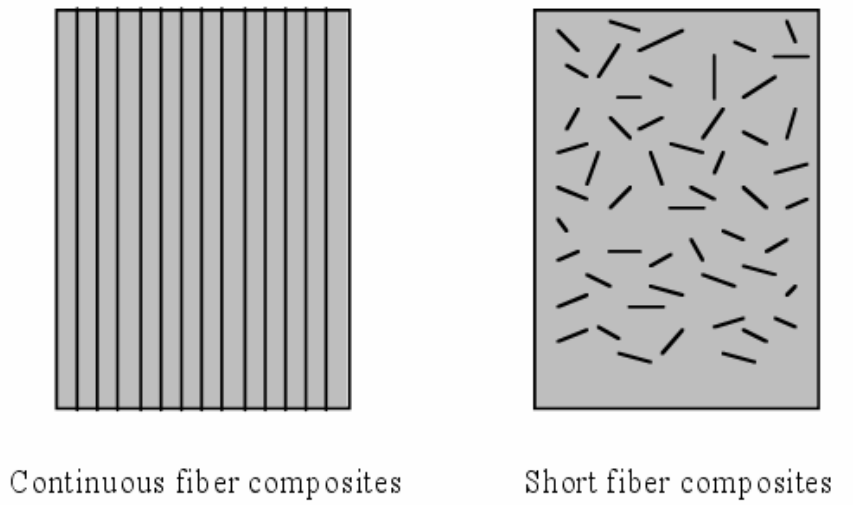

Figure 3.2 Continuous fiber and short fiber composites.

3.2.1 Functions of Fibers and Matrix

A composite material is formed by reinforcing plastics with fibers. To develop a good understanding of composite behaviour, one should have a good knowledge of the roles of fibers and matrix materials in a composite. The important functions of fibers and matrix materials are discussed below.

The main functions of the fibers in a composite are:

- To carry the load. In a structural composite, 70 to 90 % of the load is carried by fibers.
- To provide stiffness, strength, thermal stability, and other structural properties in the composites.
- To provide electrical conductivity or insulation, depending on the type of fiber used.

A matrix material fulfills several functions in a composite structure, most of which are vital to the satisfactory performance of the structure. Fibers in and of themselves are of little use without the presence of a matrix material or binder. The important functions of a matrix material include the following:

- The matrix material binds the fibers together and transfers the load to the fibers. It provides rigidity and shape to the structure.
- The matrix isolates the fibers so that individual fibers can act separately. This stops or slows the propagation of a crack.
- The matrix provides a good surface finish quality and aids in the production of net-shape or near-net-shape parts.
- The matrix provides protection to reinforcing fibers against chemical attack and mechanical damage (wear).
- Depending on the matrix material selected, performance characteristics such as ductility, impact strength, etc. are also influenced. A ductile matrix will increase the toughness of the structure. For higher toughness requirements, thermoplastic-based composites are selected.
- The failure mode is strongly affected by the type of matrix material used in the composite as well as its compatibility with the fiber.

3.2.2 Special Features of Composites

Composites have been routinely designed and manufactured for applications in which high performance and light weight are needed. They offer several advantages over traditional engineering materials as discussed below.

- Composite materials provide capabilities for part integration. Several metallic components can be replaced by a single composite component.
- Composite structures provide in-service monitoring or online process monitoring with the help of embedded sensors. This feature is used to monitor fatigue damage in aircraft structures or can be utilized to monitor the resin flow in an RTM (resin transfer molding) process. Materials with embedded sensors are known as “smart” materials.
- Composite materials have a high specific stiffness (stiffness-to-density ratio), as shown in Table 3.1. Composites offer the stiffness of steel at one fifth the

weight and equal the stiffness of aluminum at one half the weights.

- The specific strength (strength-to-density ratio) of a composite material is very high. Due to this, airplanes and automobiles move faster and with better fuel efficiency due to light weight and less projected areas taking the air flow into account. The specific strength is typically in the range of 3 to 5 times that of steel and aluminum alloys. Due to this higher specific stiffness and strength, composite parts are lighter than their counterparts.
- The fatigue strength (endurance limit) is much higher for composite materials. Steel and aluminum alloys exhibit good fatigue strength up to about 50% of their static strength. Unidirectional carbon/epoxy composites have good fatigue strength up to almost 90% of their static strength.
- Composite materials offer high corrosion resistance. Iron and aluminum corrode in the presence of water and air, require special coatings and alloying. Because the outer surface of composites is formed by plastics, corrosion and chemical resistance are very good.
- Composite materials offer increased amounts of design flexibility. For example, the coefficient of thermal expansion (CTE) of composite structures can be made zero by selecting suitable materials and lay-up sequence. Because the CTE for composites is much lower than for metals, composite structures provide good dimensional stability.
- Net-shape or near-net-shape parts can be produced with composite materials. This feature eliminates several machining operations and thus reduces process cycle time and cost.
- Complex parts, appearance, and special contours, which are sometimes not possible with metals, can be fabricated using composite materials without welding or riveting the separate pieces. This increases reliability and reduces production times. It offers greater manufacturing feasibility.
- Composite materials offer greater feasibility for employing design for manufacturing (DFM) and design for assembly (DFA) techniques. These techniques help minimize the number of parts in a product and thus reduce assembly and joining time. By eliminating joints, high-strength structural parts

can be manufactured at lower costs. Cost benefit comes by reducing the both assembly time and cost.

• Composites offer good impact properties, as shown in Figures 3.3 and Figure 3.4 shows impact properties of aluminum, steel, glass/epoxy, kevlar/epoxy, and carbon/epoxy continuous fiber composites. Glass and Kevlar composites provide higher impact strength than steel and aluminum. Figure 3.4 compares impact properties of short and long glass fiber thermoplastic composites with aluminum and magnesium. Among thermoplastic composites, impact properties of long glass fiber nylon 66 composite (NylonLG60) with 60% fiber content, short glass fiber nylon 66 composite (NylonSG40) with 40% fiber content, long glass fiber polypropylene composite (PPLG40) with 40% fiber content, short glass fiber polypropylene composite (PPSG40) with 40% fiber content, long glass fiber PPS composite (PPSLG50) with 50% fiber content, and long glass fiber polyurethane composite (PULG60) with 60% fiber content are described. Long glass fiber provides three to four times improved impact properties than short glass fiber composites.

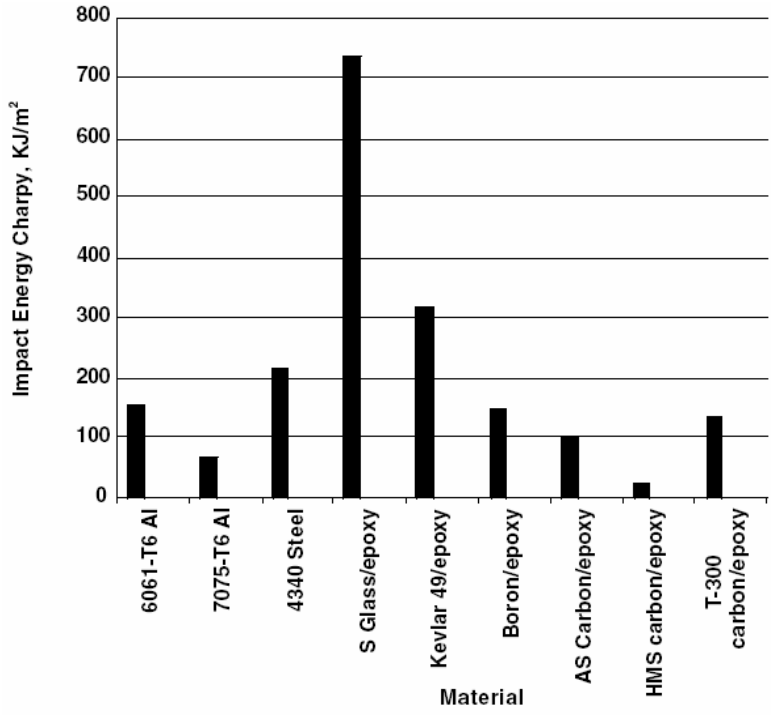

Figure 3.3 Impact properties of various engineering materials. Unidirectional composite materials with about 60 % fiber volume fraction are used.

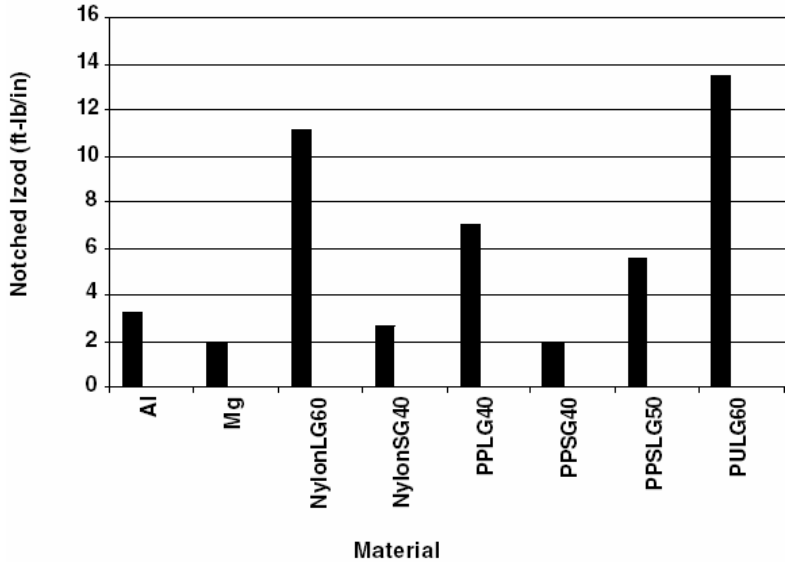

Figure 3.4 Impact properties of long glass (LG) and short glass (SG) fibers reinforced thermoplastic composites. Fiber weight percent is written at the end in two digits..

- Noise, vibration, and harshness (NVH) characteristics are better for composite materials than metals. Composite materials dampen vibrations in an order of magnitude better than metals. These characteristics are used in a variety of applications, from the leading edge of an airplane to golf clubs.
- By utilizing proper design and manufacturing techniques, cost-effective composite parts can be manufactured. Composites offer design freedom by tailoring material properties to meet performance specifications, thus avoiding the over-design of products. This is achieved by changing the fiber orientation, fiber type, and/or resin systems.
- Glass-reinforced and aramid-reinforced phenolic composites meet FAA and JAR requirements for low smoke and toxicity. This feature is required for aircraft interior panels, stowbins, and galley walls.
- The cost of tooling required for composites processing is much lower than that for metals processing because of lower pressure and temperature requirements. This offers greater flexibility for design changes in this competitive market where product lifetime is continuously reducing.

3.2.3 Disadvantages of Composites

Although composite materials offer many benefits, they suffer from the following disadvantages:

- The materials cost for composite materials is very high compared to that of steel and aluminum. It is almost 5 to 20 times more than aluminum and steel on a weight basis. For example, glass fiber costs $1.00 to $8.00/lb; carbon fiber costs $8 to $40/lb; epoxy costs $1.50/lb; glass/epoxy prepreg costs $12/lb; and carbon/epoxy prepreg costs $12 to $60/lb. The cost of steel is $0.20 to $1.00/lb and that of aluminum is $0.60 to $1.00/lb.
- In the past, composite materials have been used for the fabrication of large structures at low volume (one to three parts per day). The lack of high-volume production methods limits the widespread use of composite materials. Recently, pultrusion, resin transfer molding (RTM), structural reaction injection molding (SRIM), compression molding of sheet molding compound (SMC), and filament winding have been automated for higher production rates. Automotive parts require the production of 100 to 20,000 parts per day. For example, Corvette volume is 100 vehicles per day, and Ford-Taurus volume is 2000 vehicles per day. Steering system companies such as Delphi Saginaw Steering Systems and TRW produce more than 20,000 steering systems per day for various models. Sporting good items such as golf shafts are produced on the order of 10,000 pieces per day.
- Classical ways of designing products with metals depend on the usage of machinery and metals handbooks, and design and data handbooks. Large design databases are available for metals. Designing parts with composites lacks such books because of the lack of a database.
- The temperature resistance of composite parts depends on the temperature resistance of the matrix materials. Because a large proportion of composites use polymer-based matrices, temperature resistance is limited by the plastics' properties. Average composites work in the temperature range –40 to +100°C. The upper temperature limit can range between +150 and +200°C for high-

temperature plastics such as epoxies, bismaleimides, and PEEK. Table 3.2 shows the maximum continuous-use temperature for various polymers.

- Solvent resistance, chemical resistance, and environmental stress cracking of composites depend on the properties of polymers. Some polymers have low resistance to solvents and environmental stress cracking.
- Some composites absorb moisture, which affects the properties and dimensional stabilities of the them.

Table 3.2 Maximum Continuous-Use Temperatures for Various Thermosets and Thermoplastics

Materials	Maksimum Continuous-Use Temperature (˚C)
Thermosets	
Vinylester	60-150
Polyester	60-150
Phenolics	70-150
Epoxy	80-215
Cyanate esters	150-250
Bismaleimide	230-320
Thermoplastics	
Polyethylene	50-80
Polypropylene	50-75
Acetal	70-95
Nylon	75-100
Polyester	70-120
PPS	120-220
PEEK	120-250
Teflon	200-260

3.2.4 Classification of Composites Processing

Processing is the science of transforming materials from one shape to the other. As composite materials involve two or more different materials, the processing techniques used with composites are quite different than those for metals processing. There are various types of composites processing techniques available to process the various types of reinforcements and resin systems. It is the job of a manufacturing

engineer to select the correct processing technique and processing conditions to meet the performance, production rate, and cost requirements of an application. The engineer must make informed judgements regarding the selection of a process that can accomplish the most for the least resources. For this, engineers should have a good knowledge of the benefits and limitations of each process. This paper discusses the various manufacturing processes frequently used in the fabrication of thermoset and thermoplastic composites, as well as the processing conditions, fabrication steps, limitations, and advantages of each manufacturing method. Figure 3.5 classifies the frequently used composites processing techniques in the composites industry.

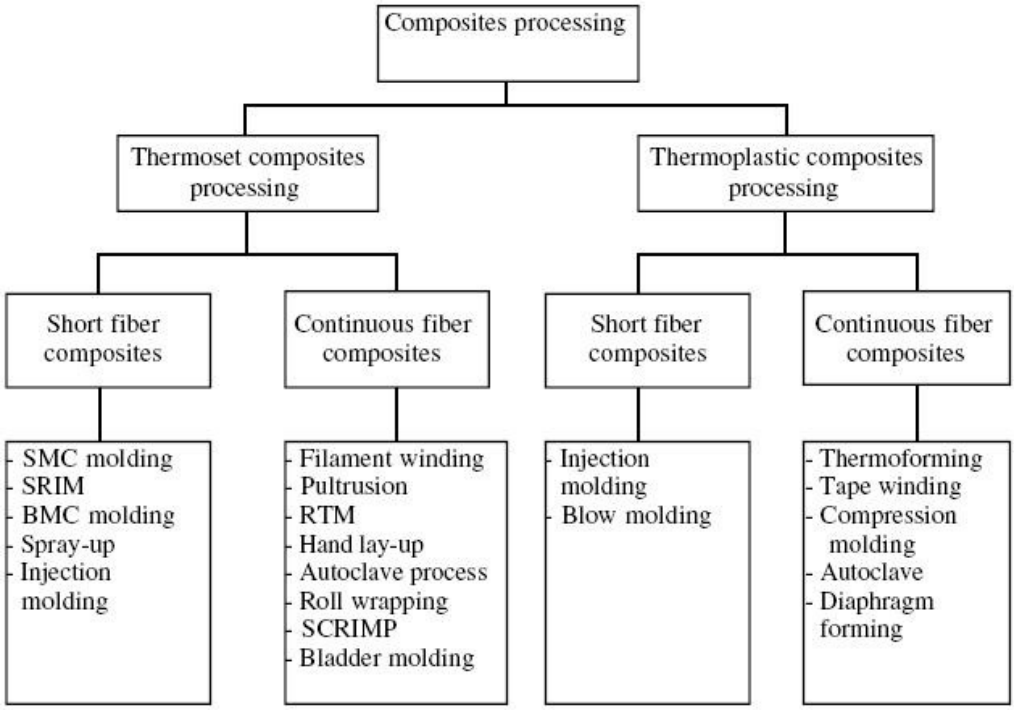

Figure 3.5 Classification of composites processing techniques.

3.3 Manufacturing Processes of Composite Materials

If you want to design a product using composites, there are many choices to make in the area of resins, fibers and core materials etc, each of them having their own unique set of properties. However, the end properties of a product built from these different materials are not only a function of the individual material properties. The

way the materials are designed into the product and the way the materials are processed to make the product, contribute largely to the overall end properties.

The choice for a specific manufacturing process is based on the form and complexity of the product, the tooling and processing costs and, most importantly, the required properties for the product. We will describe the most commonly used manufacturing processes.

3.3.1 Hand Lay-up

Hand lay-up, also known as wet lay-up, uses fibers in the form of woven, knitted, stitched or bonded fabrics. These fibers, after being placed in a mould, are impregnated by hand using rollers or brushes. The laminates are left to cure under standard atmospheric conditions.

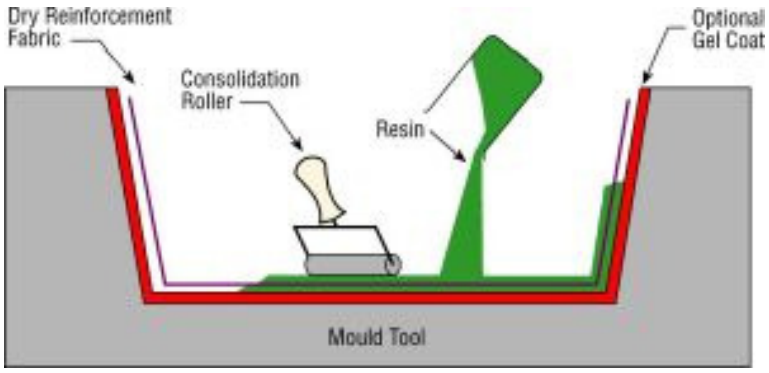

Figure 3.6 Hand lay-up process technique.

Materials

•Any kind of fiber and any kind of resin can be processed by hand lay-up.

Advantages

- Low molding/tooling costs
- Widely used
- Possibility for large products
- Possibility for small series
- Wide choice of suppliers and material types

Disadvantages

- Overall quality of the composite depends on the skill of the processors
- Health and safety precautions during processing are necessary
- Resins need to be low in viscosity to be workable by hand. This generally compromises their mechanical and thermal properties.

3.3.2 Spray Lay-up

Spray lay-up uses a hand-held spray gun which chops the fibers and then feeds it into a spray of resin aimed at the mould. The materials are left to cure under standard atmospheric conditions.

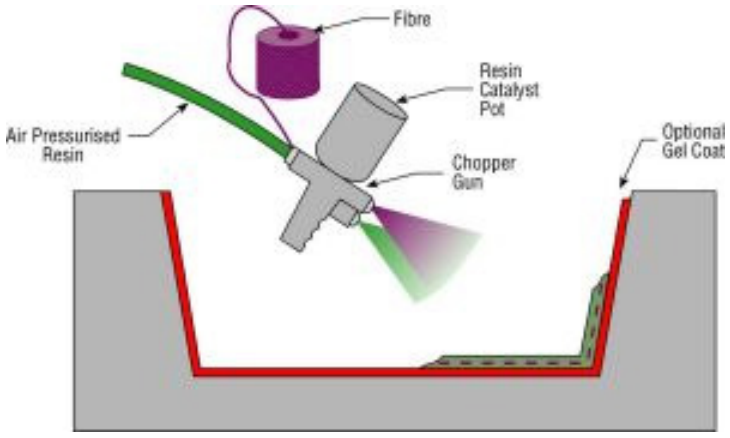

Figure 3.7 Spray lay-up process technique.

Materials

- Spray lay-up can only make use of glass fibers. Polyester is primarily used as matrix.

Advantages

- Low molding/tooling costs
- Widely used
- Possibility for large products
- Possibility for small series

Disadvantages

- Laminates tend to be very resin-rich and therefore excessively heavy
- Mechanical properties are limited by the use of short fibers
- Health and safety precautions during processing are necessary
- Resins need to be low in viscosity to be sprayable. This generally compromises their mechanical and thermal properties

3.3.3 Vacuum Bagging

Vacuum bagging is basically an extension of wet lay-up. In order to improve the consolidation of the laminate laid-up by hand or spray, pressure up to 1 atmosphere is applied. A plastic film is sealed over the laminate and onto the mould. After that the air underneath the plastic film is extracted by a vacuum pump.

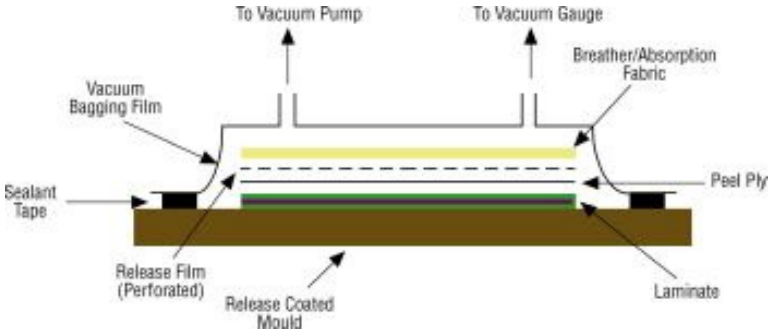

Figure 3.8 Vacuum bagging process technique.

Materials

• Primarily epoxy is used in combination with any kind of fibers and fabrics. Even heavy fabrics can be wet-out due to the consolidation pressure.

Advantages

• Higher fiber content can be achieved compared to standard wet lay-up

• Better fiber wet-out due to pressure

• The vacuum bag reduces the amount of volatiles emitted during cure

Disadvantages

• Extra costs compared to wet lay-up (tooling, labour and bagging material)

• Quality determined by the skills of the operator (mixing and controlling of resin)

3.3.4 Filament Winding

The process of filament winding is discussed in section 3.5.

3.3.5 Prepregs

'Prepreg' stands for pre-impregnated, which basically means 'already impregnated'. Fabrics and fibers are pre-impregnated by the materials manufacturer, under heat and pressure or with solvent, with a pre-catalysed resin. Although the catalyst is reasonably stable at ambient temperatures, allowing these materials to be used / processed for several weeks or even months, they are mostly stored frozen to prolong storage life.

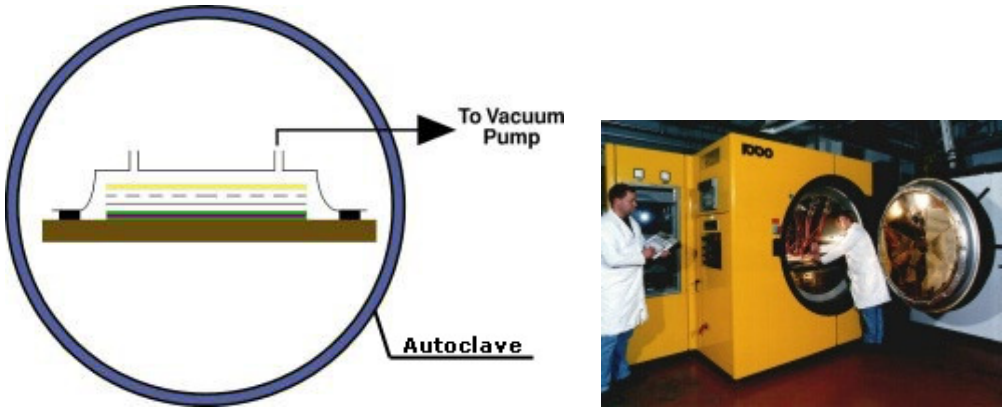

Figure 3.9 Prepregs process technique.

Unidirectional materials take fiber direct from a creel, and are held together by the resin alone. The prepregs are laid up by hand or machine onto a mould surface, vacuum bagged and then heated to typically 120-180°C. This allows the resin to initially reflow and eventually to cure. Additional pressure for the molding is usually provided by an autoclave (effectively a pressurized oven) which can apply up to 5 atmospheres to the laminate.

Materials

• Generally epoxy, polyester, phenolic and high temperature resins such as polyimides, cyanate esters and bismaleimides, combined with any kind of fiber (directly from creel or as a fabric)

Advantages

• Resin/catalyst level set by manufacturer

- Materials are clean to work with
- Extended working times at room temperature
- Automation and labour saving possible
- Resin chemistry can be optimised for mechanical and thermal performance, with the high viscosity resins being impregnable due to the manufacturing process

Disadvantages

- Material cost is higher
- Autoclave required: expensive, slow and limited in size

3.3.6 Resin Transfer Moulding (RTM)

RTM is a relatively high performance production method. Although the fiber-to-resin ratio of about 60% is not as high as using prepregs, RTM offers possibilities that are very difficult to meet with other manufacturing processes.

RTM makes production of complex structures, for example with ribs or with network structures, relatively easy. The male and the female mould have the advantage that the surfaces are all of high quality and within certain tolerances. The size of the composite parts just depends on the size of the mould tool.

A less obvious but nevertheless important advantage of RTM is that the workers are much less affected by the chemicals compared to other production methods (hand lay-up). This is also true with respect to health problems; especially allergic reactions caused by chemicals for example solvents.

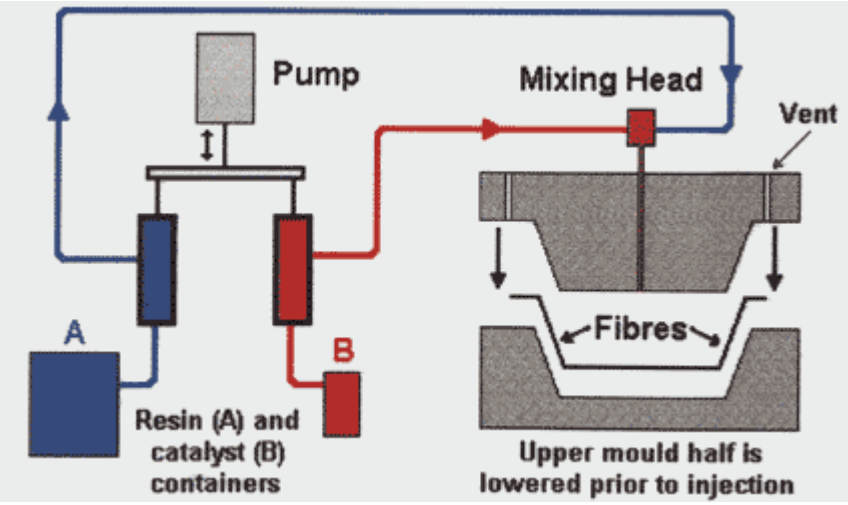

Figure 3.10 Resin transfer moulding technique.

Materials

- Generally polyester, vinylester and epoxy are used in combination with any kind of fiber.

Advantages

- Large, complex products possible
- Closed mould; no vapour emissions
- Excellent surface quality on both sides

Disadvantages

- Moulds can be expensive
- Unimpregnated areas can occur resulting in very expensive scrap parts

3.3.7 Rubber Pressing

Rubber pressing is a process for forming sheet materials (both composites and sheet metals) into products. It uses one product shaped mould, made out of

aluminium or wood, and one universal rubber ‘cushion’. For rubber pressing composites, a thermoplastic resin is required. Thermoplastic prepreg sheets are heated by infrared heaters. The next step is pressing the sheet material into its final form.

Rubber pressing is used for economical forming of sheet materials into (complex double curved) products. Because only one mould is required, the costs and the time necessary for making the mould are both low. This makes this process especially interesting for small series, prototyping and establishing short time-to-market.

Materials

- Rubber pressing composites require thermoplastic prepregs. Any type of fiber can be used, as long as they can withstand the temperature necessary for heating the prepregs.

Advantages

- Low tooling costs
- Fast mould production
- Good surface quality
- Flexibility

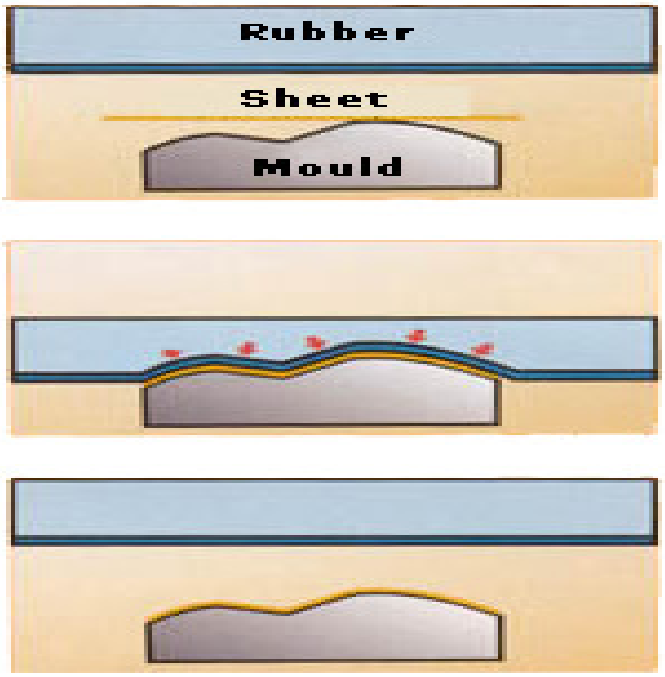

Figure 3.11 Rubber pressing technique.

Disadvantages

- Limited deformation ability
- Longer cycle times

3.3.8 Pultrusion

Fibers are pulled from a creel through a resin bath and then on through a heated die. The die completes the impregnation of the fiber, controls the resin content and cures the material into its final shape as it passes through the die. This cured profile is then automatically cut to length. Fabrics may also be introduced into the die to provide fiber direction other than at 0°. Although pultrusion is a continuous process, producing a profile of constant cross-section, a variant known as 'pulforming' allows for some variation to be introduced into the cross-section. The process pulls the materials through the die for impregnation, and then clamps them in a mould for curing. This makes the process non-continuous, but accommodating of small changes in cross-section.

Materials

- Pultrusion can process any kind of continuous fiber. Generally used resins are polyester, vinylester and epoxy.

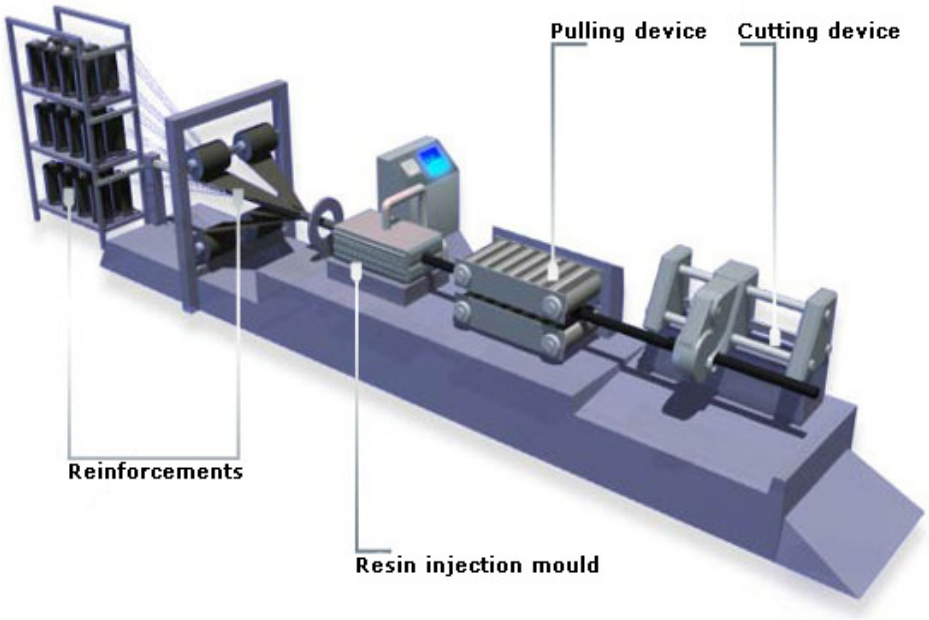

Figure 3.12 Pultrusion technique.

Advantages

- Fast and economic way of impregnating and curing materials
- Resin content can be accurately controlled
- Minimized fiber costs (come directly from creel)
- Very good structural properties (fibers lay straight in loading direction)
- Impregnation area can be enclosed thus limiting volatile emissions

Disadvantages

- Tooling costs are high
- Limited to constant or near constant cross-section products

3.3.9 Sandwich Constructions

Structural sandwiches are a special form of laminated composites in which thin, strong, stiff, hard, but relatively heavy facings are combined with thick, relatively soft, light and weaker cores to provide a lightweight composite stronger and stiffer in most respects than the sum of the individual stiffness and strengths.

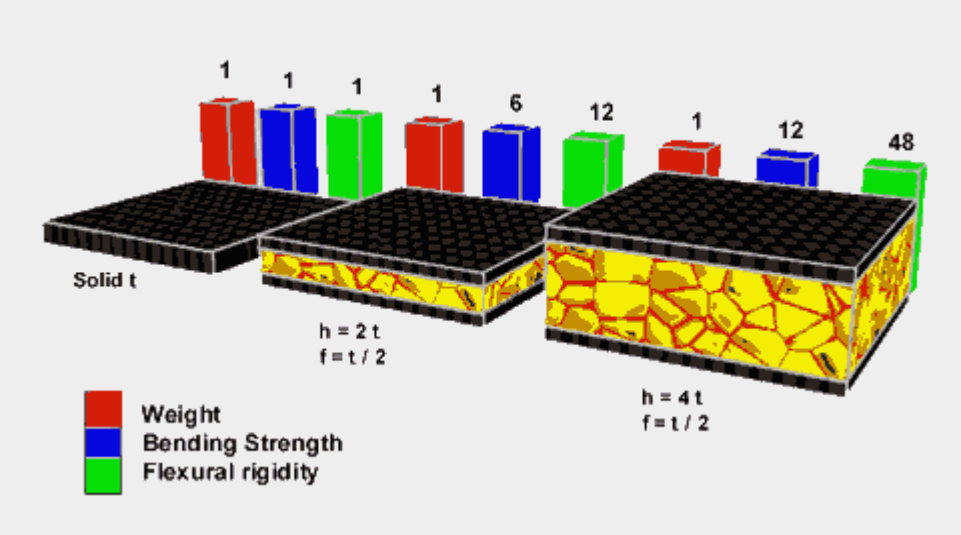

Figure 3.13 Sandwich construction technique.

The basic principle of a sandwich (spaced facings) was discovered in 1820 by a French inventor named Duleau.

A sandwich construction includes the following elements:

1. Two laminates, outer and inner

2. Core material, as a spacer

3. Adhesive for bonding of laminates.

Common materials for the laminates are: composite, metal or wood. The core can be made of paper, honeycombs made of impregnated aramid-paper or thermoplasts and all kinds of foams.

3.4 Composites Product Fabrication

Composite products are fabricated by transforming the raw material into final shape using one of the manufacturing processes discussed in Section 3.2.4.

The products thus fabricated are machined and then joined with other members as required for the application. The complete product fabrication is divided into the following four steps:

• *Forming*

In this step, feedstock is changed into the desired shape and size, usually under the action of pressure and heat.

• *Machining*

Machining operations are used to remove extra or undesired material.

•*Drilling*

Turning, cutting, and grinding come in this category. Composites machining operations require different tools and operating conditions than that required by metals.

• *Joining and Assembly*

Joining and assembly is performed to attach different components in a manner so that it can perform a desired task. Adhesive bonding, fusion bonding, mechanical fastening, etc. are commonly used for assembling two components. These operations are time consuming and cost money. Joining and assembly should be avoided as much as possible to reduce product costs.

• *Finishing*

Finishing operations are performed for several reasons, such as to improve outside appearance, to protect the product against environmental degradation, to provide a wear-resistant coating, and/or to provide a metal coating that resembles that of a metal. Golf shaft companies apply coating and paints on outer composite shafts to improve appearance and look.

It is not necessary that all of the above operations be performed at one manufacturing company. Sometimes a product made in one company is sent to another company for further operations. For example, an automotive driveshaft made in a filament winding company is sent to automakers (tier 1 or tier 2) for assembly with their final product, which is then sold to OEMs (original equipment manufacturers). In some cases, products such as golf clubs, tennis rackets, fishing rods, etc. are manufactured in one company and then sent directly to the distributor for consumer use.

3.5 Filament Winding

In a filament winding process, a band of continuous resin impregnated rovings or monofilaments is wrapped around a rotating mandrel and then cured either at room temperature or in an oven to produce the final product. The technique offers high speed and precise method for placing many composite layers. The mandrel can be cylindrical, round or any shape that does not have re-entrant curvature. Among the applications of filament winding are cylindrical and spherical pressure vessels, pipe lines, oxygen & other gas cylinders, rocket motor casings, helicopter blades, large underground storage tanks (for gasoline, oil, salts, acids, alkalies, water etc.). The process is not limited to axis-symmetric structures: prismatic shapes and more complex parts such as tee-joints, elbows may be wound on machines equipped with the appropriate number of degrees of freedom. Modern winding machines are numerically controlled with higher degrees of freedom for laying exact number of layers of reinforcement. Mechanical strength of the filament wound parts not only depends on composition of component material but also on process parameters like winding angle, fibre tension, resin chemistry and curing cycle.

3.5.1 Filament Winding Technology

In 1964, the authors, Rosato D.V and Grove C.S. in their book entitled, Filament winding: Its Development, Manufacture, Applications and Design, defined it as a technique which "…produces high-strength and lightweight products; consists basically of two ingredients; namely, a filament or tape type reinforcement and a matrix or resin". The unique characteristics of these materials made great revolutions for many years .The concept of filament winding process had been introduced in early 40's and the first attempt was made to develop filament-winding equipment. The equipment that was designed in 1950's was very basic; performing the simplest tasks using only two axes of motion (spindle rotation and horizontal carriage). Machine design consisted of a beam, a few legs and cam rollers for support. The simplistic design was sufficient to create the first filament wound parts: rocket motor cases. Initial advancements came in the form of mechanical systems that allowed an operator to program a machine by the use of gears, belts, pulleys and chains. These machines had limited capabilities and capacities, but were accurate.

Eventually through technical innovations, engineers were able to design servo-controlled photo-optic machines with hydraulic systems. The desired fibre path was converted into machine path motion through a black-white interface on a drum; which was followed by a photo-optic device that controlled the machine function. During this time the filament winding machine became increasingly sophisticated in design; the addition of a third axis of motion (radial or crossfeed carriage), profile rails and ball shafts in combination with improved gearboxes resulted in smoother, more accurate filament winding.

By mid-70’s, machine design once again made a dramatic shift. This time the advancement of servo technology entered the realm of the machine design. High-speed computers allowed for rapid data processing, resulting in smoother motion and greater fibre placement accuracy. Increasingly, function that historically was controlled through the use of belts, gears, pulley and chains was eventually being controlled through the use of computers.

The 1980s and 90s saw the increased use of computer technology. Computers and motion control cards became essential pieces of hardware that were included in almost every machine. Machine speed control was greatly improved; computer control systems could track position and velocity with increased accuracy. Additional axes of motions were also incorporated into machine design; allowing for four, five and even six axes of controlled motion.

At the same time a number of different companies began to experiment with the notion and development of pattern generation software. By creating pattern generation software, more complex configurations, such as tapered shafts, T-shaped parts and non-axisymmetric parts could be successfully wound.

3.5.2 Industrial Importance of Filament Winding Process

Since this fabrication technique allows production of strong, lightweight parts, it has proved particularly useful for components of aerospace, hydrospace and military applications and structures of commercial and industrial use. Both the reinforcement and the matrix can be tailor- made to satisfy almost any property demand. This aids in widening the applicability of filament winding to the production of almost any commercial items wherein the strength to weight ratio is important. Apart from the strength-to-weight advantages and low cost of manufacturing, filament wound composite parts have better corrosion and electrical resistance properties.

3.5.3 Filament Winding: Process Technology

The process of filament winding is primarily used for hollow, generally circular or oval sectioned products. Fibers can either be used dry or be pulled through a resin bath before being wound onto the mandrel. The winding pattern is controlled by the rotational speed of the mandrel and the movement of the fiber feeding mechanism. Filament winding usually refers to the conventional filament winding process. However some industrial companies use a device called 'Fast Filament Winder' for producing pressure vessels. Basically the processes are the same (the fibers are

wound around a mandrel following a certain pattern), but the way the machines work and the way the mandrel moves differs.

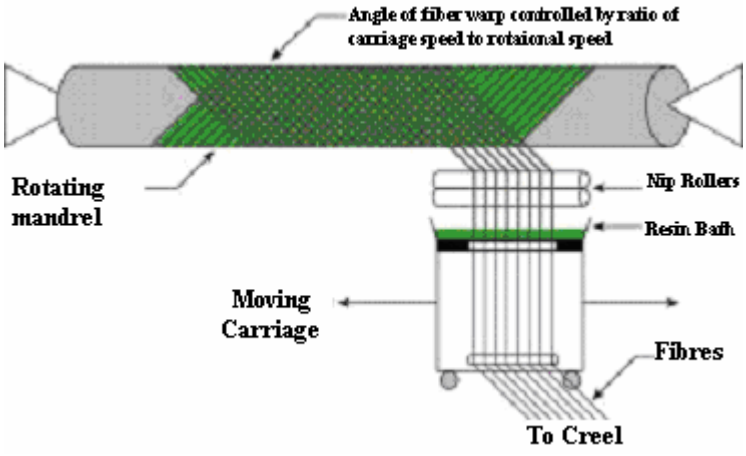

Figure 3.14 Schematic representation of the filament winding process.

After winding, the filament wound mandrel is subjected to curing and post curing operations during which the mandrel is continuously rotated to maintain uniformity of resin content around the circumference. After curing, product is removed from the mandrel, either by hydraulic or mechanical extractor.

Materials

- Any kind of continuous fiber and any kind of resin can be processed by filament winding.

Advantages

- Fast process
- Low material costs because the fibers come straight from the creel (no need to convert fibers into fabrics prior to use)
- Structural properties of laminates can be very good since straight fibers can be laid in a complex pattern to match the applied loads
- Resin content can be controlled by metering the resin onto each fiber tow

through nips or dies

CNC Filament Winding Set-up

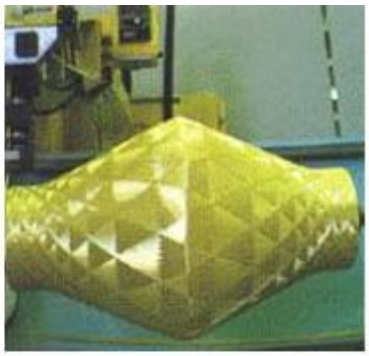

Winding of Kevlar Pressure Vessel

Filament Wound Pressure Vessel

Storage Tanks

Filament Wound

GRE Pipe Fittings

Figure 3.15 Some diagrams of filament wound products

Disadvantages

- Limited to convex shaped components
- Mandrel costs can be high

3.5.4 Filament Winding Materials

3.5.4.1 Fiber types (Reinforcement)

The mechanical properties of fibers dominantly contribute to the overall mechanical properties of the fiber/resin composite. The contribution of the fibers depends on four main factors:

- The basic mechanical properties of the fiber;
- The surface interaction of fiber and resin (interface);
- The amount of fibers in the composite (Fiber Volume Fraction);
- The orientation of the fibers in the composite.

The surface interaction of fiber and resin depends on the degree of bonding between the two. This interfacial bonding is heavily influenced by the kind of surface treatment given to the fiber surface (sizing). Also, sizing minimizes the damage due to handling. The choice in sizing depends on the desired performance of the composite, the kind of fiber and the way the fibers are going to be processed.

The amount of fibers in a composite determines the strength and stiffness. As a general rule, strength and stiffness of a laminate will increase proportional to the amount of fibers. However, above 60-70% Fiber Volume Fraction, tensile stiffness will continue to increase, while the laminate's strength reaches a peak and then slowly decreases. In this situation there's too little resin present to sufficiently hold the fibers together.

The orientation of the fibers in a composite largely contributes to the overall strength. Reinforcing fibers are designed to be loaded along their length, which means that the properties of the composite are highly direction-specific. By placing the fibers in the loading directions, the amount of material put in directions where there is little or no load can be minimized.

Carbon

Fibers show excellent mechanical properties compared to other fibers: high specific stiffness, very high strength in both compression and tension and a high resistance to corrosion, creep and fatigue. They are used as structural components and reinforcements in aerospace structures, for example airplanes' vertical fins, flaps, satellite platforms and in turbofan engines.

Carbon fibers provide the designer with the following properties:

- low density
- high tensile modulus
- high tensile strength
- good creep resistance
- good fatigue resistance
- good wear resistance
- low thermal expansion
- low friction
- good electrical conductivity
- good thermal conductivity, good chemical resistance
- bio compatibility
- low shrinkage
- reduced moisture absorption

Aramid

Fibers (most commonly known as 'Kevlar' or 'Twaron'), which have been commercially available since the 1960s, have found a wide field of applications. Their thermal properties facilitated their use as a substitute for asbestos. Aramid fibers, which show high energy absorption and ballistic properties as no other fibers, are used for bullet and fragment or impact resistance applications as well as for ropes and cables.

Aramid fibers provide the designer with the following properties:

- low density
- high tensile modulus
- high tensile strength
- good vibration damping
- high energy absorption
- high impact resistance
- low material fatigue, low compression strength
- good temperature resistance, good chemical resistance
- moderate adhesive properties
- low thermal conductivity

Glass

Fibers can be divided into groups according to their chemical composition. Well known are A-glass, C-glass, S-glass and E-glass fibers, whereof only the last one is widely used in aerospace applications. Glass fibers are produced from molten glass which is either produced directly or by melting glass marbles. The molten glass is poured into a tank and held at a constant temperature to retain a constant viscosity. The flowing glass forms filaments with diameters that can range from 1-25 10e-6 m.

Glass fibers provide the designer with the following properties

- high tensile strength
- high shear modulus
- low Poisson's ratio
- good electrical resistance
- good thermal resistance
- low thermal expansion
- low price

3.5.4.2 Resin types (Matrix)

Resins (or matrix) are an important part of any composite. It's basically the glue that keeps the composite together. A resin must have good mechanical properties, good adhesive properties, good toughness properties and good environmental properties.

For the mechanical properties this means that an ideal resin must be initially stiff but may not suffer brittle failure. And in order to achieve the full mechanical properties of the fiber, the resin must deform at least the same extend as the fiber.

Good adhesion between resin and reinforcement fibers ensures that the loads will be transferred efficiently and cracks and fiber/resin debonding will be prevented. The resistance to crack propagation is a measure for the material's toughness. Because this is hard to measure accurately in composites, you can generally say that the more deformation a resin will accept before failure, the tougher the material will be. It's important to match the toughness with the elongation of the fiber.

The environment in which the composite is used can be harsh. The resin must have good resistance to the environment it's used in, especially water and other aggressive substances. Furthermore, the resin must be able to withstand constant stress cycling.

There are two different groups of so called matrix systems: Thermoset matrix systems and Thermoplastic matrix systems.

Thermoset matrix system

Thermosetting materials are formed from a chemical reaction, where the resin is mixed with a hardener or catalyst to undergo an irreversible chemical reaction. The result is a hard, infusible matrix. Although there are many different types of resin in use in the composite industry, the three most commonly used types of resin are thermosets: Polyester, Vinylester and Epoxy.

Thermoplastic matrix system

Thermoplastics, like metals, soften with heating and eventually melt, hardening is established again with cooling. This process of crossing the softening or melting point on the temperature scale can be repeated as often as desired without any appreciable effect on the material properties in either state. Typical thermoplastics include nylon, polypropylene and ABS, and these can be reinforced, although usually only with short, chopped fibers such as glass.

Polyester

Polyester resins, or simply polyesters, are the most commonly used and cheapest matrix in the marine and composite industry. In organic chemistry the reaction of an alcohol with an organic acid produces an ester and water. Using special alcohols, such as glycol, and adding different kind of compounds (different acids and monomers), results in a whole range of polyesters having varying properties.

Basically there are two types of polyesters used in composites: orthophthalic polyester and Isophthalic polyester. The first one is the standard economic resin used by many people; the second one is becoming the preferred material in industries where superior water resistance is required.

Compared to the epoxy and vinylester, polyester shows the lowest adhesive and mechanical properties. The shrinkage due to curing is around 8%, which is higher than epoxy. This high shrinkage leads to build-in stresses and so called ‘print-through’ of the pattern of the reinforcing fibers. These cosmetic defects are difficult and expensive to ‘correct’.

Vinylester

The molecular structure of vinylester is the same as polyester, but differs in the location of the reactive sites of the structure. This difference makes vinylester tougher and more resilient than polyester. Because vinylester has fewer ester groups, which are susceptible to water degradation, it exhibits better resistance to water and many other chemicals than polyester. Because of this property, vinylester is

frequently used in applications such as pipelines and chemical storage tanks.

Compared to polyester, vinylester shows better adhesive and mechanical properties and a better resistance to water and chemicals. The shrinkage due to curing is the same as polyester, around 8%, giving the same problems with build-in stresses and ‘print-through’. The price level of vinylester is about two times the price level of polyester.

Epoxy

Epoxies generally out-perform most other resin types in terms of mechanical properties and resistance to environmental degradation. For this reason, epoxy resins are the most used resins in the aerospace industry for high performance fiber reinforced composites. It’s also the most expensive resin, exceeding the price level of polyester by 3 to 8 times.

The term 'epoxy' refers to a chemical group consisting of an oxygen atom bonded to two carbon atoms that are already bonded in some way. Epoxies differ from polyester and vinylester resins in that they are cured by a 'hardener' rather than a catalyst. Low shrinkage (around 2%), due to the different curing method, is in part responsible for the improved mechanical properties over polyester and vinylester.

3.5.4.3 Additives

By using various additives liquid resin systems can be made suitable to provide specific performance. Fillers constitute the greatest proportion of a formulation, second to the base resin. The most commonly used fillers are calcium carbonate, alumina silicate (clay) and alumina trihydrate. *Calcium carbonate* is primarily used as a *volume extender* to provide the lowest-cost-resin formulation in areas in which performance is not critical. *Alumina trihydrate* is an additive that is used for its ability to *suppress flame and smoke generation*. Fillers can be incorporated into the resins in quantities up to 50% of the total resin formulation by weight (100 parts filler per 100 parts resin). The usual volume limitation is based on the development

of usable viscosity, which depends on the particle size and the characteristics of the resin.

Special purpose additives include ultraviolet radiation screens for improved weatherability, *antimony oxide for flame retardance, pigments for coloration* and low-profile agents for surface smoothness and crack suppression characteristics. Mould release agents (metallic stearates, silicon gel or organic phosphate esters etc.) are important for adequate release from the mandrel to provide smooth surfaces and low processing friction.

3.5.5 Winding Patterns

In filament winding, one can vary winding tension, winding angle and/or resin content in each layer of reinforcement until desired thickness and strength of the composite are achieved. The properties of the finished composite can be varied by the type of winding pattern selected. Three basic filament winding patterns are:

3.5.5.1 Hoop Winding

It is known as girth or circumferential winding. Strictly speaking, hoop winding is a high angle helical winding that approaches an angle of 90 degrees. Each full rotation of the mandrel advances the band delivery by one full bandwidth as shown in Figure 3.16.

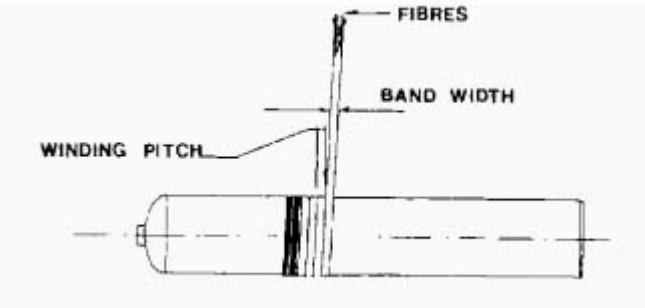

Fig 3.16 Circumferential or hoop winding

3.5.5.2 Helical Winding

In helical winding, mandrel rotates at a constant speed while the fibre feed carriage transverses back and forth at a speed regulated to generate the desired helical angles as shown in figure 3.17.

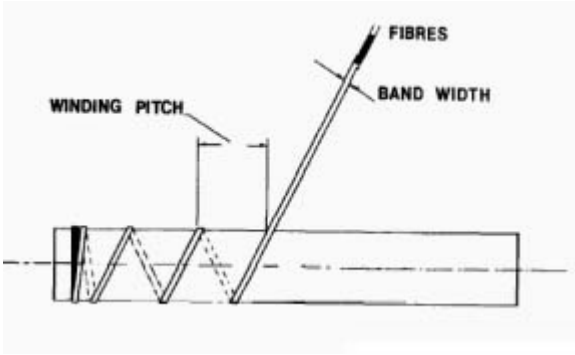

Fig 3.17 Helical winding

3.3.5.3 Polar Winding

In polar winding, the fibre passes tangentially to the polar opening at one end of the chamber, reverses direction, and passes tangentially to the opposite side of the polar opening at the other end. In other words, fibres are wrapped from pole to pole, as the mandrel arm rotates about the longitudinal axis as shown in figure 3.18. It is used to wind almost axial fibres on domed end type of pressure vessels. On vessels with parallel sides, a subsequent circumferential winding would be done.

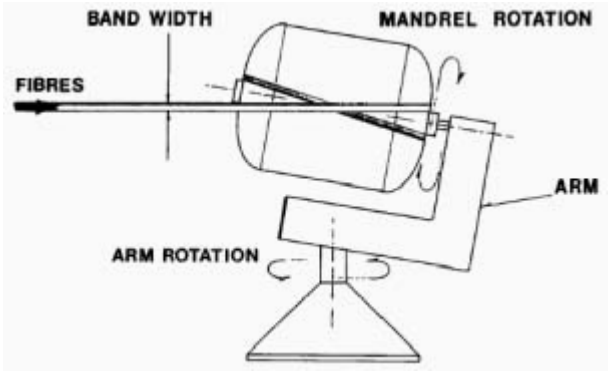

Fig 3.18 Polar winding

In the above three, helical winding has great versatility. Almost any combination of diameter and length may be wound by trading off wind angle and circuits to close the patterns. Usually, all composite tubes and pressure vessels are produced by means of helical winding.

3.5.6 Mechanical Properties of Filament Wound Products

Table 3.3 Typical properties of filament wound pipes (glass fibre reinforced)

Property	Typical Values	Predominant Process Variables *
Density	1.88-2.26	Glass/Resin Ratio
Tensile Strength, MPa (Helical Windings)	344-1034	Glass Type, Glass/Resin Ratio, Wind Pattern
Compressive Strength, MPa (Helical Windings)	276-551	Glass/Resin Ratio, Resin Type, Wind Pattern
Shear Strength, MPa: --Interlaminar --Cross	21-137 55-206	Resin Type, Wind Pattern, Glass/Resin Ratio, Resin Type
Modulus of Elasticity (Tension), GPa	21-41	Glass type, Wind Pattern
Modulus of Rigidity (Torsion), GPa	11-14	Wind Pattern
Flexural Strength	344-517	Wind Pattern, Glass/Resin Ratio
*The Predominant Process Variables are those, which have the greatest influence upon the range in the particular values reported.		

Table: 3.3 Property comparison: Filament wound composite vis-à-vis others

Material *	Density (g/cm^3)	Tensile Strength (MPa)	Tensile Modulus (MPa)	Specific Tensile Strength
Filament Wound Composite	1.99	1034	31.02	519.60
Aluminium 7075-T6	2.76	565	71.01	204.71
Stainless Steel -301	8.02	1275	199.94	158.98
Titanium Alloy (Ti-13 V-12 Cr-3 Al)	4.56	1275	110.3	279.61

*For unidirectional composites, the reported modulus and tensile strength values are measured in the direction of fibers.

(Source: C-K Composites, Mount Pleasant, PA)

Table 3.4 Filament wound products: Applications Vs. Resin systems used

Industry	Typical Application	Typical Resin Systems
Corrosion	• Underground Storage Tanks • Aboveground Storage Tanks	Polyester (Ortho- and Iso-phthalic), Vinyl Ester
	• Piping Systems • Stack Liners • Ducting Systems	Polyester (Ortho- and Iso-phthalic), Vinyl Ester, Epoxy, Phenolic
Oilfield	• Piping Systems • Drive Shafts • Tubular Structures	Epoxy, Phenolic
Paper and Pulp	• Paper Rollers • Piping Systems • Ducting Systems	Vinyl Ester, Epoxy
Infrastructure and Civil Engineering	• Column Wrapping • Tubular Support Structures • Power Poles • Light Standards	Polyester (Ortho- and Iso-phthalic), Vinyl Ester, Epoxy
Commercial Pressure Vessels	• Water Heaters • Solar Heaters • Reverse Osmosis Tanks • Filter Tanks • SCBA (Self-Contained Breathing Apparatus) Tanks • Compressed Natural Gas Tanks	Polyester (Ortho- and Iso-phthalic), Vinyl Ester, Epoxy
Aerospace	• Rocket Motor Cases • Drive Shafts • Launch Tubes • Aircraft Fuselage • High Pressure Tanks • Fuel Tanks	Epoxy, Bismaleimide (BMI), Phenolic, Vinyl Ester
Marine	• Drive Shafts • Mast and Boom Structures	Epoxy
Sports and Recreation	• Golf Shafts • Bicycle Tubular Structures • Wind Surfing Masts • Ski Poles	Epoxy

CHAPTER FOUR
MECHANICS OF COMPOSITE MATERIALS

4.1 General

Linear elastic theories of fiber reinforced composite are developed and are widely used in engineering. In this chapter, elastic constitutive equations and micromechanical behaviour of composites are presented.

4.2 Elastic Constitutive Equation

The Elastic Constitutive Equations for a general linear elastic solid relates the stress and strain tensors through the expression.

$$\sigma_{ij} = C_{ijkl}\varepsilon_{kl} \tag{4.1}$$

where; σ_{ij}, ε_{kl} = Stress tensor and strain tensor respectively
C_{ijkl} = The fourth order tensor of elastic constants

Fiber reinforced composite materials are considered to have orthotropic elasticity because these materials posses three mutually perpendicular planes of the elastic symmetry. Constitutive equation orthotropic elasticity can be defined by giving nine individual elastic stiffness parameters. In this case the stress-strain relations are of the forms

$$\begin{Bmatrix} \sigma_1 \\ \sigma_2 \\ \sigma_3 \\ \tau_{12} \\ \tau_{13} \\ \tau_{23} \end{Bmatrix} = \begin{bmatrix} C_{1111} & C_{1122} & C_{1133} & 0 & 0 & 0 \\ & C_{2222} & C_{2233} & 0 & 0 & 0 \\ & & C_{3333} & 0 & 0 & 0 \\ & & & C_{1212} & 0 & 0 \\ & sym & & & C_{1313} & 0 \\ & & & & 0 & C_{2323} \end{bmatrix} \begin{Bmatrix} \varepsilon_{11} \\ \varepsilon_{22} \\ \varepsilon_{33} \\ \gamma_{12} \\ \gamma_{13} \\ \gamma_{23} \end{Bmatrix} \tag{4.2}$$

where, material stiffness parameters C_{ijkl} are defined by engineering constant:

$$
\begin{aligned}
C_{1111} &= \frac{1-\nu_{23}\nu_{32}}{E_2E_3\Delta} \\
C_{2222} &= \frac{1-\nu_{13}\nu_{31}}{E_1E_3\Delta} \\
C_{3333} &= \frac{1-\nu_{12}\nu_{21}}{E_1E_2\Delta} \\
C_{1122} &= \frac{\nu_{21}+\nu_{31}\nu_{23}}{E_2E_3\Delta} = \frac{\nu_{12}+\nu_{32}\nu_{13}}{E_1E_3\Delta} \\
C_{1133} &= \frac{\nu_{31}+\nu_{21}\nu_{32}}{E_2E_3\Delta} = \frac{\nu_{13}+\nu_{12}\nu_{23}}{E_1E_2\Delta} \\
C_{2233} &= \frac{\nu_{32}+\nu_{12}\nu_{31}}{E_1E_3\Delta} = \frac{\nu_{23}+\nu_{21}\nu_{13}}{E_1E_2\Delta} \\
C_{1212} &= G_{12} \\
C_{1313} &= G_{13} \\
C_{2323} &= G_{23}
\end{aligned}
\tag{4.3}
$$

where;

$$
\Delta = \frac{1-\nu_{12}\nu_{21}-\nu_{23}\nu_{32}-\nu_{31}\nu_{13}-2\nu_{21}\nu_{32}\nu_{13}}{E_1E_2E_3} \tag{4.4}
$$

Due to composite material's stability there are restrictions on the elastic constants as follows:

$$
\begin{aligned}
&C_{ijkl} > 0 \\
&|C_{1122}| < \sqrt{C_{1111}C_{2222}} \\
&|C_{1133}| < \sqrt{C_{1111}C_{3333}} \\
&|C_{2233}| < \sqrt{C_{2222}C_{3333}}
\end{aligned}
\tag{4.5}
$$

Composite materials are compressible. Therefore, the determinant of the stiffness matrix should be positive,

$$\det(C_{ijkl}) > 0 \tag{4.6a}$$

or

$$C_{1111}C_{2222}C_{3333} + 2C_{1122}C_{1133}C_{2233} - C_{2222}C_{1133}^2 - C_{1111}C_{2233}^2 - C_{3333}C_{1122}^2 > 0 \tag{4.6b}$$

It is obvious that elastic constants C_{ijkl} depend on the elastic modulus, shear modulus and Poisson's ratio. However, these material parameters are difficult to obtain by experimental investigation. The alternative choice is to evaluate these material parameters by a micro mechanics approach.

4.3 Micromechanical Behaviour of Composites

Fiber reinforced composite materials (FRC) are built from fibers and a resin matrix. Mechanical properties of FRC materials not only depend on properties fibers and resin used but also depend on the organization and the envelopment of fibers in the resin matrix. The interfacial bonding strength between fiber and resin is another factor that affects the strength of the composite. Filament wound composite pressure vessels maybe regarded as an assembly of unidirectional FRC are the focus of this work.

Currently, there are several models to describe and evaluate the properties of composites, as found from literature review. The rule of mixtures based on a simple one-dimensional model is the simplest. In terms of longitudinal modulus and in-plane Poisson's ratio the results match the experimental data very well and are written as follows.

$$E_1 = \varphi E_f + (1-\varphi)E_m \tag{4.7}$$

$$\nu_{12} = \varphi \nu_f + (1-\varphi)\nu_m \tag{4.8}$$

where: φ = Fiber volume fraction

The most advanced theory to evaluate the transverse modulus of the unidirectional laminates was derived by Hashin. The equations are complex, and some of material constants are difficult to establish. Highly sophisticated mathematical models are not useful when if the required data are not available. When Chamis's formula is compared with Hashin's theory, it is found that the results are similar, though Chamis's formula is very simple. Thus it is recommended to employ Chamis's formula for transverse elastic modulus as follows

$$E_{22} = \frac{E_m}{1-(1-\frac{E_m}{E_{22}{}^f})\sqrt{\varphi}} \tag{4.9}$$

where $E_{22}{}^f$ = Fiber transversal elastic modulus

For similar reasons, the shear modulus proposed by Chamis is also recommended

$$G_{12} = \frac{G_m}{1-(1-\frac{G_m}{G_{12}{}^f})\sqrt{\varphi}} \tag{4.10}$$

The in-plain Poisson's ratio ν_{21} can be derived by the reciprocity relationship

$$\nu_{21} = \frac{\nu_{12} E_{11}}{E_{22}} \tag{4.11}$$

The out of plane shear modulus transverse to the fiber direction G_{23} is proposed by Hashin with upper and lower bound values. Tsai also presented equations (4.6, 4.7) for G_{23} which agrees quite well with Hashin's upper bound and is relatively simple.

$$G_{23} = \frac{\varphi + \delta(1-\varphi)}{\frac{\varphi}{G_{23}{}^{f}} + \frac{\delta(1-\varphi)}{G_m}} \tag{4.12}$$

and

$$\delta = \frac{3 - 4\nu_m + \frac{G_m}{G_{23}{}^{f}}}{4(1-\nu_m)} \tag{4.13}$$

Equations (4 .1) to (4.13) are based on the assumption that both fiber and resin deform elastically and there are no voids within the resin. In fact void content has a significant effect on mechanical properties and is not discussed here.

4.4 Macromechanical Behaviour of A Lamina

4.4.1 Stress-Strain Relations for Plane Stress in An Orthotropic Material

For a unidirectionally reinforced lamina in the 1-2 plane as shown in Figure 2.1, a plane stress state is defined by setting

$$\sigma_3 = 0 \qquad \tau_{23} = 0 \qquad \tau_{31} = 0 \tag{4.14}$$

so that

$$\sigma_1 \neq 0 \qquad \sigma_2 \neq 0 \qquad \tau_{12} \neq 0 \tag{4.15}$$

Plane stress on a lamina is not merely an idealization of reality, but instead is a practical and achievable objective of how we must use a lamina with fibers in its plane. After all, the lamina cannot withstand high stresses in any direction other than that of the fibers, so why would we subject it to unnatural stresses such as σ_3? That is, we except to load a lamina *only* in plane stress because carrying in-plane stresses is its fundamental capability. A unidirectionally reinforced lamina would need 'help' carrying in-plane stress perpendicular to its fibers, but that help can be provided by

other (parallel) layers that have their fibers in the direction of the stress. Thus, a laminate is needed, but we concentrate on the characteristics of a lamina in this section.

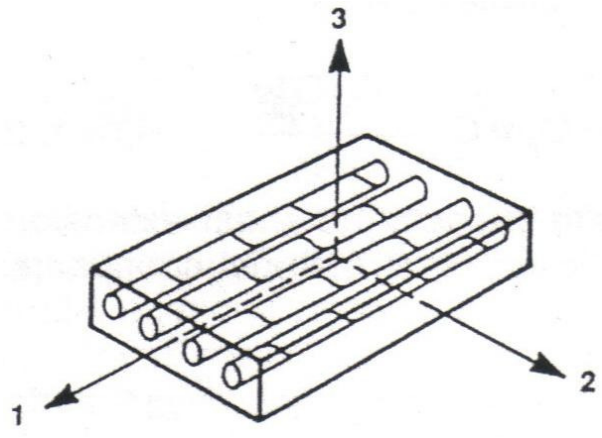

Figure 4.1 Unidirectionally reinforced lamina

For orthotropic materials, imposing a state of plane stress results in implied out-of-plane strains of

$$\varepsilon_3 = S_{13}\sigma_1 + S_{23}\,\sigma_2 \qquad \gamma_{23} = 0 \qquad \gamma_{31} = 0 \tag{4.16}$$

where

$$S_{13} = -\frac{\nu_{13}}{E_1} = -\frac{\nu_{31}}{E_3} \qquad S_{23} = -\frac{\nu_{23}}{E_2} = -\frac{\nu_{32}}{E_3} \tag{4.17}$$

Moreover, the strain-stress relations

$$\begin{bmatrix} \varepsilon_1 \\ \varepsilon_2 \\ \gamma_{12} \end{bmatrix} = \begin{bmatrix} S_{11} & S_{12} & 0 \\ S_{12} & S_{22} & 0 \\ 0 & 0 & S_{66} \end{bmatrix} \begin{bmatrix} \sigma_1 \\ \sigma_2 \\ \tau_{12} \end{bmatrix} \tag{4.18}$$

supplemented by Equation (4.16) where

$$S_{11}=\frac{1}{E_1} \qquad S_{12}=-\frac{\nu_{12}}{E_1}=-\frac{\nu_{21}}{E_2} \qquad S_{22}=\frac{1}{E_2} \qquad S_{66}=\frac{1}{G_{12}} \tag{4.19}$$

Note that in order to determinate ε_3 in Equation (4.16), ν_{13} and ν_{23} must be known in addition to the engineering constants in Equation (4.19). That is, ν_{13} and ν_{23} arise from S_{13} and S_{23} in Equation (4.16).

The strain-stress relations in Equation (4.18) can be inverted to obtain the stress-strain relations;

$$\begin{bmatrix}\sigma_1\\ \sigma_2\\ \tau_{12}\end{bmatrix}=\begin{bmatrix}Q_{11} & Q_{12} & 0\\ Q_{12} & Q_{22} & 0\\ 0 & 0 & Q_{66}\end{bmatrix}\begin{bmatrix}\varepsilon_1\\ \varepsilon_2\\ \gamma_{12}\end{bmatrix} \tag{4.20}$$

where the Q_{ij} are the so-called reduced stiffnesses for a plane stress state in the 1-2 plane which are determined either (1) as the components of the inverted compliance matrix in Equation (4.18) or (2) from the C_{ij} directly by applying the condition $\sigma_3 = 0$ to the strain-stress relations to get an expression for ε_3 and simplifying the results to get

$$Q_{ij}=C_{ij}-\frac{C_{i3}C_{j3}}{C_{33}} \qquad \text{i,j=1,2,6} \tag{4.21}$$

The term C_{63} is zero because no shear-extension coupling exists for an orthotropic lamina in principal material coordinates. For the orthotropic lamina, the Q_{ij} are

$$\begin{aligned} Q_{11}&=\frac{S_{22}}{S_{11}S_{22}-S_{12}^2} & Q_{22}&=\frac{S_{11}}{S_{11}S_{22}-S_{12}^2}\\ Q_{12}&=\frac{S_{12}}{S_{11}S_{22}-S_{12}^2} & Q_{66}&=\frac{1}{S_{66}}\end{aligned} \tag{4.22}$$

or, in terms of the engineering constants,

$$Q_{11} = \frac{E_1}{1-\nu_{12}\nu_{21}} \qquad Q_{22} = \frac{E_2}{1-\nu_{12}\nu_{21}}$$
$$Q_{12} = \frac{\nu_{12}E_2}{1-\nu_{12}\nu_{21}} = \frac{\nu_{21}E_1}{1-\nu_{12}\nu_{21}} \qquad Q_{66} = G_{12} \tag{4.23}$$

Note that there are four independent material properties; E_1, E_2, ν_{12} and G_{12}, in Equations (4.18) and (4.20) are considered in addition to the reciprocal relation

$$\frac{\nu_{12}}{E_1} = \frac{\nu_{21}}{E_2} \tag{4.24}$$

The preceding stress-strain and strain-stress relations are the basis for stiffness and stress analysis of an individual lamina subjected to forces in its own plane. Thus, the relations are indispensable in laminate analysis.

4.4.2 Stress-Strain Relations for a Lamina of Arbitrary Orientation

The stresses and strains were defined in the principal material coordinates for an orthotropic material. However, the principal directions of orthotropic materials often do not coincide with coordinate directions that are geometrically natural to the solution of the problem. For example, consider the helically wound fiber-reinforced circular cylindrical shell in Figure 2.2. There, the coordinates natural to the solution of the shell problem are the shell coordinates x', y', z'. The filament-winding angle is defined by cos(y', y) = cos α; also, z' = z. Other examples include laminated plates with different laminates at different orientations. Thus, a relation is needed between the stresses and strains in the principal material coordinates and those in the body coordinates. Then, a method of transforming stress-strain relations from one coordinate system to another is also needed.

At this point, we recall from elementary mechanics of materials the transformation equations for expressing stresses in a z-y coordinate system in terms of stresses in a 1-2 coordinate system,

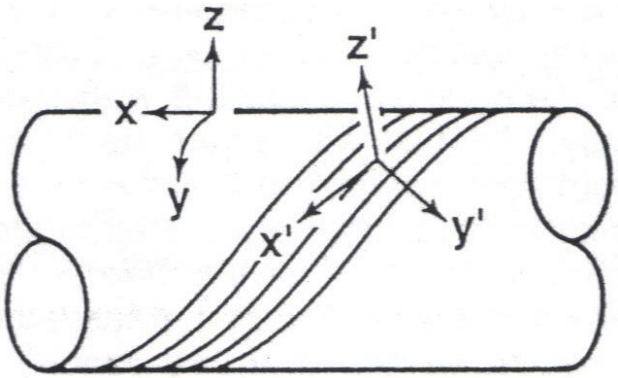

Figure 4.2 Helically wound fiber-reinforced circular cylindrical shell.

$$\begin{bmatrix} \sigma_x \\ \sigma_y \\ \tau_{xy} \end{bmatrix} = \begin{bmatrix} \cos^2\theta & \sin^2\theta & -2\sin\theta\cos\theta \\ \sin^2\theta & \cos^2\theta & 2\sin\theta\cos\theta \\ \sin\theta\cos\theta & -\sin\theta\cos\theta & \cos^2\theta - \sin^2\theta \end{bmatrix} \begin{bmatrix} \sigma_1 \\ \sigma_2 \\ \tau_{12} \end{bmatrix} \tag{4.25}$$

where θ is the angle *from* the z-axis to the 1-axis (see Figure 4.3). Note especially that the transformation has nothing to do with the material properties but is merely a rotation of stress directions. Also, the *direction* of rotation is crucial.

Similarly, the strain-transformation equations are

$$\begin{bmatrix} \varepsilon_x \\ \varepsilon_y \\ \frac{\gamma_{xy}}{2} \end{bmatrix} = \begin{bmatrix} \cos^2\theta & \sin^2\theta & -2\sin\theta\cos\theta \\ \sin^2\theta & \cos^2\theta & 2\sin\theta\cos\theta \\ \sin\theta\cos\theta & -\sin\theta\cos\theta & \cos^2\theta - \sin^2\theta \end{bmatrix} \begin{bmatrix} \varepsilon_1 \\ \varepsilon_2 \\ \frac{\gamma_{12}}{2} \end{bmatrix} \tag{4.26}$$

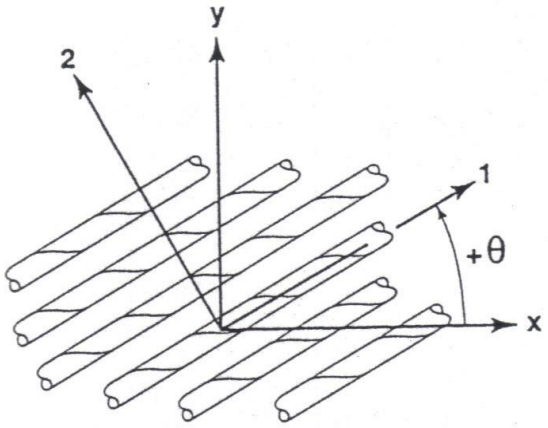

Figure 4.3 Positive rotation of principal material axes from x-y axes.

where we observe that strains do transform with the same transformation as stresses if the tensor definition of shear strain is used (which is equivalent to dividing the engineering shear strain by two).

The transformations are commonly written as

$$\begin{bmatrix} \sigma_x \\ \sigma_y \\ \tau_{xy} \end{bmatrix} = [T]^{-1} \begin{bmatrix} \sigma_1 \\ \sigma_2 \\ \tau_{12} \end{bmatrix} \tag{4.27}$$

$$\begin{bmatrix} \varepsilon_x \\ \varepsilon_y \\ \frac{\gamma_{xy}}{2} \end{bmatrix} = [T]^{-1} \begin{bmatrix} \varepsilon_1 \\ \varepsilon_2 \\ \frac{\gamma_{12}}{2} \end{bmatrix} \tag{4.28}$$

where the superscript -1 denotes the matrix inverse and

$$[T] = \begin{bmatrix} \cos^2\theta & \sin^2\theta & 2\sin\theta\cos\theta \\ \sin^2\theta & \cos^2\theta & -2\sin\theta\cos\theta \\ -\sin\theta\cos\theta & \sin\theta\cos\theta & \cos^2\theta - \sin^2\theta \end{bmatrix} \tag{4.29}$$

However, if the simplex matrix

$$[\mathrm{R}]=\begin{bmatrix}1 & 0 & 0\\ 0 & 1 & 0\\ 0 & 0 & 2\end{bmatrix} \tag{4.30}$$

due to Reuter is introduced, then the engineering strain vectors

$$\begin{bmatrix}\varepsilon_1\\ \varepsilon_2\\ \gamma_{12}\end{bmatrix}=[\mathrm{R}]\begin{bmatrix}\varepsilon_1\\ \varepsilon_2\\ \dfrac{\gamma_{12}}{2}\end{bmatrix} \tag{4.31}$$

$$\begin{bmatrix}\varepsilon_x\\ \varepsilon_y\\ \gamma_{xy}\end{bmatrix}=[\mathrm{R}]\begin{bmatrix}\varepsilon_x\\ \varepsilon_y\\ \dfrac{\gamma_{xy}}{2}\end{bmatrix} \tag{4.32}$$

can be used instead of the tensor strain vectors in the strain transformations as well as in stress-strain law transformations, the advantage of Reuter's transformation is that concise matrix notation can then be used. As a result, the ordinary expressions for stiffness and compliance matrices with awkward factors of 1/2 and 2 in various rows and columns are avoided.

A so-called *specially orthotropic lamina* is an orthotropic lamina whose principal material axes are aligned with the natural body axes:

$$\begin{bmatrix}\sigma_1\\ \sigma_2\\ \tau_{12}\end{bmatrix}=\begin{bmatrix}\sigma_x\\ \sigma_y\\ \tau_{xt}\end{bmatrix}=\begin{bmatrix}Q_{11} & Q_{12} & 0\\ Q_{12} & Q_{22} & 0\\ 0 & 0 & Q_{66}\end{bmatrix}\begin{bmatrix}\varepsilon_1\\ \varepsilon_2\\ \gamma_{12}\end{bmatrix} \tag{4.33}$$

where the principal material axes are shown in Figure 4.1. These stress-strain relations apply when the principal material directions of an orthotropic lamina are used as coordinates

However, as mentioned previously, orthotropic laminae are often constructed in such a manner that the principal material coordinates do not to be interpreted as

meaning that the principal material coordinates do not coincide with the natural coordinates of the body. This statement is not to be interpreted as meaning that the material itself is no longer orthotropic; instead, we are just looking at an orthotropic material in an unnatural manner, i.e., in a coordinate system that is oriented at some angle to the principal material coordinate system. Then, the basic question is: given the stress-strain relations in the principal material coordinates, what are the stress-strain relations in x-y coordinates?

Accordingly, we use the stress and strain transformations of Equations (4.27) and (4.28) along with Reuter's matrix, Equation (4.30), after abbreviating Equation (4.33) as

$$\begin{bmatrix} \sigma_1 \\ \sigma_2 \\ \tau_{12} \end{bmatrix} = [Q] \begin{bmatrix} \varepsilon_1 \\ \varepsilon_2 \\ \gamma_{12} \end{bmatrix} \tag{4.34}$$

to obtain

$$\begin{bmatrix} \sigma_x \\ \sigma_y \\ \tau_{xy} \end{bmatrix} = [T]^{-1} \begin{bmatrix} \sigma_1 \\ \sigma_2 \\ \tau_{12} \end{bmatrix} = [T]^{-1}[Q][R][T][R]^{-1} \begin{bmatrix} \varepsilon_x \\ \varepsilon_y \\ \gamma_{xy} \end{bmatrix} \tag{4.35}$$

However, [R] [T] $[R]^{-1}$ can be shown to be $[R]^{-T}$ where the superscript T denotes the matrix transpose. Then, if we use the abbreviation

$$\left[\overline{Q}\right] = [T]^{-1}[Q][T]^{-T} \tag{4.36}$$

the stress-strain relations in x-y coordinates are

$$\begin{bmatrix} \sigma_x \\ \sigma_y \\ \tau_{xy} \end{bmatrix} = \left[\overline{Q}\right] \begin{bmatrix} \varepsilon_x \\ \varepsilon_y \\ \gamma_{xy} \end{bmatrix} = \begin{bmatrix} \overline{Q}_{11} & \overline{Q}_{12} & \overline{Q}_{16} \\ \overline{Q}_{12} & \overline{Q}_{22} & \overline{Q}_{26} \\ \overline{Q}_{16} & \overline{Q}_{26} & \overline{Q}_{66} \end{bmatrix} \begin{bmatrix} \varepsilon_x \\ \varepsilon_y \\ \gamma_{xy} \end{bmatrix} \tag{4.37}$$

in which

$$
\begin{aligned}
\overline{Q}_{11} &= Q_{11}\cos^4\theta + 2(Q_{12}+2Q_{66})\sin^2\theta\cos^2\theta + Q_{22}\sin^4\theta \\
\overline{Q}_{12} &= (Q_{11}+Q_{12}-4Q_{66})\sin^2\theta\cos^2\theta + Q_{12}(\sin^4\theta+\cos^4\theta) \\
\overline{Q}_{22} &= Q_{11}\sin^4\theta + 2(Q_{12}+2Q_{66})\sin^2\theta\cos^2\theta + Q_{22}\cos^4\theta \\
\overline{Q}_{16} &= (Q_{11}-Q_{12}-2Q_{66})\sin\theta\cos^3\theta + (Q_{12}-Q_{22}+2Q_{66})\sin^3\theta\cos\theta \\
\overline{Q}_{26} &= (Q_{11}-Q_{12}-2Q_{66})\sin^3\theta\cos\theta + (Q_{12}-Q_{22}+2Q_{66})\sin\theta\cos^3\theta \\
\overline{Q}_{66} &= (Q_{11}+Q_{22}-2Q_{12}-2Q_{66})\sin^2\theta\cos^2\theta + Q_{66}(\sin^4\theta+\cos^4\theta)
\end{aligned}
\tag{4.38}
$$

where the bar over the $\overline{Q}_{ij}$ matrix denotes that we are dealing with the transformed reduced stiffnesses instead of the reduced stiffnesses, Q_{ij}.

Note that the transformed reduced stiffness matrix $\overline{Q}_{ij}$ has terms in all nine positions in contrast to the presence of zeros in the reduced stiffness matrix Q_{ij}. However, there are still only *four* independent material constants because the lamina is orthotropic. In the general case with body coordinates x and y, there is coupling between shear strain and normal stresses and between shear stress and normal strains, i.e., shear-extension coupling exists. Thus, in body coordinates, even an orthotropic lamina appears to be anisotropic. However, because such a lamina does have orthotropic characteristics in principal material coordinates, it is called a *generally orthotropic lamina* because it can be represented by the stress-strain relations in Equation (4.37). That is, a *generally orthotropic lamina* is an orthotropic lamina whose principal material axes are not aligned with the natural body axes.

The only advantage associated with generally orthotropic laminae as opposed to anisotropic laminae is that generally orthotropic laminae are easier to characterize experimentally. However, if we do not realize that principal material axes exist, then a generally orthotropic lamina is indistinguishable from an anisotropic lamina. That is we cannot take away the inherent orthotropic character of a lamina, but we can orient the lamina in such a manner so as to make that character quite difficult to recognize.

As an alternative to the foregoing procedure, we can express the strains in terms of the stresses in body coordinates by either (1) inversion of the stress-strain relations

in Equation (4.37) or (2) transformation of the strain-stress relations in principal material coordinates from Equation (4.18),

$$\begin{bmatrix} \varepsilon_1 \\ \varepsilon_2 \\ \gamma_{12} \end{bmatrix} = \begin{bmatrix} S_{11} & S_{12} & 0 \\ S_{12} & S_{22} & 0 \\ 0 & 0 & S_{66} \end{bmatrix} \begin{bmatrix} \sigma_1 \\ \sigma_2 \\ \tau_{12} \end{bmatrix} \tag{4.39}$$

to body coordinates. We choose the second approach and apply the transformations of Equations (4.27) and (4.28) along with Reuter's matrix, Equation (4.30), to obtain

$$\begin{bmatrix} \varepsilon_x \\ \varepsilon_y \\ \gamma_{xy} \end{bmatrix} = [T]^T [S][T] \begin{bmatrix} \sigma_x \\ \sigma_y \\ \tau_{xy} \end{bmatrix} = \begin{bmatrix} \overline{S}_{11} & \overline{S}_{12} & \overline{S}_{16} \\ \overline{S}_{12} & \overline{S}_{22} & \overline{S}_{26} \\ \overline{S}_{16} & \overline{S}_{26} & \overline{S}_{66} \end{bmatrix} \begin{bmatrix} \sigma_x \\ \sigma_y \\ \tau_{xy} \end{bmatrix} \tag{4.40}$$

where $[R]\,[T]^{-1}\,[R]^{-1}$ was found to be $[T]^{T}$ and

$$\begin{aligned}
\overline{S}_{11} &= S_{11}\cos^4\theta + (2S_{12} + S_{66})\sin^2\theta\cos^2\theta + S_{22}\sin^4\theta \\
\overline{S}_{12} &= S_{12}(\sin^4\theta + \cos^4\theta) + (S_{11} + S_{22} - S_{66})\sin^2\theta\cos^2\theta \\
\overline{S}_{22} &= S_{11}\sin^4\theta + (2S_{12} + S_{66})\sin^2\theta\cos^2\theta + S_{22}\cos^4\theta \\
\overline{S}_{16} &= (2S_{11} - 2S_{12} - S_{66})\sin\theta\cos^3\theta - (2S_{22} - 2S_{12} - S_{66})\sin^3\theta\cos\theta \\
\overline{S}_{26} &= (2S_{11} - 2S_{12} - S_{66})\sin^3\theta\cos\theta - (2S_{22} - 2S_{12} - S_{66})\sin\theta\cos^3\theta \\
\overline{S}_{66} &= 2(2S_{11} + 2S_{22} - 4S_{12} - S_{66})\sin^2\theta\cos^2\theta + S_{66}(\sin^4\theta + \cos^4\theta)
\end{aligned} \tag{4.41}$$

Recall that the S_{ij} are defined in terms of the engineering constants in Equation (4.19)

Because of the presence of Q_{16} and Q_{26} in Equation (4.37) and of S_{16} and S_{26} in Equation (4.40), the solution of problems involving so-called generally orthotropic laminae is more difficult than problems with so-called specially orthotropic laminae. That is, shear-extension coupling complicates the solution of practical problems. As a matter of fact, there is no difference between solutions for generally orthotropic laminae and those for anisotropic laminae whose stress-strain relations, under conditions of plane stress, can be written as

$$\begin{bmatrix}\sigma_1\\ \sigma_2\\ \tau_{12}\end{bmatrix}=\begin{bmatrix}Q_{11} & Q_{12} & 0\\ Q_{12} & Q_{22} & 0\\ 0 & 0 & Q_{66}\end{bmatrix}\begin{bmatrix}\varepsilon_1\\ \varepsilon_2\\ \gamma_{12}\end{bmatrix} \tag{4.42}$$

or in inverted form as

$$\begin{bmatrix}\varepsilon_1\\ \varepsilon_2\\ \gamma_{12}\end{bmatrix}=\begin{bmatrix}S_{11} & S_{12} & S_{16}\\ S_{12} & S_{22} & S_{26}\\ S_{16} & S_{26} & S_{66}\end{bmatrix}\begin{bmatrix}\sigma_1\\ \sigma_2\\ \tau_{12}\end{bmatrix} \tag{4.43}$$

where the anisotropic compliances in terms of the engineering constants are

$$\begin{aligned} S_{11} &= \frac{1}{E_1} & S_{12} &= \frac{1}{E_2} & S_{16} &= \frac{\eta_{12,1}}{E_1} = \frac{\eta_{1,12}}{G_{12}}\\ S_{12} &= -\frac{\nu_{12}}{E_1} = -\frac{\nu_{21}}{E_2} & S_{66} &= \frac{1}{G_{12}} & S_{26} &= \frac{\eta_{12,1}}{E_2} = \frac{\eta_{2,12}}{G_{12}} \end{aligned} \tag{4.44}$$

Note that some new engineering constants have been used. The new constants are called *coefficients of mutual influence* by Lekhnitskii [x] and are defined as

$\eta_{i,ij}$ = coefficient of mutual influence of the first kind that characterizes stretching in the i-direction caused by shear stress in the ij-plane

$$\eta_{i,ij} = \frac{\varepsilon_i}{\gamma_{ij}} \tag{4.45}$$

for $\tau_{ij} = \tau$ and all other stresses are zero.

$\eta_{ij,i}$ = coefficient of mutual influence of the second kind characterizing shearing in the ij-plane caused by normal stress in the i-direction

$$\eta_{ij,i} = \frac{\gamma_{ij}}{\varepsilon_i} \tag{4.46}$$

for $\sigma_{ij} = \sigma$ and all other stresses are zero.

Lekhnitskii defines the coefficients of mutual influence and the Poisson's ratios with subscripts that are reversed from the present notation. The coefficients of mutual influence are not named very effectively because the Poisson's ratios could also be called coefficients of mutual influence. Instead, the $\eta_{ij,i}$ and $\eta_{i,ij}$ are more appropriately called by the functional name shear-extension coupling coefficients.

Other anisotropic elasticity relations are used to define *Chentsov coefficients* that are to shearing strains what Poisson's ratios are to shearing stresses and shearing strains. However, the Chentsov coefficients do not affect the in-plane behaviour of laminae under plane stress. The Chentsov coefficients are defined as

$\mu_{ij,kl}$ = Chentsov coefficient that characterizes the shearing strain in the kl-plane due to shearing stress in the ij-plane, i.e.,

$$\mu_{ij,kl} = \frac{\gamma_{kl}}{\gamma_{ij}} \tag{4.47}$$

for $\tau_{ij} = \tau$ and all other stresses are zero.

The Chentsov coefficients are subject to the reciprocal relations

$$\frac{\mu_{kl,ij}}{G_{kl}} = \frac{\mu_{ij,kl}}{G_{ij}} \tag{4.48}$$

Note that the Chentsov coefficients are more effectively called the functional name of shear-shear coupling coefficients.

The out-of-plane shearing strains of an anisotropic lamina due to in-plane shearing stress and normal stresses are

$$\begin{aligned} \gamma_{13} &= \frac{\eta_{1,13}\sigma_1 + \eta_{2,13}\sigma_2 + \mu_{12,13}\tau_{12}}{G_{13}} \\ \gamma_{23} &= \frac{\eta_{1,13}\sigma_1 + \eta_{2,13}\sigma_2 + \mu_{12,13}\tau_{12}}{G_{23}} \end{aligned} \tag{4.49}$$

wherein both the shear-shear coupling coefficients and the shear-extension coupling coefficients are required. Note that neither of these shear strains arise in an orthotropic material unless it is stressed in coordinates other than the principal material coordinates. In such cases, the shear-shear coupling coefficients and the shear-extension coupling coefficients are obtained from the transformed compliances as in the following paragraph.

Compare the transformed orthotropic compliances in Equation (4.41) with the anisotropic compliances in terms of engineering constants in Equations (4.44). Obviously an *apparent* shear-extension coupling coefficient results when an orthotropic lamina is stressed in non-principal material coordinates. Redesignate the coordinates 1 and 2 in Equation (4.43) as x and y because, by definition, an anisotropic material has *no* principal material directions. Then, substitute the redesignated S_{ij} from Equation (4.44) in Equation (4.41) along with the orthotropic compliances in Equation (4.19). Finally, the apparent engineering constants for an orthotropic lamina that is stressed in non-principal x-y coordinates are

$$
\begin{aligned}
\frac{1}{E_x} &= \frac{1}{E_1}\cos^4\theta + \left[\frac{1}{G_{12}} + \frac{2\nu_{12}}{E_1}\right]\sin^2\theta\cos^2\theta + \frac{1}{E_2}\sin^4\theta \\
\nu_{xy} &= E_x\left[\frac{\nu_{12}}{E_1}(\sin^4\theta + \cos^4\theta) - \left[\frac{1}{E_1} + \frac{1}{E_2} - \frac{1}{G_{12}}\right]\sin^2\theta\cos^2\theta\right] \\
\frac{1}{E_y} &= \frac{1}{E_1}\sin^4\theta + \left[\frac{1}{G_{12}} - \frac{2\nu_{12}}{E_1}\right]\sin^2\theta\cos^2\theta + \frac{1}{E_2}\cos^4\theta \\
\frac{1}{G_{xy}} &= 2\left[\frac{2}{E_1} + \frac{2}{E_2} + \frac{4\nu_{12}}{E_1} - \frac{1}{G_{12}}\right]\sin^2\theta\cos^2\theta + \frac{1}{G_{12}}(\sin^4\theta\cos^4\theta) \\
\eta_{xy,x} &= E_x\left[\left[\frac{2}{E_1} + \frac{2\nu_{12}}{E_1} - \frac{1}{G_{12}}\right]\sin\theta\cos^3\theta - \left[\frac{2}{E_1} + \frac{2\nu_{12}}{E_1} - \frac{1}{G_{12}}\right]\sin^3\theta\cos\theta\right] \\
\eta_{xy,y} &= E_y\left[\left[\frac{2}{E_1} + \frac{2\nu_{12}}{E_1} - \frac{1}{G_{12}}\right]\sin^3\theta\cos\theta - \left[\frac{2}{E_2} + \frac{2\nu_{12}}{E_1} - \frac{1}{G_{12}}\right]\sin\theta\cos^3\theta\right]
\end{aligned}
\tag{4.50}
$$

4.5 Macromechanical Behaviour of a Laminate

4.5.1 Classical Lamination Theory

Classical lamination theory consists of a collection of mechanics-of-materials type of stress and deformation hypotheses that is re described in the section. By use of this theory, we can consistently proceed directly from the basic building block, the lamina, to the end result, a structural laminate. The whole process is one of finding effective and reasonably accurate simplifying assumptions that enable us to reduce our attention from a complicated three-dimensional elasticity problem to a solvable two-dimensional mechanics of deformable bodies problem.

Actually, because of the stress and deformation hypotheses that are an inseparable part of classical thin lamination theory, or even classical laminated plate theory. We will use the common term classical lamination theory, but recognize that it is a convenient oversimplification of the rigorous nomenclature. In the composite materials literature, classical lamination theory is often abbreviated as CLT.

First, the stress-strain behaviour of an individual lamina is reviewed in Section 4.5.2, and expressed in equation form for the k^{th} lamina of a laminate. Then, the variations of stress and strain through the thickness of the laminate are determined in Section 4.5.3. Finally, the relation of the laminate forces and moments to the strains and curvatures is founding Section 4.5.4 where the laminate stiffnesses are the link from the forces and moments to the strains and curvatures.

4.5.2 Lamina Stress-Strain Behaviour

The stress-strain relations in principal material coordinates for a lamina of an orthotropic material under plane stress are

$$\begin{bmatrix} \sigma_1 \\ \sigma_2 \\ \tau_{12} \end{bmatrix} = \begin{bmatrix} Q_{11} & Q_{12} & 0 \\ Q_{12} & Q_{22} & 0 \\ 0 & 0 & Q_{66} \end{bmatrix} \begin{bmatrix} \varepsilon_1 \\ \varepsilon_2 \\ \gamma_{12} \end{bmatrix} \tag{4.51}$$

The reduced stiffnesses, Q_{ij}, are defined in terms of the engineering constants in Equation (4.23). in any other coordinate system in the plane of the lamina, the stresses are

$$\begin{bmatrix} \sigma_x \\ \sigma_y \\ \tau_{xy} \end{bmatrix} = \begin{bmatrix} \overline{Q}_{11} & \overline{Q}_{12} & \overline{Q}_{16} \\ \overline{Q}_{12} & \overline{Q}_{22} & \overline{Q}_{26} \\ \overline{Q}_{16} & \overline{Q}_{26} & \overline{Q}_{66} \end{bmatrix} \begin{bmatrix} \varepsilon_x \\ \varepsilon_y \\ \gamma_{xy} \end{bmatrix} \tag{4.52}$$

where the transformed reduced stiffnesses, $\overline{Q}_{ij}$, are given in terms of the reduced stiffnesses, Q_{ij}, in Equation (4.38).

The stress-strain relations in arbitrary in-plane coordinates, namely Equation (4.52), are useful in the definition of the laminate stiffnesses because of the arbitrary orientation of the constituent laminae. Both Equations (4.51) and (4.52) can be thought of as stress-strain relations for the k^{th} layer of a multilayered laminate. Thus, Equation (4.52) can be written as

$$\{\sigma\}_k = \left[\overline{Q}\right]_k \{\varepsilon\}_k \tag{4.53}$$

We will proceed in the next section to define the strain, and stress variations through the thickness of a laminate will then be obtained in Section 4.5.4 by integrating the stress-strain relations for each layer, Equation (4.53), through the laminate thickness subject to the stress and strain variations determined in Section 4.5.3.

4.5.3 Strain and Stress Variation in a Laminate

Knowledge of the variation of stress and strain though the laminate thickness is essential to the definition of the extensional and bending stiffnesses of a laminate. The laminate is presumed to consist of perfectly bonded laminae. Moreover, the

bonds are presumed to be infinitesimally thin as well as non-shear-deformable. That is, the displacements are continuous across lamina boundaries so that no lamina can slip relative to another. Thus, the laminate acts as a single layer with very special properties that later we will see as a constitute a structural element.

Accordingly, if the laminate is thin, a line originally straight and perpendicular to the middle surface of the laminate, i.e., a normal to the middle surface, is assumed to remain straight and perpendicular to the middle surface when the laminate is deformed, e.g., bent, extended, contracted, sheared, or twisted. Requiring the normal to the middle surface to remain straight and normal under deformation is equivalent to ignoring the shearing strains in planes perpendicular to the middle surface, that is, $y_{xz} = y_{yz} = 0$ where z is the direction of the normal to the middle surface in Figure 4.4 (note that y_{xz} and y_{yz} are the angles that a deformed normal would make with the deformed middle surface.) In addition, the normals are presumed to have constant length so that the strain perpendicular to the middle surface is ignored as well, that is, $\varepsilon_z = 0$. The foregoing collection of assumptions of the behaviour of the single layer that represents the laminate, constitutes the familiar Kirchhoff hypothesis for plates and the Kirchhoff-Love hypothesis for shells (and is the two-dimensional analog of the ordinary one-dimensional beam theory assumption that plane sections, i.e., sections normal to the beam axis, remain plane after bending- thus, the physical justification of the collection of assumptions should be obvious). Note that no restriction has been made to flat laminates; the laminates can, in fact, be curved or shell like.

The implications of Kirchhoff hypothesis on the laminate displacements u, v, and w in the x-, y-, and z-directions are derived by use of the laminate cross section in the x-z plane shown in Figure 4.4. The displacement in the x-direction of point B from the undeformed middle surface to the deformed middle surface is u_0 (the symbol 'nought' (^{o}) is used to designate middle-surface values of variable). Because line ABCD remains straight under deformations of the laminate, the displacement at point C is

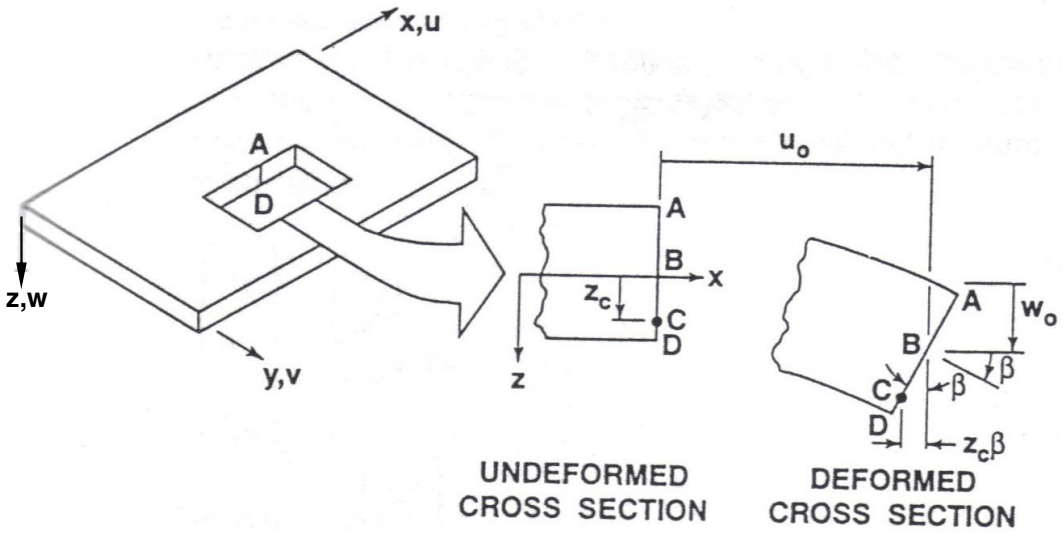

Figure 4.4 Geometry of Deformation in the x-z plane

$$U_C = U_0 - Z_C\beta \tag{4.54}$$

But because, under deformation, line ABCD further remains perpendicular to the middle surface, ß is the slope of the laminate middle surface in the x-direction, that is,

$$\beta = \frac{\partial w_0}{\partial x} \tag{4.55}$$

Then, the displacement, u, at any point z through the laminate thickness is

$$u = u_o - z = \frac{\partial w_0}{\partial x} \tag{4.56}$$

By similar reasoning, the displacement, v, in the y-direction is

$$v = v_o - z = \frac{\partial w_0}{\partial y} \tag{4.57}$$

The laminate strains have been reduced to ε_x, ε_y, and γ_{xy} by virtue of the Kirchhoff hypothesis. That is $\varepsilon_z = \gamma_{xz} = \gamma_{yz} = 0$ for small strains (linear elasticity), the remaining strains are defined in terms of displacements as

$$\begin{aligned} \varepsilon_x &= \frac{\partial u}{\partial x} \\ \varepsilon_y &= \frac{\partial v}{\partial y} \\ \gamma_{xy} &= \frac{\partial u}{\partial y} + \frac{\partial v}{\partial x} \end{aligned} \tag{4.58}$$

Thus, for the derived displacements u and v in Equations (4.56) and (4.57), the strains are

$$\begin{aligned} \varepsilon_x &= \frac{\partial u_0}{\partial x} - \frac{\partial^2 w_0}{\partial x^2} \\ \varepsilon_y &= \frac{\partial v_0}{\partial y} - z\frac{\partial^2 w_0}{\partial y^2} \\ \gamma_{xy} &= \frac{\partial u_0}{\partial y} + \frac{\partial v_0}{\partial x} - 2z\frac{\partial^2 w_0}{\partial x \partial y} \end{aligned} \tag{4.59}$$

or

$$\begin{bmatrix} \varepsilon_x \\ \varepsilon_y \\ \gamma_{xy} \end{bmatrix} = \begin{bmatrix} \varepsilon_x{}^0 \\ \varepsilon_y{}^0 \\ \varepsilon_{xy}{}^0 \end{bmatrix} + z\begin{bmatrix} k_x \\ k_y \\ k_{xy} \end{bmatrix} \tag{4.60}$$

where the middle-surface strains are

$$\begin{bmatrix} \varepsilon_x{}^0 \\ \varepsilon_y{}^0 \\ \gamma_{xy}{}^0 \end{bmatrix} = \begin{bmatrix} \dfrac{\partial u_0}{\partial x} \\ \dfrac{\partial v_0}{\partial y} \\ \dfrac{\partial u_0}{\partial y} + \dfrac{\partial v_0}{\partial x} \end{bmatrix} \tag{4.61}$$

and the middle-surface curvatures are

$$\begin{bmatrix} k_x \\ k_y \\ k_{xy} \end{bmatrix} = -\begin{bmatrix} \dfrac{\partial^2 w_0}{\partial x^2} \\ \dfrac{\partial^2 w_0}{\partial y^2} \\ 2\dfrac{\partial^2 w_0}{\partial x \partial y} \end{bmatrix} \tag{4.62}$$

(The last term in Equation (4.62) is the twist curvature of the middle surface.) We refer only to curvatures of the middle surface as a reference surface and not of any other surface, so nought superscripts are not needed on k_x, k_y, and k_{xy}. Thus, the Kirchhoff hypothesis has been readily verified to imply a linear variation of strain through the laminate thickness because the strains in Equation (4.60) have the form of a straight line, i.e., y = mx + b. The foregoing strain analysis is valid only for plates because of the strain-displacement relations in Equation (4.58). For circular cylindrical shells, the ε_y term in Equation (4.58) must be supplemented by w_0/r where r is the shell radius; other shells have more complicated strain-displacement relations.

By substitution of the strain variation through the thickness, Equation (4.60), in the stress-strain relation, Equation (4.53), the stresses in the k^{th} layer can be expressed in terms of the laminate middle-surface strains and curvature as

$$\begin{bmatrix} \sigma_x \\ \sigma_y \\ \tau_{xy} \end{bmatrix} = \begin{bmatrix} \overline{Q}_{11} & \overline{Q}_{12} & \overline{Q}_{16} \\ \overline{Q}_{12} & \overline{Q}_{22} & \overline{Q}_{26} \\ \overline{Q}_{16} & \overline{Q}_{26} & \overline{Q}_{66} \end{bmatrix}_k \begin{bmatrix} \varepsilon_x^0 \\ \varepsilon_y^0 \\ \gamma_{xy}^0 \end{bmatrix} + \begin{bmatrix} k_x \\ k_y \\ k_{xy} \end{bmatrix} \tag{4.63}$$

The $\overline{Q}_{ij}$ can be different for each layer of the laminate, so the stress variation through the strain variation is linear. Instead, typical strain and stress variations are shown in Figure 4.5 where the stresses are piecewise linear (i.e., linear in each layer, but discontinuous at boundaries between laminae).

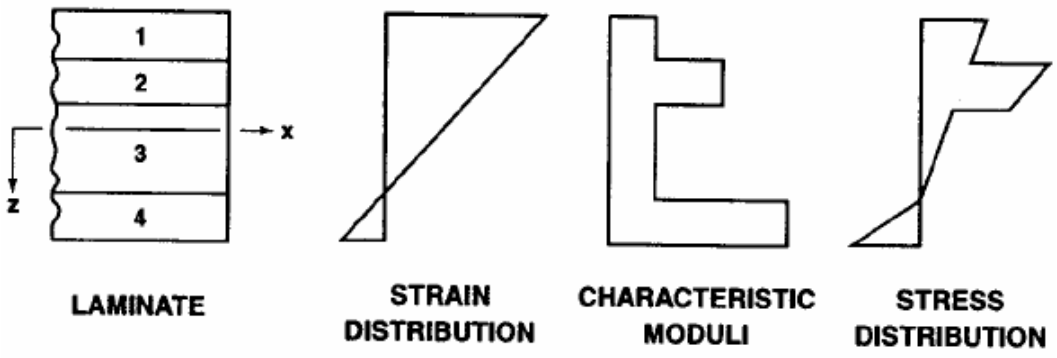

Figure 4.5 Hypothetical variations of strain and stress through the laminate thickness.

4.5.4 Resultant Laminate Forces and Moments

The resultant forces and moments acting on a laminate are obtained by integration of the stresses in each layer or lamina through the laminate thickness, for example,

$$N_x = \int_{-t/2}^{t/2} \sigma_x dz \qquad M_x = \int_{-t/2}^{t/2} \sigma_x z dz \tag{4.64}$$

Note that in Figure 4.5, the stresses vary within each lamina as well as from lamina to lamina, so the integration is not trivial. Actually N_x is a force per unit width of the cross section of the laminate as shown in Figure 4.6.

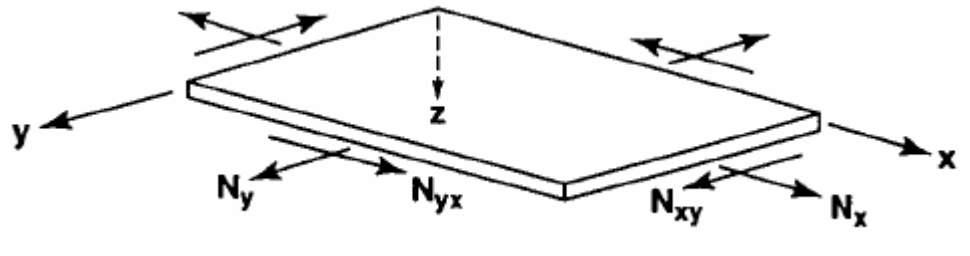

Figure 4.6 In-plane forces on a flat laminate.

Similarly, M_x is a moment per unit width as shown in Figure 4.7. However, N_x, etc., and M_x, etc., will be referred to as forces and moments with the stipulation of 'per

unit width' being dropped for convenience. The entire collection of force and moment resultants for an N-layered laminate is depicted in Figure 4.6 and 4.7 and is defined as

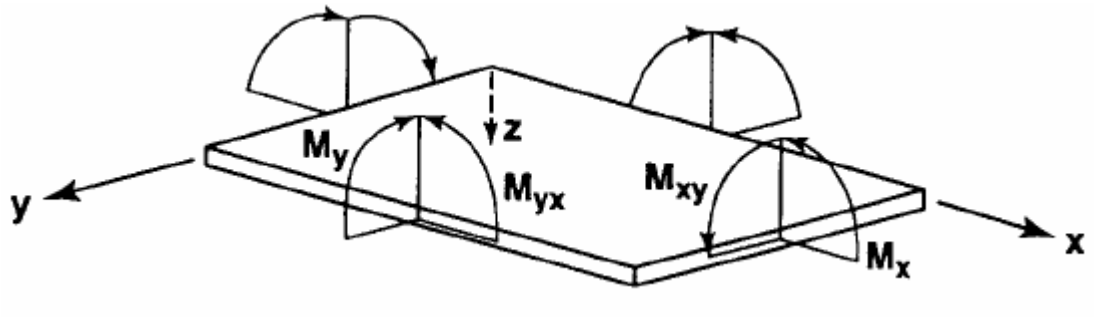

Figure 4.7 Moments on a flat laminate.

$$\begin{bmatrix} N_x \\ N_y \\ N_{xy} \end{bmatrix} = \int_{-t/2}^{t/2} \begin{bmatrix} \sigma_x \\ \sigma_y \\ \tau_{xy} \end{bmatrix} dz = \sum_{k=1}^{N} \int_{z_{k-1}}^{z_k} \begin{bmatrix} \sigma_x \\ \sigma_y \\ \tau_{xy} \end{bmatrix} dz \tag{4.65}$$

and

$$\begin{bmatrix} M_x \\ M_y \\ M_{xy} \end{bmatrix} = \int_{-t/2}^{t/2} \begin{bmatrix} \sigma_x \\ \sigma_y \\ \tau_{xy} \end{bmatrix} z\, dz = \sum_{k=1}^{N} \int_{z_{k-1}}^{z_k} \begin{bmatrix} \sigma_x \\ \sigma_y \\ \tau_{xy} \end{bmatrix} z\, dz \tag{4.66}$$

where z_k and z_{k-1} are defined in the basic laminate geometry of Figure 4.8. Note that the z_i's are directed distances (coordinates) in accordance with the convention that z_i is positive downward. That is, z_k is the directed distance to the bottom of the k^{th} layer, and z_{k-1} is the directed distance to the top of the k^{th} layer. Moreover, $z_0 = -t/2$ $z_1 = -t/2 + t_1$, etc., whereas $z_N = +t/2$, $z_{N-1} = +t/2 - t_N$ etc. These force and moment resultants do not depend on z after integration, but are functions of x and y, the coordinates in the plane of the laminate middle surface.

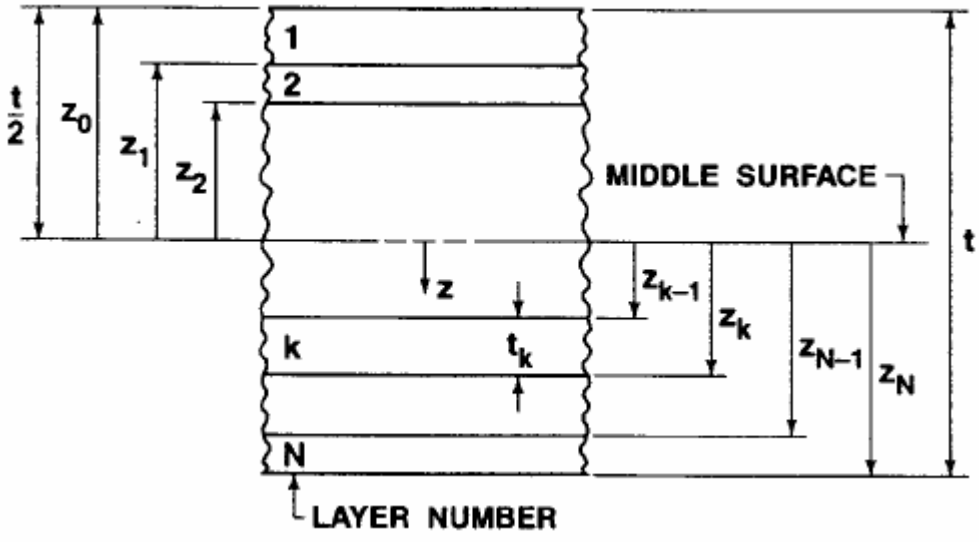

Figure 4.8 Geometry of an N-layered laminate.

Equations (4.65) and (4.66) can be rearranged to take advantage of the fact that the stiffness matrix for a lamina is often constant within the lamina (unless the lamina has temperature-dependent or moisture-dependent properties and a temperature gradient or a moisture gradient exists across the lamina). If the elevated temperature or moisture is constant through the thickness of the lamina (a 'soaked' condition), then the values of $[\overline{Q}_{ij}]_k$ are constant in the layer but probably degraded because of the temperature and/or moisture. Thus, the stiffness matrix goes outside the integration over each layer, but is within the summation of force and moment resultant for each layer. When the lamina stress-strain relations, Equation (4.63), become;

$$\begin{bmatrix} N_x \\ N_y \\ N_{xy} \end{bmatrix} = \sum_{k=1}^{N} \begin{bmatrix} \overline{Q}_{11} & \overline{Q}_{12} & \overline{Q}_{16} \\ \overline{Q}_{12} & \overline{Q}_{22} & \overline{Q}_{26} \\ \overline{Q}_{16} & \overline{Q}_{26} & \overline{Q}_{66} \end{bmatrix}_k \left[\int_{z_{k-1}}^{z_k} \begin{bmatrix} \varepsilon_x^0 \\ \varepsilon_y^0 \\ \gamma_x^0 \end{bmatrix} dz + \int_{z_{k-1}}^{z_k} \begin{bmatrix} k_x \\ k_y \\ k_{xy} \end{bmatrix} z\, dz \right] \tag{4.67}$$

$$\begin{bmatrix} M_x \\ M_y \\ M_{xy} \end{bmatrix} = \sum_{k=1}^{N} \begin{bmatrix} \overline{Q}_{11} & \overline{Q}_{12} & \overline{Q}_{16} \\ \overline{Q}_{12} & \overline{Q}_{22} & \overline{Q}_{26} \\ \overline{Q}_{16} & \overline{Q}_{26} & \overline{Q}_{66} \end{bmatrix}_k \left[\int_{z_{k-1}}^{z_k} \begin{bmatrix} \varepsilon_x^0 \\ \varepsilon_y^0 \\ \gamma_x^0 \end{bmatrix} z\, dz + \int_{z_{k-1}}^{z_k} \begin{bmatrix} k_x \\ k_y \\ k_{xy} \end{bmatrix} z^2 dz \right] \tag{4.68}$$

Sometimes the stiffness matrix for a lamina, $\left[\overline{Q}_{ij}\right]_k$, is not constant through the thickness of the lamina. For example, if a temperature gradient or moisture gradient exists in the lamina and the lamina material properties are temperature dependent and/or moisture dependent, then $\left[\overline{Q}_{ij}\right]_k$ is a function of z and must be left inside the integral. In such cases, the laminate is nonhomogeneous within each layer, so a more complicated numerical solution is required then the one addressed here.

We should now recall that ε_x^0, ε_y^0, γ_{xy}^0, k_x, k_y, and k_{xy} are not functions of z, but are middle-surface values so they can be removed from within the summation signs. Thus, Equations (4.67) and (4.68) can be written as

$$\begin{bmatrix} N_x \\ N_y \\ N_{xy} \end{bmatrix} = \begin{bmatrix} A_{11} & A_{12} & A_{16} \\ A_{12} & A_{22} & A_{26} \\ A_{16} & A_{26} & A_{66} \end{bmatrix} \begin{bmatrix} \varepsilon_x^0 \\ \varepsilon_y^0 \\ \gamma_x^0 \end{bmatrix} + \begin{bmatrix} B_{11} & B_{12} & B_{16} \\ B_{12} & B_{22} & B_{26} \\ B_{16} & B_{26} & B_{66} \end{bmatrix} \begin{bmatrix} k_x \\ k_y \\ k_{xy} \end{bmatrix} \tag{4.69}$$

$$\begin{bmatrix} M_x \\ M_y \\ M_{xy} \end{bmatrix} = \begin{bmatrix} B_{11} & B_{12} & B_{16} \\ B_{12} & B_{22} & B_{26} \\ B_{16} & B_{26} & B_{66} \end{bmatrix} \begin{bmatrix} \varepsilon_x^0 \\ \varepsilon_y^0 \\ \gamma_x^0 \end{bmatrix} + \begin{bmatrix} D_{11} & D_{12} & D_{16} \\ D_{12} & D_{22} & D_{26} \\ D_{16} & D_{26} & D_{66} \end{bmatrix} \begin{bmatrix} k_x \\ k_y \\ k_{xy} \end{bmatrix} \tag{4.70}$$

where

$$\begin{aligned} A_{ij} &= \sum_{k=1}^{N} (\overline{Q}_{ij})_k (z_k - z_{k-1}) \\ B_{ij} &= \frac{1}{2} \sum_{k=1}^{N} (\overline{Q}_{ij})_k (z_k^2 - z_{k-1}^2) \\ D_{ij} &= \frac{1}{3} \sum_{k=1}^{N} (\overline{Q}_{ij})_k (z_k^3 - z_{k-1}^3) \end{aligned} \tag{4.71}$$

CHAPTER FIVE

NUMERICAL STUDY

5.1 Overview of Pressure Vessels

5.1.1 Introduction

Vessels, tanks, and pipelines that carry, store, or receive fluids are called pressure vessels. A pressure vessel is defined as a container with a pressure differential between inside and outside. The inside pressure is usually higher than the outside, except for some isolated situations. The fluid inside the vessel may undergo a change in state as in the case of steam boilers, or may combine with other reagents as in the case of a chemical reactor. Pressure vessels often have a combination of high pressures together with high temperatures, and in some cases flammable fluids or highly radio- active materials. Because of such hazards it is imperative that the design be such that no leakage can occur. In addition these vessels have to be designed carefully to cope with the operating temperatures and pressures. It should be borne in mind that the rupture of a pressure vessel has a potential to cause extensive physical injury and property damage. Plant safety and integrity are of fundamental concern in pressure vessel design and these of course depend on the adequacy of design codes.

When discussing pressure vessels we must also consider tanks. Pressure vessels and tanks are significantly different in both design and construction: tanks, unlike pressure vessels, are limited to atmospheric pressure; and pressure vessels often have internals while most tanks do not (and those that do are limited to heating coils or mixers).

Pressure vessels are used in a number of industries; for example, the power generation industry for fossil and nuclear power, the petrochemical industry for storing and processing crude petroleum oil in tank farms as well as storing gasoline in service stations, and the chemical industry (in chemical reactors) to

name but a few. Their use has expanded throughout the world. Pressure vessels and tanks are, in fact, essential to the chemical, petroleum, petrochemical and nuclear industries. It is in this class of equipment that the reactions, separations, and storage of raw materials occur. Generally speaking, pressurized equipment is required for a wide range of industrial plant for storage and manufacturing purposes.

The size and geometric form of pressure vessels vary greatly from the large cylindrical vessels used for high-pressure gas storage to the small size used as hydraulic units for aircraft. Some are buried in the ground or deep in the ocean, but most are positioned on ground or supported in platforms. Pressure vessels are usually spherical or cylindrical, with domed ends. The cylindrical vessels are generally preferred, since they present simpler manufacturing problems and make better use of the available space. Boiler drums, heat exchangers, chemical reactors, and so on, are generally cylindrical. Spherical vessels have the advantage of requiring thinner walls for a given pressure and diameter than the equivalent cylinder. Therefore they are used for large gas or liquid containers, gas-cooled nuclear reactors, containment buildings for nuclear plant, and so on. Containment vessels for liquids at very low pressures are sometimes in the form of lobed spheroids or in the shape of a drop. This has the advantage of providing the best possible stress distribution when the tank is full.

5.2 Design of Pressure Vessels

5.2.1 Thin-shell Equations

A shell is a curved plate-type structure. Here, the discussions are limited to the shells of revolutions. Referring to Figure 5.1 this is denoted by an angle φ, the meridional radius r_1 and the conical radius r_2, from the centre line. The horizontal radius when the axis is vertical is r.

If the shell thickness is t, with z being the coordinate across the thickness, following the convention of Flugge, we have the following stress resultants:

$$N_\theta = \int_{-t/2}^{t/2} \sigma_\theta \left(\frac{r_1 + z}{r_1}\right) dz \tag{5.1}$$

$$N_\phi = \int_{-t/2}^{t/2} \sigma_\phi \left(\frac{r_2 + z}{r_2}\right) dz \tag{5.2}$$

$$N_{\theta\varphi} = \int_{-t/2}^{t/2} \sigma_{\theta\varphi} \left(\frac{r_2 + z}{r_2}\right) dz \tag{5.3}$$

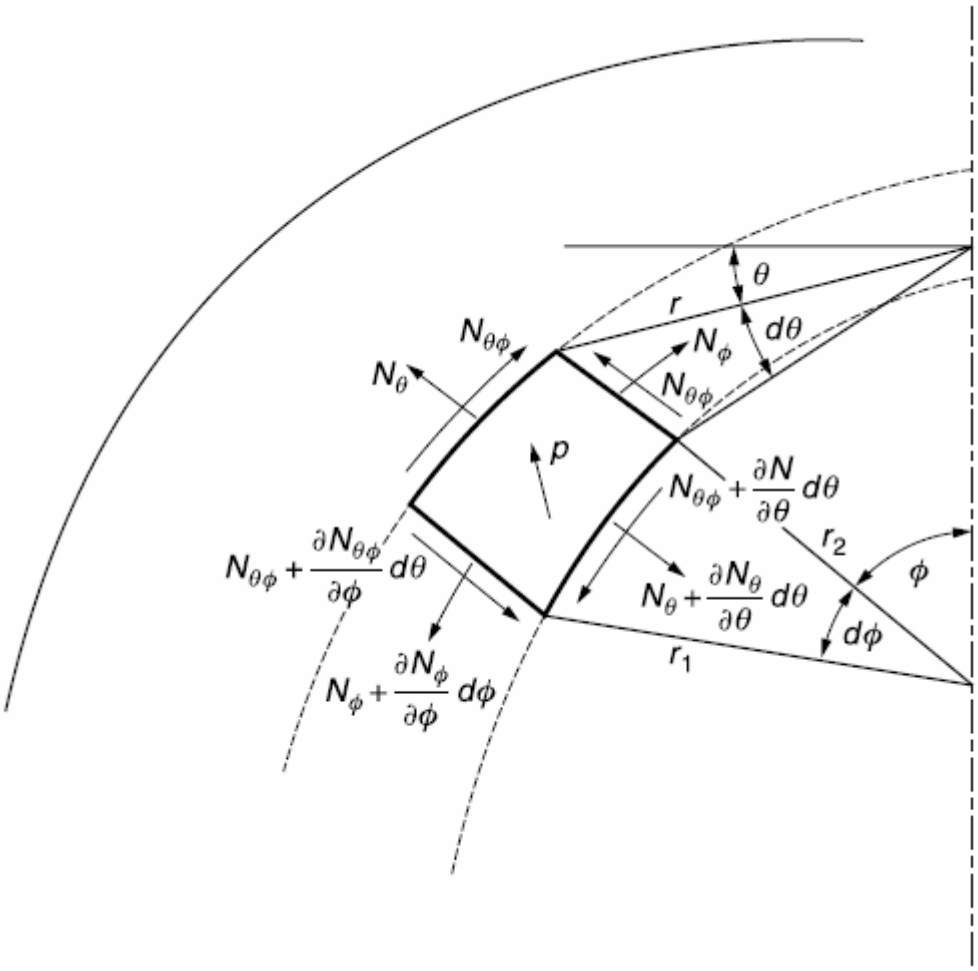

Figure 5.1 Thin shell of revolution.

$$N_{\varphi\theta} = \int_{-t/2}^{t/2} \sigma_{\theta\varphi} \left(\frac{r_1 + z}{r_1}\right) dz \tag{5.4}$$

These stress resultants are assumed to be due only to an internal pressure, p, acting in the direction of r. For membrane shells where the effects of bending can be ignored, all the moments are zero and further development leads to

$$N_{\theta\varphi}=N_{\varphi\theta} \tag{5.5}$$

The following equations result from considering force equilibrium along with the additional requirement of rotational symmetry:

$$\frac{d(rN_{\phi})}{d\phi}-r_1 N_{\theta}\cos\phi=0 \tag{5.6}$$

$$N_{\theta}=pr_2-\frac{r_2}{r_1}N_{\phi} \tag{5.7}$$

Noting that $r=r_2\sin\phi$, by solving Equations (5.6) and (5.7), we have

$$N_{\phi}=\frac{pr_2}{2} \tag{5.8}$$

$$N_{\theta}=pr_2\left(2-\frac{r_2}{r_1}\right) \tag{5.9}$$

The above two equations are the results for a general shell of revolution. Two specific cases result:

1. For a spherical shell of radius R, $r_1=r_2=R$, which gives

$$N_{\theta}=N_{\phi}=\frac{pR}{2} \tag{5.10}$$

2. For a cylindrical pressure vessel of radius R, we have $r_1=\infty$, $r_2=R$, which gives

$$N_{\phi}=\frac{pR}{2} \tag{5.11}$$

$$N_\theta = pR \tag{5.12}$$

This gives the hoop stress

$$\sigma_{hoop} = \sigma_\theta = \frac{N_\theta}{t} = \frac{pR}{t} \tag{5.13}$$

and the longitudinal stress

$$\sigma_{long} = \sigma_\phi = \frac{N_\phi}{t} = \frac{pR}{2t} \tag{5.14}$$

These results will be shown to be identical to the results that follow. Let us consider a long thin cylindrical shell of radius R and thickness t, subject to an internal pressure p. By thin shells we mean the ones having the ratio R/t typically greater than about 10. If the ends of the cylindrical shell are closed, there will be stresses in the hoop as well as the axial (longitudinal) directions.

A section of such a shell is shown in Figure 5.2. The hoop (circumferential) stress, σ_{hoop} and the longitudinal stress, σ_{long} are indicated in the figure. The shell is assumed to be long and thin resulting in σ_{hoop} and σ_{long} to be uniform through the thickness. Therefore in this case σ_{hoop} and σ_{long} are also referred to as membrane stress (there are no bending stresses associated with this type of loading).

Considering equilibrium across the cut section, we have,

$$pL(2R) = 2\sigma_{hoop}tL$$

which gives

$$\sigma_{hoop} = \frac{pR}{t} \tag{5.15}$$

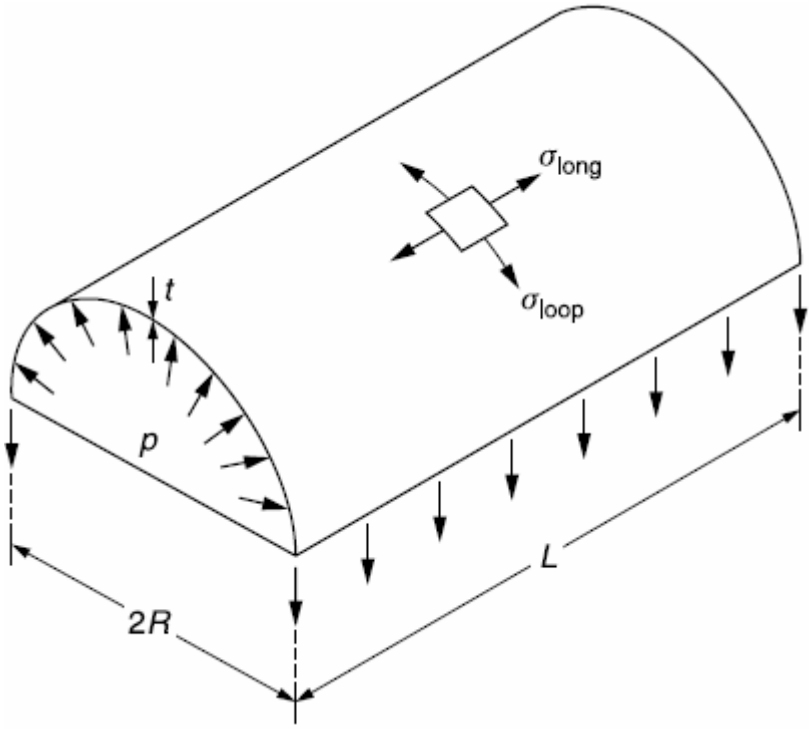

Figure 5.2 Thin cylindrical shell.

Considering a cross-section of the shell perpendicular to its axis, we have

$$p\pi r^2 = \sigma_{long}(2\pi Rt)$$

which gives

$$\sigma_{long} = \frac{pR}{2t} \tag{5.16}$$

5.2.2 Thick-shell Equations

For R/t ratios typically less than 10, Equations (5.15) and (5.16) tend not to be accurate, and thick-shell equations have to be used.

Consider a thick cylindrical shell of inside radius R_i and outside radius R_o subjected to an internal pressure p as shown in Figure 5.3.

The stress function for this case is given as a function of radius r as

$$\phi = A \ln r + Br^2 \tag{5.17}$$

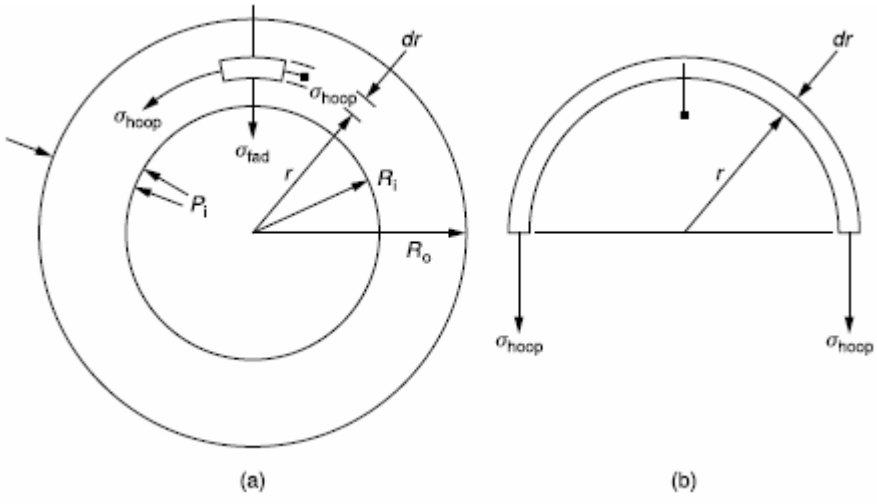

Figure 5.3 Thick cylindrical shell.

with A and B to be determined by the boundary conditions.

If we indicate the radial stress as σ_{rad} and the hoop and longitudinal stress as indicated previously by σ_{hoop} and σ_{long}, we have

$$\sigma_{rad} = \frac{1}{r}\frac{d\phi}{dr} = \frac{A}{r^2} + 2B \tag{5.18}$$

$$\sigma_{hoop} = \frac{d^2\phi}{dr^2} = -\frac{A}{r^2} + 2B \tag{5.19}$$

The constants A and B are determined from the following boundary conditions:

$$\sigma_{rad} = -p \quad \text{at} \quad r=R_i,$$
$$\sigma_{rad} = 0 \quad \text{at} \quad r=R_0 \tag{5.20}$$

Substituting (5.20) into (5.18) and (5.19), we have

$$A = -\frac{R_i^2 R_0^2 p}{(R_0^2 - R_i^2)}$$

$$B = \frac{R_i^2 p}{2(R_0^2 - R_i^2)} \tag{5.21}$$

Denoting the ratio of the outside to inside radii as m, so that $m = R_0/R_i$, we obtain the radial and hoop stresses

$$\sigma_{rad} = \frac{p}{(m^2 - 1)}\left[1 - \frac{R_0^2}{r^2}\right] \tag{5.22}$$

$$\sigma_{hoop} = \frac{p}{(m^2 - 1)}\left[1 + \frac{R_0^2}{r^2}\right] \tag{5.23}$$

Figure 5.4 shows the radial and hoop stress distributions.

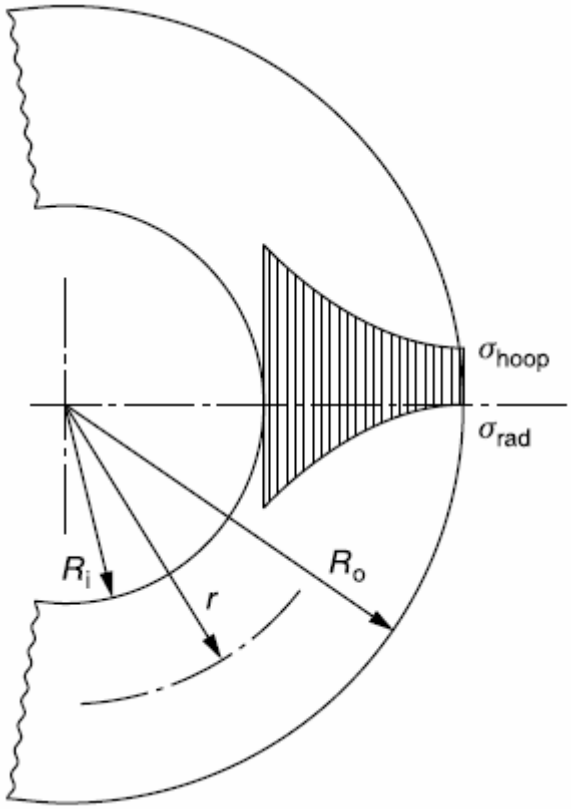

Figure 5.4 Hoop and radial stress distribution.

The longitudinal stress, σ_{long} is determined by considering the equilibrium of forces across a plane normal to the axis of the shell, which gives

$$p\pi R_i^2 = \sigma_{long}\pi(R_0^2 - R_i^2) \tag{5.24}$$

This is of course based on the assumption that the longitudinal stress is a form of membrane stress in that there is no variation across the thickness of the shell. Thus we have

$$\sigma_{long} = \frac{pR_i^2}{(R_0^2 - R_i^2)} = \frac{p}{(m^2 - 1)} \tag{5.25}$$

It should be noted however that the solutions indicated by Equations (5.22), (5.23), and (5.25) are valid for regions remote from discontinuities.

5.3 Stress Analysis of Composite Pressure Vessels

Properties of composite materials, as well as properties of all structural materials are affected by environmental and operational conditions. Moreover, for polymeric composites this influence is more pronounced than for conventional metal alloys because polymers are more sensitive to temperature, moisture, and time than metals. There exists also a specific feature of composites associated with the fact that they do not exist apart from composite structures and are formed while these structures are fabricated. As a result, material characteristics depend on the type and parameters of the manufacturing process, e.g., unidirectional composites made by pultrusion, hand lay-up, and filament winding can demonstrate different properties.

This section of the research is concerned with the effect of environmental, with hygrothermal loading on mechanical properties and behaviour of composites. A general hygrothermal stress analysis is presented in the multi-layered thin or thick composite cylinders for the axially symmetric case under

uniform temperature distributions. The solution is carried out for closed end conditions. The stacking sequences are chosen as $[45^o/-45^o]_s$, $[55^o/-55^o]_s$, $[60^o/-60^o]_s$, $[75^o/-75^o]_s$ and $[88^o/-88^o]_s$ for both symmetric and antisymmetric orientations.

5.3.1 Internal Pressure with Hygrothermal Loading

A composite pressure vessel is shown in figure 5.5. r, θ, z are the radial, tangential and axial directions. The solution is based on the Lekhnitkii's theory. In this theory, it is assumed that a body in the form of a hollow circular cylinder with an axis of anisotropy coincides with the geometrical axis of the cylinder.

$$\begin{Bmatrix} \varepsilon_r \\ \varepsilon_\theta \\ \varepsilon_z \\ \gamma_{\theta z} \\ \gamma_{\theta r} \\ \gamma_{r\theta} \end{Bmatrix} = \begin{bmatrix} a_{11} & a_{12} & a_{13} & a_{14} & a_{15} & a_{16} \\ a_{21} & a_{22} & a_{23} & a_{24} & a_{25} & a_{26} \\ a_{31} & a_{32} & a_{33} & a_{34} & a_{35} & a_{36} \\ a_{41} & a_{42} & a_{43} & a_{44} & a_{45} & a_{46} \\ a_{51} & a_{52} & a_{53} & a_{54} & a_{55} & a_{56} \\ a_{61} & a_{62} & a_{63} & a_{64} & a_{65} & a_{66} \end{bmatrix} \begin{Bmatrix} \sigma_r \\ \sigma_\theta \\ \sigma_z \\ \tau_{\theta z} \\ \tau_{\theta r} \\ \tau_{r\theta} \end{Bmatrix} \tag{5.26}$$

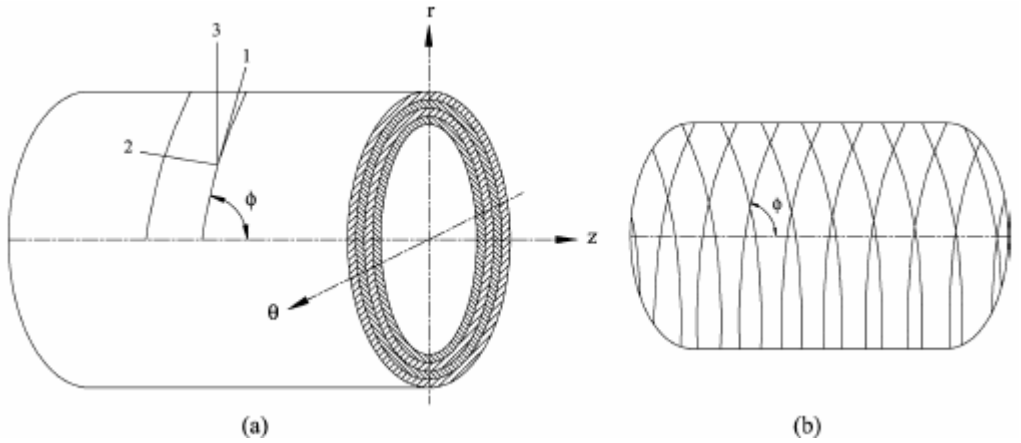

Figure 5.5 Multilayerd E-glass/epoxy cylinder (a) and pressure vessel (b)

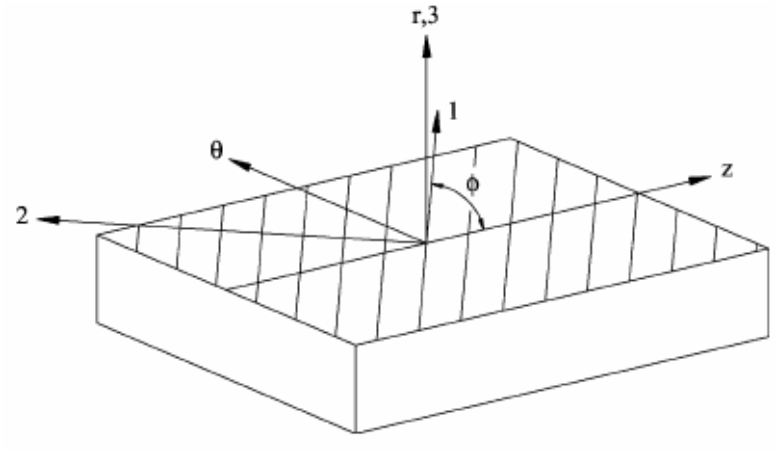

Figure 5.6 Principal material directions.

For an axially symmetric case, the shear stresses $\tau_{r\theta}$ and τ_{rz} are equal to zero. $\tau_{\theta z}$ also equals to zero because there is no twisting moment applied to the cylinder. The stress-strain relation for the axially symmetric case, figure 5.6, can be written in terms of the compliance matrix;

$$\begin{aligned}
\varepsilon_r &= a_{rr}\sigma_r + a_{r\theta}\sigma_\theta + a_{rz}\sigma_z + \alpha_r T + \beta_r c \\
\varepsilon_\theta &= a_{r\theta}\sigma_r + a_{\theta\theta}\sigma_\theta + a_{\theta z}\sigma_z + \alpha_\theta T + \beta_\theta c \\
\varepsilon_z &= a_{rz}\sigma_r + a_{\theta z}\sigma_\theta + a_{zz}\sigma_z + \alpha_z T + \beta_z c
\end{aligned} \tag{5.27}$$

where $\alpha_r, \alpha_\theta, \alpha_z$ are the thermal expansion coefficients and $\beta_r, \beta_\theta, \beta_z$ and c are hygroscopic expansion coefficients and moisture concentration.

The hygrothermal stresses are obtained by using a parameter, C

$$\varepsilon_z = a_{rz}\sigma_r + a_{\theta z}\sigma_\theta + a_{zz}\sigma_z + \alpha_z T + \beta_z c = C$$

$$\sigma_z = \frac{C}{a_{zz}} - \frac{a_{rz}}{a_{zz}}\sigma_r - \frac{a_{\theta z}}{a_{zz}}\sigma_\theta - \frac{\alpha_z}{a_{zz}}T - \frac{\beta_z}{a_{zz}}c \tag{5.28}$$

When σ_z is substituted into relations, ε_r and ε_θ becomes,

$$\varepsilon_r = \frac{\partial u}{\partial r} = \beta_{rr}\sigma_r + \beta_{r\theta}\sigma_\theta + \bar{\alpha}_r T + \bar{\beta}_r c + a_{rz}\frac{C}{a_{zz}},$$
$$\varepsilon_\theta = \frac{1}{r}\frac{\partial v}{\partial \theta} + \frac{u}{r} = \beta_{r\theta}\sigma_r + \beta_{\theta\theta}\sigma_\theta + \bar{\alpha}_\theta T + \bar{\beta}_\theta c + a_{\theta z}\frac{C}{a_{zz}} \quad (5.29)$$

where

$$\beta_{rr} = a_{rr} - \frac{a_{rz}^2}{a_{zz}}, \quad \beta_{r\theta} = a_{r\theta} - \frac{a_{\theta z}a_{rz}}{a_{zz}}, \quad \beta_{\theta\theta} = a_{\theta\theta} - \frac{a_{\theta z}^2}{a_{zz}},$$
$$\bar{a}_r = \alpha_r - \frac{a_z a_{rz}}{a_{zz}}, \quad \bar{\beta}_r = \beta_r - \frac{\beta_z a_{rz}}{a_{zz}}, \quad \beta_d = \frac{a_{rz} - a_{\theta z}}{a_{zz}} \quad (5.30)$$
$$\bar{a}_\theta = \alpha_\theta - \frac{a_z a_{\theta z}}{a_{zz}}, \quad \bar{\beta}_\theta = \beta_\theta - \frac{\beta_z a_{\theta z}}{a_{zz}}, \quad \beta_{d0} = \frac{\beta_d}{\beta_{\theta\theta}}$$

β, coefficient of hygroscopic expansion

c, moisture concentration

A stress function (F) under the Lekhnitskii's theory can be written as

$$\sigma_r = \frac{1}{r}\frac{\partial F}{\partial r} + \frac{1}{r^2}\frac{\partial^2 F}{\partial_\theta^{\,2}} = \frac{1}{r}\frac{dF}{dr}, \quad \sigma_\theta = \frac{d^2F}{dr^2} \quad (5.31)$$

Writing $\varepsilon_r = du/dr$ and $\varepsilon_\theta = u/r$ for an axially symmetric case gives the compatibility equation. By differentiating

$u = r\varepsilon_\theta$ with respect to r, the compatibility equation is obtained as follows,

$$\frac{du}{dr} = \varepsilon_\theta + r\frac{d\varepsilon_\theta}{dr}$$

then,

$$\varepsilon_r = \varepsilon_\theta + r\frac{d\varepsilon_\theta}{dr} \quad (5.32)$$

When the compatibility equation is used between ε_r and ε_θ, an ordinary differential equation is obtained for the stress function F as,

$$r^3\beta_{\theta\theta}\frac{d^3F}{dr^3}+r^2\beta_{\theta\theta}\frac{d^2F}{dr^2}-r\beta_{rr}\frac{dF}{dr}=Tr^2(\bar{\alpha}_r-\bar{\alpha}_\theta)+cr^2(\bar{\beta}_r-\bar{\beta}_\theta)-\bar{\alpha}_\theta r^3\frac{dT}{dr}+Cr^2\beta_d \quad (5.33)$$

$$r^3\frac{d^3F}{dr^3}+r^2\frac{d^2F}{dr^2}-rk^2\frac{dF}{dr}=Tr^2\alpha_1'+cr^2\beta_1'-\bar{\alpha}_\theta r^3\frac{dT}{dr}+Cr^2\beta_d \quad (5.34)$$

where $\dfrac{\beta_{rr}}{\beta_{\theta\theta}}=k^2,\ (\bar{\alpha}_r-\bar{\alpha}_\theta)=\alpha_1',\ (\bar{\beta}_r-\bar{\beta}_\theta)=\beta_1'$

The equation (5.34) is solved by using the transformation of $F=r^\alpha$. Uniform temperature distributions is chosen in the solution and we have

$$\frac{dT}{dr}=\alpha r^{\alpha-1},\ \frac{d^2F}{dr^2}=\alpha(\alpha-1)r^{\alpha-2},\ \frac{d^3F}{dr^3}=\alpha(\alpha-1)(\alpha-2)r^{\alpha-3} \quad (5.35)$$

Putting (5.35) into equation (5.34), we get characteristic equation

$$\begin{aligned} &r^\alpha\alpha(\alpha-1)(\alpha-2)+r^\alpha\alpha(\alpha-1)-r^\alpha k^2\alpha=0\\ &r^\alpha[\alpha(\alpha-1)(\alpha-2)+\alpha(\alpha-1)-k^2\alpha]=0 \end{aligned} \quad (5.36)$$

Here $r^\alpha\neq 0,\quad k^2\neq 0$ and

$$\begin{aligned} &\alpha[(\alpha-1)(\alpha-2)+(\alpha-1)-k^2]=0\\ &\alpha(\alpha^2-2\alpha+1-k^2)=0 \end{aligned} \quad (5.37)$$

Roots of (5.37) are found as;

$$\begin{aligned} &\alpha_1=0\\ &\alpha_2=1+k\\ &\alpha_3=1-k \end{aligned} \quad (5.38)$$

So we get homogeneous solution of differential problem

$$\begin{aligned} F_h &= C_0 r^{\alpha 1} + C_1 r^{\alpha 2} + C_2 r^{\alpha 1} \\ F_h &= C_0 + C_1 r^{1+k} + C_2 r^{1-k} \end{aligned} \tag{5.39}$$

We must have private solution (F_p) for exact solution of F function.

$$F = F_p + F_h \tag{5.40}$$

$$F_p = Ar^3 + Br^2 + Cr + D \tag{5.41}$$

Derivatives of equation (5.41)

$$\begin{aligned} F_p' &= 3Ar^2 + 2Br + C \\ F_p'' &= 6Ar + 2B \\ F_p''' &= 6A \end{aligned} \tag{5.42}$$

Putting (5.42) into (5.34) we have

$$\begin{aligned} r^3(12A - 3Ak^2) + r^2(2B - 2Bk^2) + r(-Ck^2) &= Tr^2\alpha_1' + cr^2\beta_1' - \bar{\alpha}_\theta r^3 \frac{dT}{dr} + Cr^2\beta_d \\ r^3(12A - 3Ak^2) + r^2(2B - 2Bk^2) + r(-Ck^2) &= r^3(\bar{\alpha}_\theta \frac{dT}{dr}) + r^2(T\alpha_1' + cr\beta_1' + C\beta_d) \end{aligned} \tag{5.43}$$

where $T' = \frac{dT}{dr} = 0$ (uniform temperature distribution) and unknown parameters are found

$$\begin{aligned} A &= 0 \\ C &= 0 \\ B &= \frac{T\alpha_1' + cr\beta_1' + C\beta_d}{2(1-k^2)} \end{aligned} \tag{5.44}$$

Putting (5.44) into equation (5.41) we will have private solution

$$F_p = \frac{T\alpha_1' + cr\beta_1' + C\beta_d}{2(1-k^2)} r^2 \tag{5.45}$$

Putting equations (5.45) and (5.39) into equation (5.40), the stress function F is obtained.

$$F = C_0 + C_1 r^{1+k} + C_2 r^{1-k} + \frac{T\alpha_1' + cr\beta_1' + C\beta_d}{2(1-k^2)} r^2 \tag{5.46}$$

The stress components are obtained as,

$$\begin{aligned}
\sigma_r &= \frac{1}{r}\frac{dF}{dr} = (1+k)C_1 r^{k-1} + (1-k)C_2 r^{-k-1} + \frac{T\alpha_1' + cr\beta_1' + C\beta_d}{(1-k^2)}, \\
\sigma_\theta &= \frac{d^2F}{dr^2} = k(1+k)C_1 r^{k-1} - k(1-k)C_2 r^{-k-1} + \frac{T\alpha_1' + cr\beta_1' + C\beta_d}{(1-k^2)}, \\
\sigma_z &= -\frac{C}{a_{zz}} - \frac{a_{rz} + ka_{\theta z}}{a_{zz}}(1+k)C_1 r^{k-1} + \frac{-a_{rz} + ka_{\theta z}}{a_{zz}}(1-k)C_2 r^{-k-1} \\
&\quad - 2A\frac{a_{rz} + a_{\theta z}}{a_{zz}} - \frac{\alpha_z}{a_{zz}}T_0 - \frac{\beta_z}{a_{zz}}c
\end{aligned} \tag{5.47}$$

Radial displacement,

$$\begin{aligned}
u &= (\beta_{r\theta} + k\beta_{\theta\theta})(1+k)C_1 r^k + (\beta_{r\theta} - k\beta_{\theta\theta})(1-k)r^{-k} \\
&\quad + 2(\beta_{r\theta} + \beta_{\theta\theta})Ar + \bar{\alpha}_\theta T_0 r + \bar{\beta}_\theta cr + \frac{a_{\theta z}}{a_{zz}}Cr
\end{aligned} \tag{5.48}$$

The integration constants obtained in this solution for each layer are C_1 and C_2. If the number of layers and plastic liner is *n,* the total number of the unknown integration constants is 2xn.

They are calculated by using the boundary conditions. If the vessel subjected to internal pressure at the inner surface, is free at the outer surface, the boundarry conditions are written as,

$\sigma_r = -p$ at the inner surface, $r = a$

$\sigma_r = 0$ at the outer surface, $r = b$ (5.49)

where a and b are the inner and outer radii of the composite vessel. However, the number of boundary conditions that can be written is $(2\times n)-2$. The radial stress (σ_r) and radial displacement (u) are in the direction of the normal of layers. They must be equal in neighboring layers, to ensure continuity of the layers. As a results of this, the radial stresses and displacements are written to be equal in neighboring layers as the following;

$(\sigma_r)_{i-1} = (\sigma_r)_i$

$(u)_{i-1} = (u)_i$ (5.50)

where i stands for the number of layer considered. Thus, $(2\times n)-2$ more relations can be written and then all integration constants can be calculated. In this solution, they are written in matrix form. The unknown constants are obtained by using Lordan method.

The resultant of σ_z at any cross section is equal to the total axial force at the ends of the vessel. That is,

$$P_z = \pi\alpha^2 p = \int_{r=a}^{b} 2\pi r\sigma_z dr \quad (5.51)$$

where p is the internal pressure. The parameter D can be found by using the previous Eq. (5.43). Iteration methots are used in order to calculate D, then all the stress components are obtained.

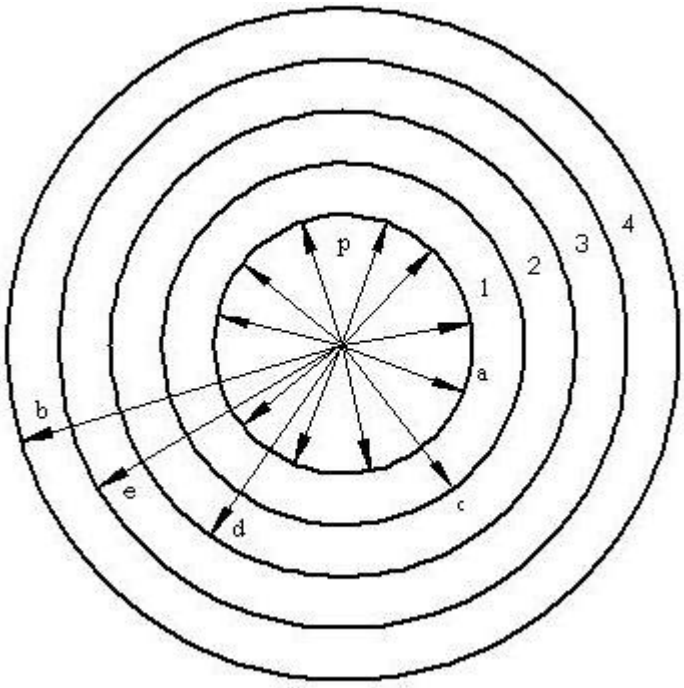

Figure 5.7 A composite cylinder with four layers.

5.4 Failure Analysis

A lamina is assumed to be homogeneous and the mechanical behaviour is characterized by a set of equivalent or effective moduli and strength properties. These properties can be obtained either by a micro-mechanics approach or by a phenomenological approach. In the micro-mechanics approach, the lamina properties are predicted in terms of the constituent (fiber, matrix) properties by using a mathematical model; in the phenomenological approach, the lamina properties are determined experimentally by conducting tests on a single lamina or a laminate. In this research, lamina properties were determined by a phenomenological approach (Section 6.2).

Once the mechanical properties of the ply are known, the initial failure of the ply within a laminate or structure can be predicted by applying an appropriate failure criterion. Failure types are dependent on loading, stacking sequence, and specimen geometry. There are many proposed theories to predict the one-set of failures. Most

of failure criterias are based on the stress state in a lamina. Hence, an accurate kinematic model of the laminate is necessary to determine three-dimensional stress/strain fields. Ideally speaking, a 3-D or layerwise model is desirable. The failure criteria, for example, the quadratic polynomial criteria consists of parameters that must be experimentally determined. Often, these parameters are difficult to determine with certainty.

To analyze the strength of any laminated composite, strength theories are required. Failure analysis is a tool for predicting the strength of a laminated composite, containing several plies with different orientations, under complex loading conditions using strength data obtained from uniaxial tests of unidirectional plies and strength theories. There are numerous failure criteria for composite materials as a direct result of the complex nature of observed failure phenomena. These criteria are only useful if they can be incorporated into a progressive damage analysis, which usually means that they must be compatible with a finite element formulation.

Different types of failure criteria have been used for failure design of composite laminates. In general, the failure criterias are categorized into two: independent and interactive (or quadratic polynomial) criteria. An independent criterion, such as maximum stress or maximum strain, is simple to apply and more significantly, tells the mode of failure, but it neglects the effect of stress interactions. For this reason, these criteria are quite conservative. An interactive criterion, such as Tsai-Wu, Tsai-Hill, Hoffmann includes stress interactions in the failure mechanism and predicts first ply failure but it requires some efforts to determine parameters.

The first-ply failure analysis of the laminated composite pressure vessel is performed via the use of a suitable failure criterion. Determination of first-ply failure pressure loads of laminated pressure vessels based on Tsai-Wu failure criteria has been used.

5.4.1 Tsai-Wu Failure Theory

Under plane stress conditions, the Tsai-Wu failure theory predicts failure in an orthotropic lamina if and when the following equality is satisfied:

$$F_1\sigma_{11} + F_2\sigma_{22} + F_6\tau_{12} + F_{11}\sigma_{11}^2 + F_{22}\sigma_{22}^2 + F_{66}\tau_{12}^2 + 2F_{12}\sigma_{11}\sigma_{22} = 1 \qquad (5.52)$$

We consider the plane stress condition of a general orthotropic lamina containing unidirectional fibers at a fiber orientation angle of θ with respect to the x axis, Figure 5.8. Four independent elastic constants, namely, E_{11}, E_{22}, G_{12}, and ν_{12} are required to define its elastic characteristics. Its strength properties are characterized by five independent strength properties:

X_t = longitudinal tensile strength
Y_t = transverse tensile strength
X_c = longitudinal compressive strength
Y_c = transverse compressive strength
S = in-plane (interlaminar) shear strength

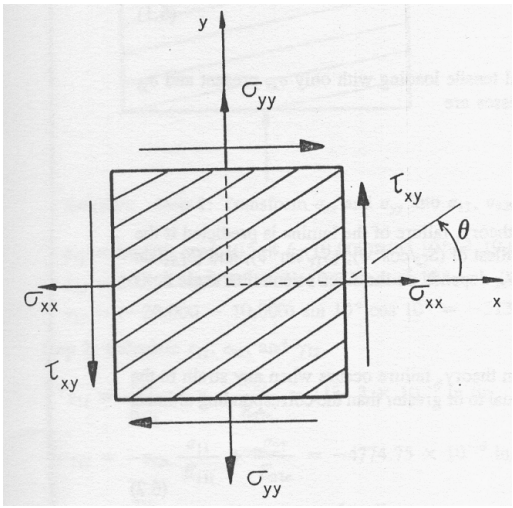

Figure 5.8 General stress states in a thin orthotropic lamina.

Where F_1, F_2, and so on are called the strength coefficients and are given by,

$$F_1 = \frac{1}{X_t} - \frac{1}{X_c} \qquad F_2 = \frac{1}{Y_t} - \frac{1}{Y_c} \qquad F_6 = 0$$

$$F_{11} = -\frac{1}{X_t X_c} \qquad F_{22} = -\frac{1}{Y_t Y_c} \qquad F_{66} = -\frac{1}{S^2}$$

and F_{12} is a strength interaction term between σ_{11} and σ_{22}. Note that F_1, F_2, F_{11}, F_{22} and F_{66} can be calculated using the tensile, compressive, and shear strength properties in the principal material directions. Determination of F_{12} requires a suitable biaxial test. For a simple example, consider an equal biaxial tension test in which $\sigma_{11} = \sigma_{22} = \sigma$ at failure. Using Eq. (5.52), we can write

$$(F_1 + F_2)\sigma + (F_{11} + F_{22} + 2F_{12})\sigma^2 = 1$$

from which

$$F_{12} = \frac{1}{2\sigma^2}\left[1 - \left(\frac{1}{X_t} + \frac{1}{X_c} + \frac{1}{Y_t} + \frac{1}{Y_c}\right)\sigma + \left(\frac{1}{X_t X_c} + \frac{1}{Y_t Y_c}\right)\sigma^2\right]$$

since reliable biaxial tests are not always easy to perform, an approximate range of values for F_{12} has been recommended,

$$-\frac{1}{2}(F_{11}F_{22})^{1/2} \le F_{12} \le 0 \tag{5.53}$$

In absence of experimental data, the lower limit of Eq. (5.53) is frequently used for F_{12}.

5.5 Finite Element Approach

In this chapter, by using Ansys 10.0 finite element analysis software, a static failure analysis was performed on an element of a composite pressure vessel in Figure 5.10.

According to thin-walled assumptions the stress of the pressure vessel subjected to internal pressure p can be given as

$$\sigma_{hoop} = \frac{pR}{t}$$
$$\sigma_{long} = \frac{pR}{2t} \qquad (5.54)$$

Equation (5.54) was mentioned in section (5.2.1).

In addition, parametric studies have been performed using various orientation angles. The first failure pressure was studied on this solution method.

5.5.1 Three-Dimensional Finite Element Method

In the three-dimensional finite element formulation, the displacements, traction components, and distributed body force values are the functions of the position coordinates indicated by (x, y, z). The displacement vector u is given as

$$u = [u, v, w]^T \qquad (5.55)$$

where *u, v* and *w* are *x, y* and *z* components of u, respectively. The stress and strains are given

$$\sigma = [\sigma_{xx}, \sigma_{yy}, \sigma_{zz}, \sigma_{yz}, \sigma_{xz}, \sigma_{xy}]^T$$

$$\varepsilon = \left[\varepsilon_{xx}, \varepsilon_{yy}, \varepsilon_{zz}, \gamma_{yz}, \gamma_{xz}, \gamma_{xy}\right]^T \tag{5.56}$$

From Figure 5.9, representing the three-dimensional problem in a general setting, the body force and traction vector are given by

$$f = \left[f_x, f_y, f_x\right]^T, \qquad T = \left[T_x, T_y, T_x\right]^T \tag{5.57}$$

The body force f has dimensions of force per unit volume, while the traction force T has dimensions of force per unit area.

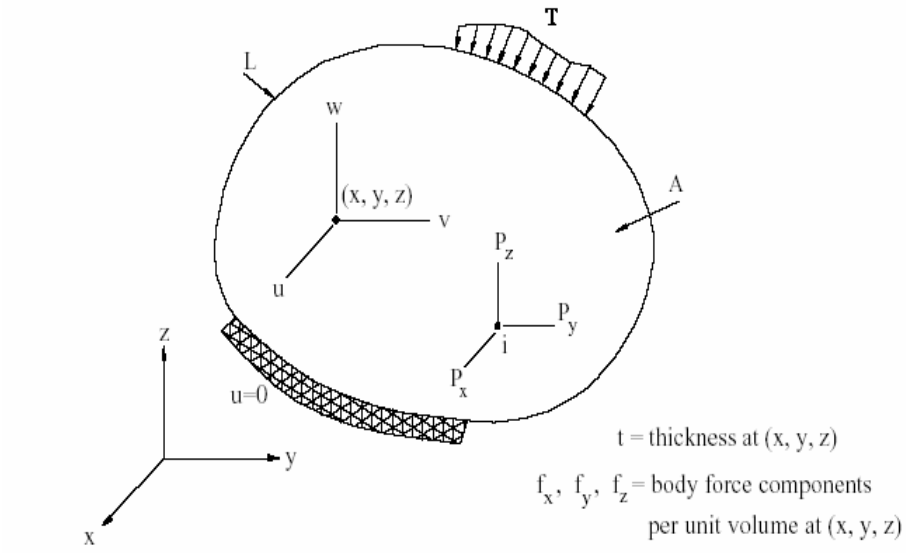

Figure 5.9 Three-dimensional problem.

5.5.2 Modelling of the Pressure Vessel

In this study, maximum failure pressure value was found by finite element analysis using Ansys. In order to modeling the problem, a small element was taken from on the boundary surface of pressure vessel which is shown in Figure 5.10. This element was modeled using Ansys and some operations were done respectively as explained below.

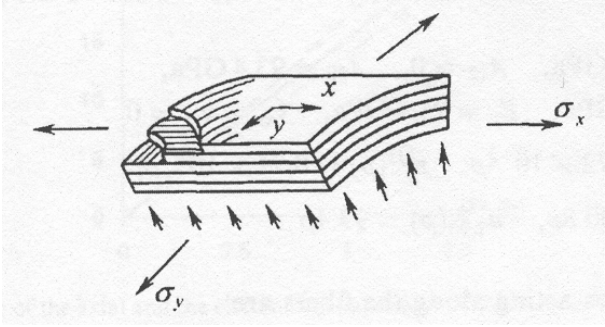

Figure 5.10 Element of a composite pressure vessel.

First element type was defined with solid layered 46 in Figure 5.11. Solid46 is a layered version of the 8-node structural solid element designed to model layered thick shells or solids. The element allows up to 250 different material layers. The element may also be stacked as an alternative approach. The element has three degrees of freedom at each node: translations in the nodal x, y, and z directions.

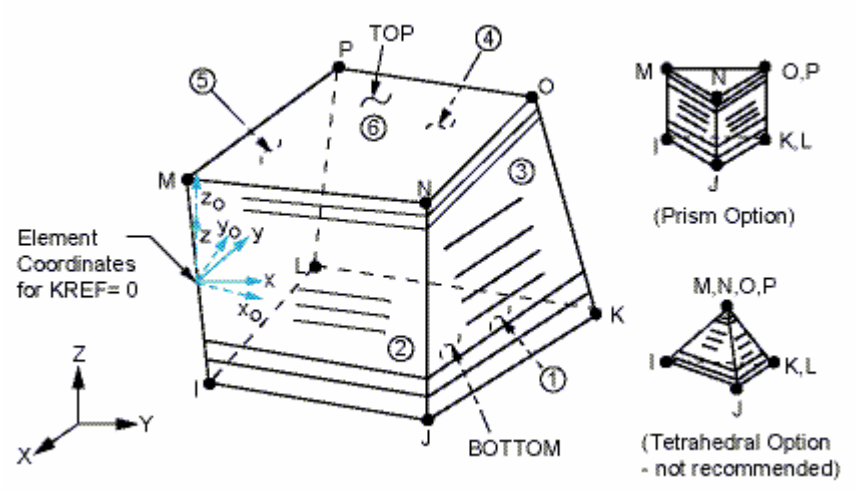

Figure 5.11 SOLID46 geometry.

Real constant sets were defined for 4 layers, various orientation angles and each layers thickness was entered 0.45 mm., Figure 5.12.

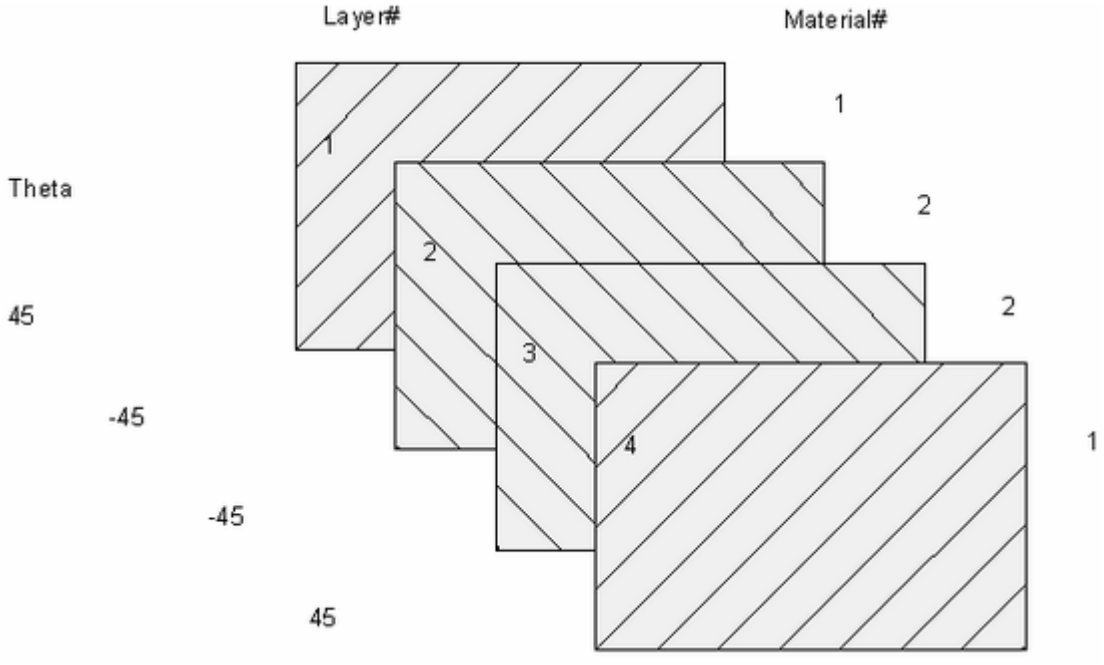

Figure 5.12 Sample layplot display for [45/-45/ - 45/45] sequence.

After material properties was defined, linear orthotropic material was chosen and the mechanical properties of E-glass/epoxy composite material was added as EX, EY, EZ, PRXY, PRYZ, PRXZ, GXY, GYZ and GXZ.

In order to calculate failure criteria, ultimate tensile strength, compressive strength and shear strength were entered both in fiber direction and in matrix direction.

Then a volume block was modelled and material properties, real constant sets and element type were appointed to the volume. After that the model was meshed by using hexahedral sweeped elements, Figure 5.13.

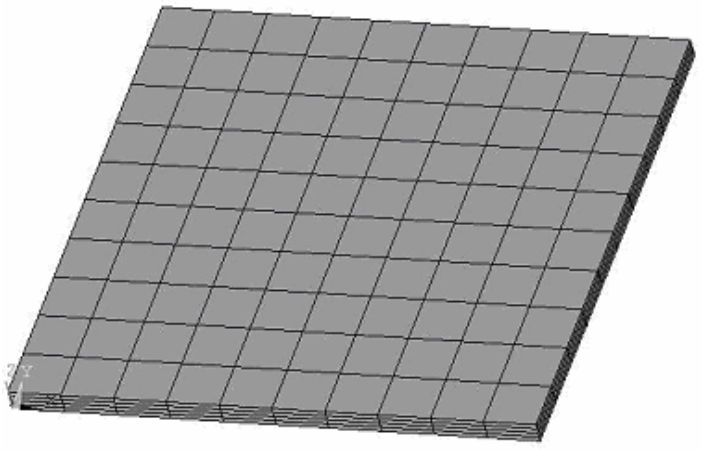

Figure 5.13. Finite element mesh.

Boundary conditions were defined corresponding to each side surfaces by using loads→pressure on areas functions as shown in Figure 5.14.

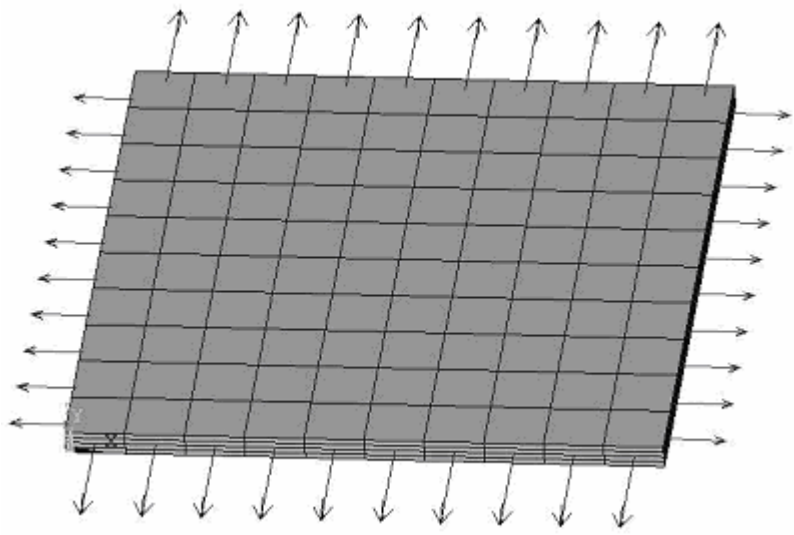

Figure 5.14 Finite element boundary conditions

Then analysis was run and the solutions were observed with plot results→nodal solutions→failure criteria→Tsai-Wu strength index. Failure criteria value was made equal to 1 by changed boundary conditions pressure value. Then this pressure values were substituted as stresses in Eq. (5.15) or Eq. (5.16) to calculate burst pressure of the composite pressure vessel.

CHAPTER SIX
EXPERIMENTAL STUDY

6.1 Production of Composite Pressure Vessels

In this study, filament wound GRP pipes with a plastic liner were manufactured using a CNC winding machine with several winding angles. Roving E-glass–fiber with 600 Tex and 17 μm diameter was used as reinforcement. The matrix material and the hardener material were used as Ciba Geigy Bisphenol an Epoxy CY-225 resin and Ciba Geigy Anhydride HY-225 in order. Mechanical properties of these matrix and reinforcement materials are given in Table 6.1. Before winding operation, resin was mixed for 4 – 5 min at 40°C resulting in an appropriate viscosity with a 4-h gel time. The filament wound composite pressure vessels were produced at the filament winding facilities of Izoreel Composite Insulating Materials Ltd., Izmir, Turkey. The fibers were wetted by passing through a resin bath for impregnation just before they were wound onto the mandrel. Helical winding was used for the desired angles of $[45^o/-45^o]_{2a}$, $[55^o/-55^o]_{2a}$, $[60^o/-60^o]_{2a}$, $[75^o/-75^o]_{2a}$ and $[88^o/-88^o]_{2a}$ which are antisymmetrical. Components were cured first at 160 °C for 2 h and at 140 °C for another 2 h. Then, the filament wound specimens were cut down to specified test length using a diamond wheel saw. The geometry of the specimen is shown in Figure 6.1. Four layers of reinforcement provided the thickness of 1.6 mm, and the inner plastic liner layer provided an additional thickness of 2 mm, resulting in 3.6 mm total wall thickness of the cylinder. The layers were oriented antisymmetrically which are shown in Table 6.2. The length and the inner diameter of the test specimens were 400 and 100 mm, respectively.

Table 6.1 Mechanical properties of the fiber and resin

	E(GPa)	σ_{TS}(MPa)	$\rho(g/cm^3)$	$\varepsilon_t(\%)$
E-glass	73	2400	2.6	4-5
Epoxy resin	3.4	50-60	1.2	6-7

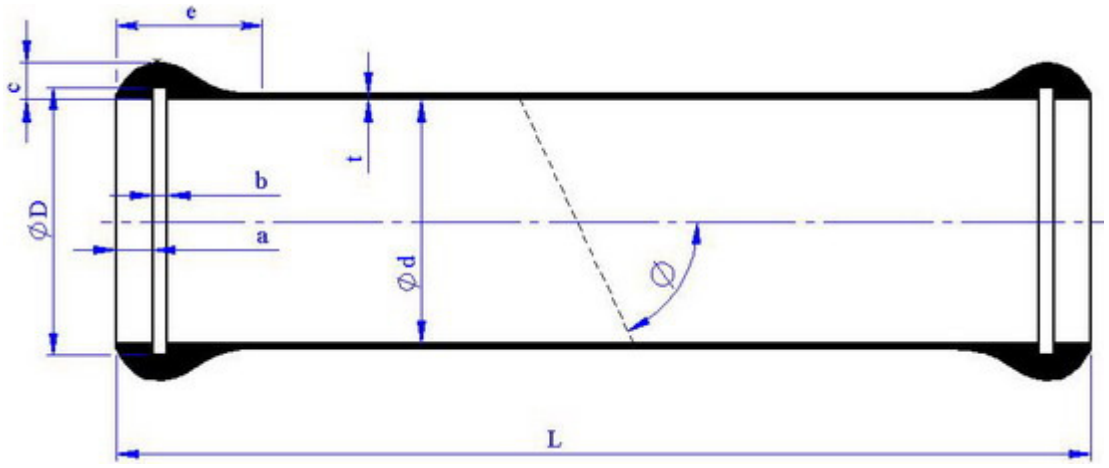

Figure 6.1 Geometry of the specimen.

L = 400 mm

D = 117.6 mm

a = 20 mm

b = 6 mm

c = 15 mm

d = 100 mm

e = 60 mm

t = 3.6 mm

ϕ = winding angle

Table 6.2 Stacking sequences of specimens.

Type		Ply angle (°)
ANTISYMMETRICAL $[\pm\Phi]_{2a}$	A	$[+45/-45/+45/-45]$
	B	$[+55/-55/+55/-55]$
	C	$[+60/-60/+60/-60]$
	D	$[+75/-75/+75/-75]$
	E	$[+88/-88/+88/-88]$

6.2 Determination of Mechanical Properties

Mechanical tests are applied to determine the engineering constants. Two strain gauges are located in the directions 1 and 2. In this way, the modulus of elasticity, E_1 and Poisson's ratio, and ν_{12} are determined. The test specimen is loaded by Instron-1114 Tensile Machine. The modulus of elasticity in the transverse direction E_2 is measured by using another strain gauge. A strain gauge is located on test specimens; the fibers are oriented 45° degrees with respect to loading direction. E_x is measured from the strain gauge measurements, ε_x. G_{12} is computed from

$$G_{12} = \frac{1}{\frac{4}{E_x} - \frac{1}{E_1} - \frac{1}{E_2} - \frac{2\nu_{12}}{E_1}} \tag{6.1}$$

Figure 6.2 shows Iosipescu test method which is used to find the shear strength S. It is computed from

$$S = \frac{P_{max}}{t\ c}$$

In addition, the strength in the first and second principal material directions is computed. They are X_t and Y_t for tensile strengths and X_c and Y_c for compressive strengths. The mechanical properties in the third principal direction are assumed to be equal to those in the second principal direction.

Thermal expansion coefficients in the principal material directions are measured by strain gauges. For this measurement, temperature is increased step by step, and then the strains in the principal material directions are determined. The thermal expansion coefficients are calculated from the strains in the principal material directions.

The strain gauges are isolated from water and the test specimens are put into the water in order to measure the hygrothermal coefficients Therefore, the specimen is waited for two hours (based on the ASTM standards), at $23^{\circ}C$, in the water in order to enable water absorption by the composite material. The coefficients of the hygrothermal expansion and moisture concentration are measured from the test specimens in the principal material directions as β_1, β_2 and c, respectively. Mechanical properties of the composite material and the plastic liner are shown in Table 6.3 and Table 6.4.

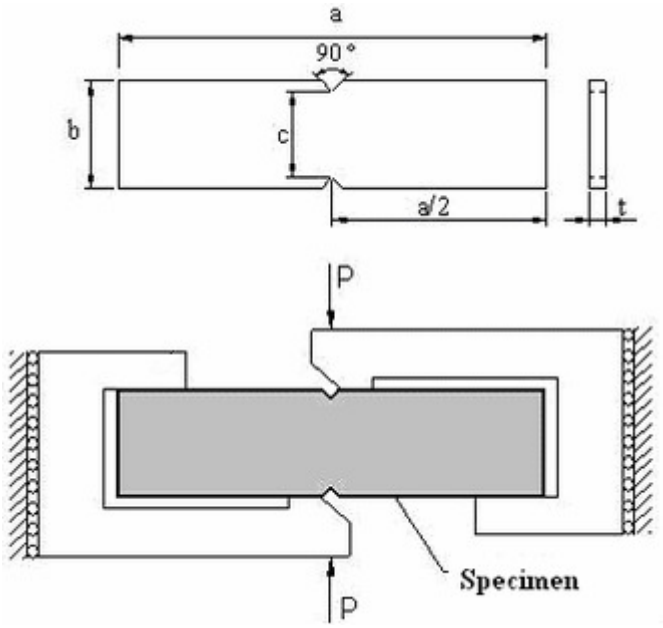

Figure 6.2 Iosipescu test method.

Table 6.3 Mechanical properties of composite material.

E_1(GPa)	E_2(GPa)	G_{12}(GPa)	ν_{12}	X_t(MPa)	Y_t(MPa)	X_c(MPa)
36.5	15.0	6.4	0,24	1050	43	938
Y_c(MPa)	S(MPa)	α_1(1/°C)	α_2(1/°C)	β_1	β_2	
106	88	$7{,}52\text{x}10^{-6}$	$47{,}77\text{x}10^{-6}$	$-46\text{x}10^{-4}$	$14\text{x}10^{-4}$	

Table 6.4 Mechanical properties of the plastic liner material.

E (GPa)	ν_{12}	σ_y(MPa)
2.66	0,38	32

6.3 Setting Experimental Equipments

Figure 6.3 shows close ended internal pressure test apparatus for GRP pipe. Figure 6.5 shows details of the test apparatus.

Figure 6.3 Closed-end internal pressure test apparatus.

Specimens were exposed to closed end internal pressure tests using the instrument design shown in Figure 6.3.

Figure 6.4 A photograph of test apparatus.

Static internal pressure tests were conducted using a 250 bar PLC controlled servo-hydraulic testing machine. The procedure for determining burst pressure of composite pressure vessel is based on ASTM standard. Test specimens were loaded with internal pressure to burst pressure using a 1 MPa/min loading rate. Figure 6.6 shows a PLC controlled servo-hydraulic testing machine.

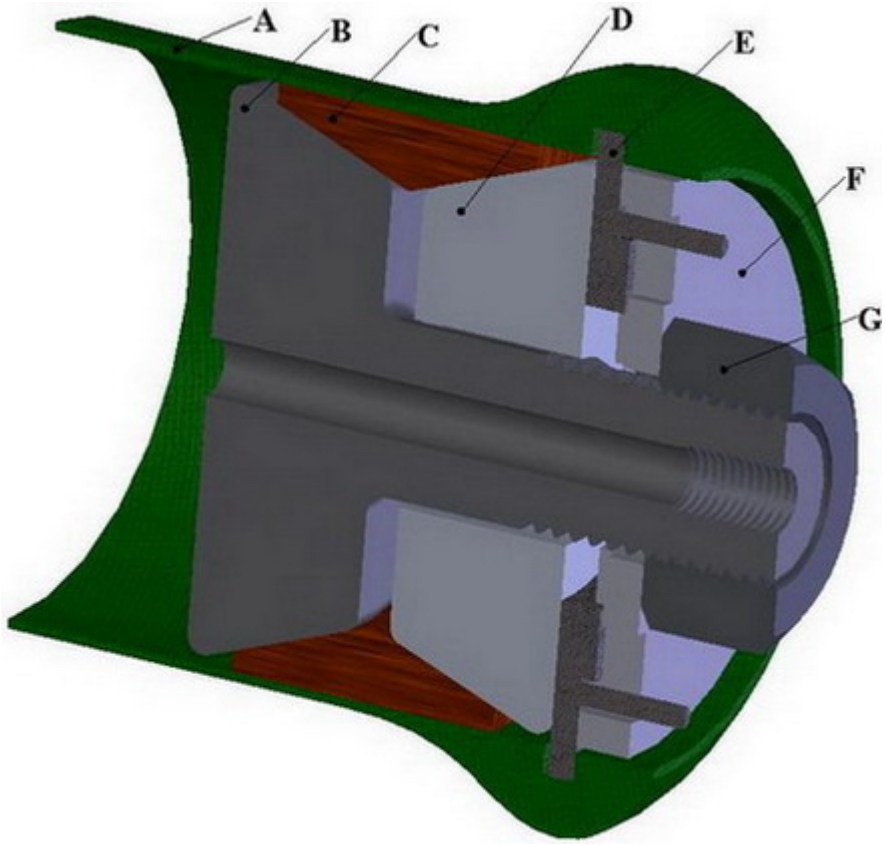

Figure 6.5 Details of test apparatus.

A = Composite pressure vessel (with plastic liner as the innermost layer)

B, D = Compressing parts

C = Rubber seal element

E = System locking member component

F = Flange

G = Nut

Figure 6.6 A PLC controlled servo-hydraulic testing machine.

A protective test box was manufactured for observing the test specimen during pressure tests. It provides the observers' protection from the test specimen while taking photos and videos. Figure 6.6 shows a photo of the protective test box.

Figure 6.7 A protective test box.

CHAPTER SEVEN
RESULTS AND DISCUSSIONS

In this study, three different methods were used to determine first failure pressure of composite pressure vessels. Analytical method, finite element method and experimental method were applied respectively.

A glass-epoxy composite layer is used in the solution. The layers are oriented antisymmetrically. The Tsai-Wu criterion and The Maximum Stress Theory are used to compute the first failure pressures of the composite layers in FEM solutions.

In order to see how structures behave, the theoretical results are necessary for a given material, geometry and loading combination. A computer program is developed with FORTRAN using the derived formulation of the stresses. In order to determine the burst pressure, the performance of the specified composite pressure vessel is taken as the only limiting value. Burst pressure is determined by using the first-ply failure criterion.

The design outputs of the computer program are optimum first-ply and burst failure pressures with respect to geometry and loading combination. Also the effect of the hygrothermal forces on the burst pressure is studied.

In the literature, the optimum winding angle for filament wound composite pressure vessels is given as 54.74^{o} by netting analysis.

Numerical solutions are studied in antisymmetrical conditions for the orientation angle of 45^{0}, 55^{0}, 60^{0}, 75^{0} and 88^{0} at 2^{0}C, 25^{0}C, 60^{0}C and 80^{0}C temperature. The first-ply and burst failure pressures of the composite vessels in corresponding orientations are studied analytically by Tsai-Wu failure criteria. Some test specimens which have different orientations were performed to test the first failure pressures of composite vessels. In these tests, the composite vessels were loaded with internal pressure until failure. In addition to some numerical solution, commercial software

Ansys 10.0 was used to determine first failure pressure of composite pressure vessel. The FEM failure criteria inputs were managed to get two different FEM solutions which are Max Stress and Tsai-Wu failure criterias.

Figure 7.1 shows the experimental, analytical and FEM first-ply failure pressure results with respect to different winding angles at 25^0C. Table 7.1 lists the corresponding of Figure 7.1 for different solutions.

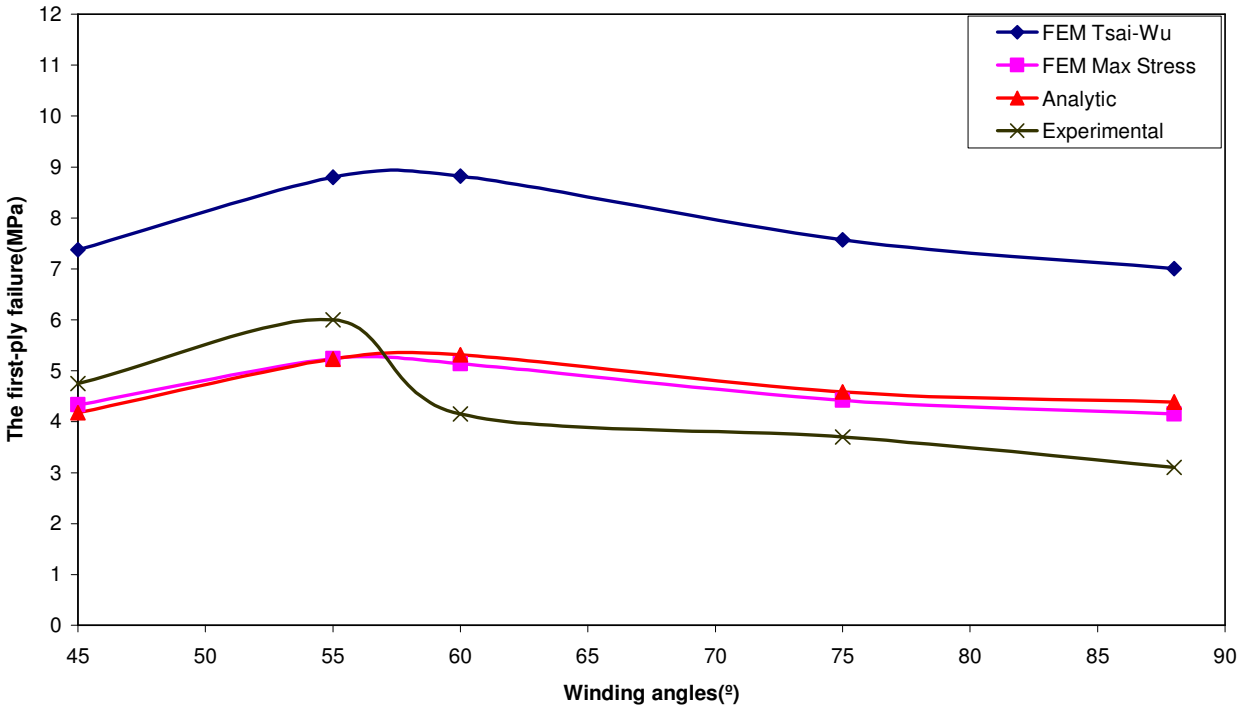

Figure 7.1 Variation of first-ply failure pressure with increasing winding angle at 25ºC.

As it can be observed from the graph, Tsai-Wu analytical results are much more closer to the experimental results than FEM Tsai-Wu results. So, it can be stated that due to FEM modelling parameters, Tsai-Wu failure does not seem to have much accuracy in our analysis as a FEM application procedure.

Also, looking at the curves for FEM Max Stress and analytical Tsai-Wu results, we can say that these solutions seem to give close results especially at 55º orientation, and slightly different results at 45º, 60º, 75º and 88º orientations. The

speciality about 55º orientation according to the FEM Max Stress and analytical Tsai-Wu first-ply failure pressure results, may be upon the full structural capacity usage of the fibers as it was previously found as the most efficient design according to the experiments performed so far both in this thesis and previous literature information. But again, this result is still a slightly bit different from the experimental data, which may be causing either from the lack of new parameters to be applied both in FEM and analytical solutions' procedure or from the experimental testing apparatus inefficiencies.

Table 7.1 First-ply failure pressure results for different methods for 20ºC. (MPa)

TYPE	winding angle(˚)	FEM Max Stress	FEM Tsai-Wu	Analytic	Experimental
Antisymmetrical	45	4.33	7.37	4.17	4.75
	55	5.24	8.80	5.23	6.00
	60	5.14	8.82	5.31	4.15
	75	4.42	7.57	4.59	3.70
	88	4.15	7.01	4.39	3.10

Figure 7.2 shows the experimental first-ply failure pressures of composite pressure vessels at different temperatures for 45º, 55º, 60º, 75º and 88º orientations. It is clearly seen that 55º oriented composite pressure vessels supply the maximum first-ply failure pressures compared to other orientations at all temperatures. Here a peak value at 25ºC is clearly seen for the composite pressure vessel of 55º orientation. This behaviour, taking the comments for Figure 7.1 into account, leads us to the fact that the most efficient design of the composite pressure vessel supplies the maximum first-ply failure pressure at 25ºC.

The peak first-ply pressure values cannot be observed exactly for composite pressure vessels of 45º, 60º, 75º and 88º fiber orientations. Hence, it can be stated that the most efficient usage of these vessels is at 55º orientation and 25ºC. Other temperatures between 20ºC and 30º C may be observed later to approve the most efficient temperature application of these designs.

Also the average position of each curve gives us a hint about the fiber orientation and the first-ply failure pressures. Here, it is clear that the first-ply pressure drops as "the difference of the orientation angle and 55º" increases. In other words, the more the fiber orientation is changed from 55º, the more the first-ply failure pressure drops. But these first-ply failure pressure change to drop ratios are not exact for a formulation. This table of ratios may also be created later for the industrial needs of specific designs.

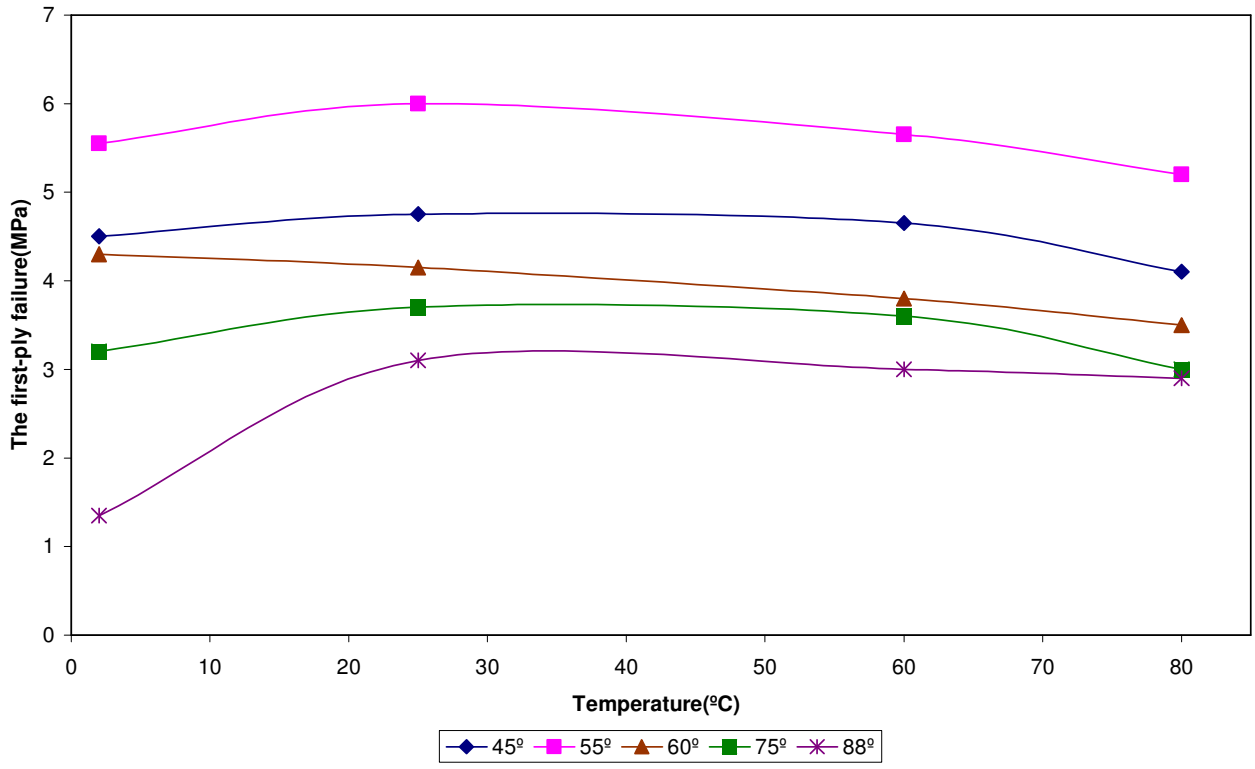

Figure 7.2 Variation of first-ply experimental failure pressures of different winding angled composite pressure vessels with increasing temperatures.

Figure 7.3 shows the experimental burst failure pressures of composite pressure vessels at different temperatures for 45º, 55º, 60º, 75º and 88º fiber orientations.

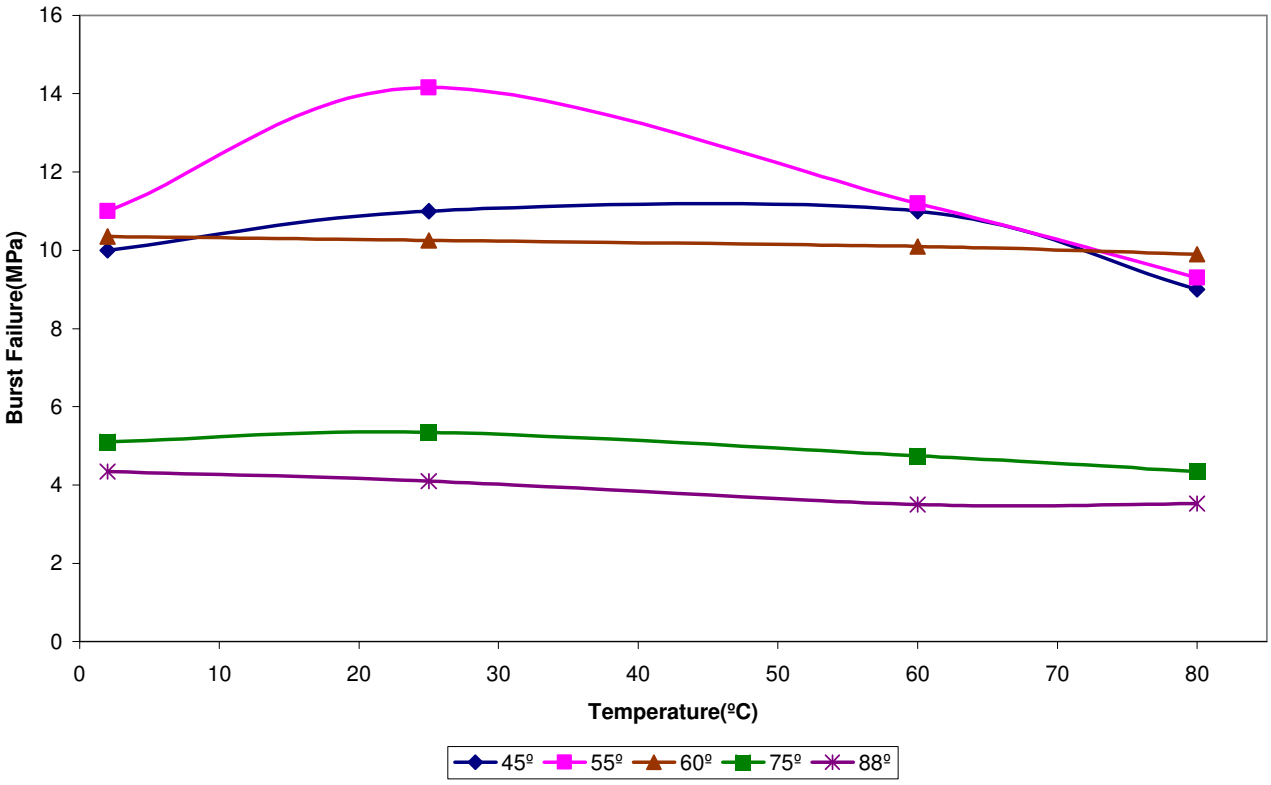

Figure 7.3 Variation of experimental burst failure pressures of different winding angled composite pressure vessels with increasing temperatures.

Taking both Figure 7.2 and Figure 7.3 into account, we can say that the behaviour of composite pressure vessels are similar at 25ºC and 60ºC both for burst and first-ply failure pressures. But for 2ºC and 80ºC, the behaviours of winding angle curves shows a little difference. This may either be caused by physical phenomena of the application, or by the inadequate number of experiments made for these burst failures, or by the very small parameters changing in the production steps of these vessels. This subject, again, may be another research project for later purposes. Shortly, depending upon our experiments, we can say that the final and first-ply failures have similar behaviours with respect to the winding angles at 25ºC and 60ºC temperature application environments.

Figure 7.4 displays the experimental burst failure pressures of composite pressure vessels at increasing winding angles for different temperatures.

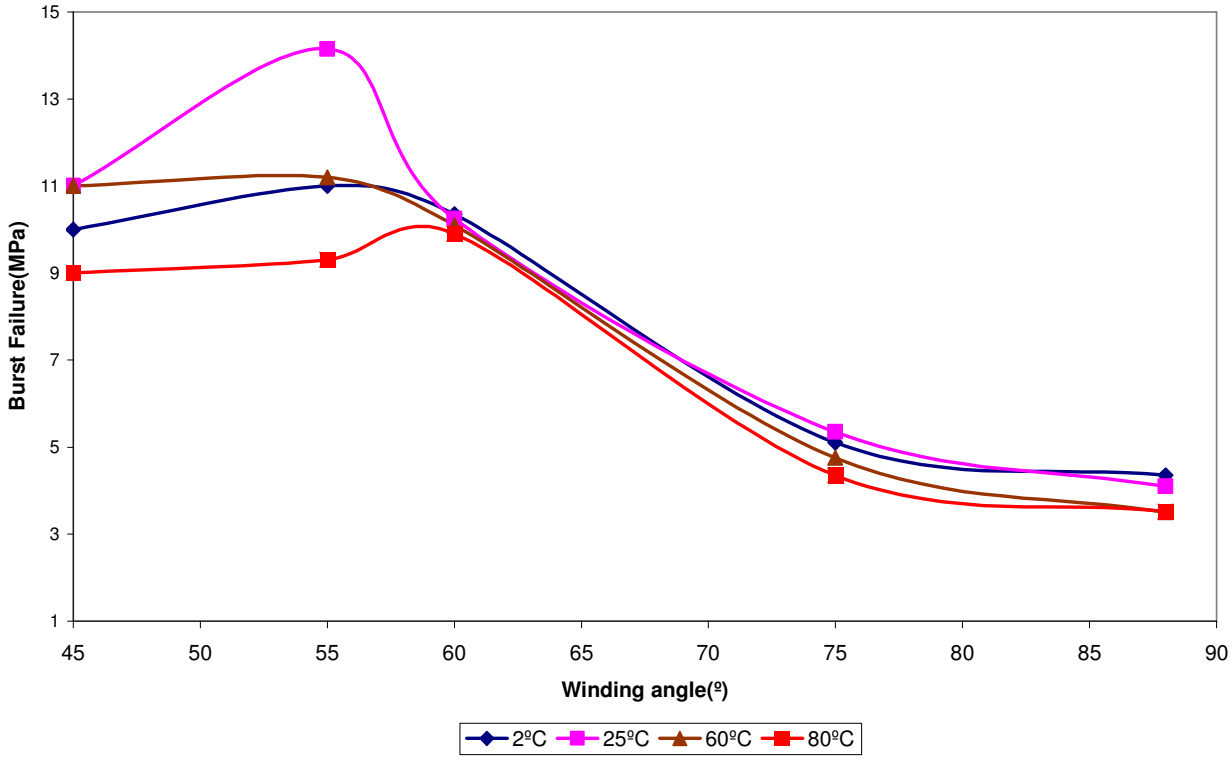

Figure 7.4 Experimental results of burst failure pressure with increasing winding angle for different temperatures.

Here, it can be observed that the designs performed at 80ºC temperature shows the lowest burst failure pressure values. The production procedure and the material properties of the composite pressure vessels are most likely to be the cause of this result. Hence, we can come up to the idea that the related production steps of this composite pressure vessel design designates 25ºC application environment as the best application temperature value.

Figure 7.5 shows the analytical and experimental burst pressure results of the composite pressure vessels with increasing winding angles. The graphs look similar to the first-ply pressure graphs of the related results in behaviour. If we look at the peak values of both curves at 55º orientation, we can easily see almost the same ratios for analytical results and experimental results both in first-ply failure and burst

failure pressure values. This also give us some clue that, the first-ply failure and burst failure pressures may act similarly for experimental and analytical results, meaning that with further research, a ratio constant "for this design" may be found, and with the use of this constant; analytical solution of burst or first-ply failure pressures may lead the designers to an approximate experimental burst or first-ply failure pressures. Though, this hypothesis has to be confirmed by sufficient number of research projects.

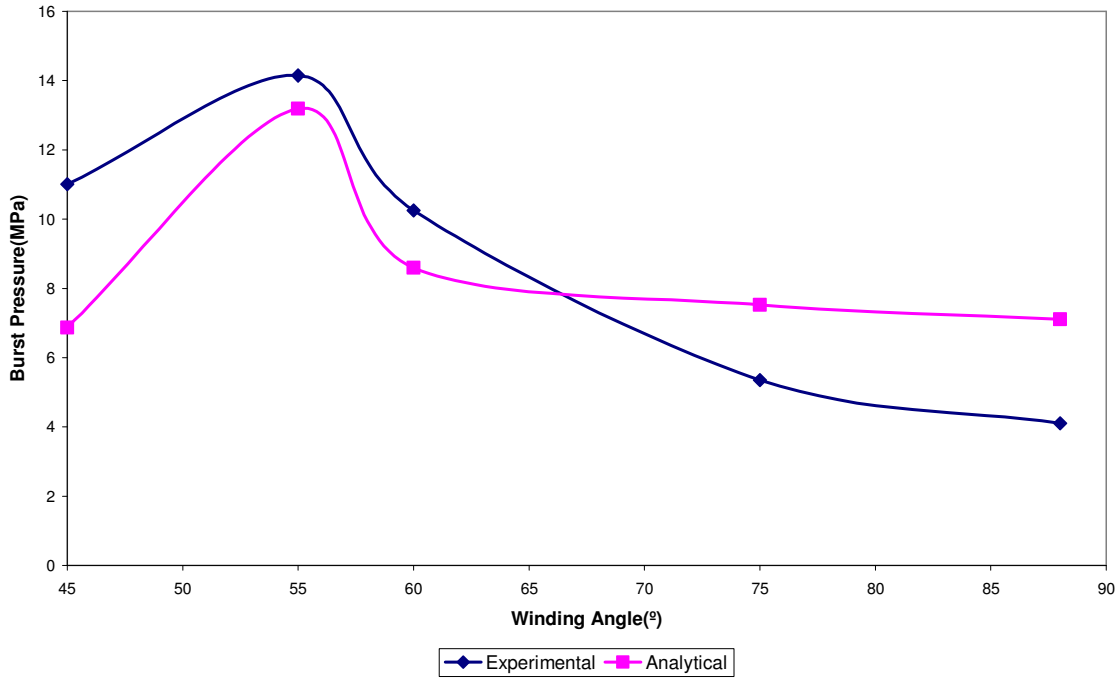

Figure 7.5 Experimental and analytical results of burst pressure with increasing winding angles at 25ºC.

Experimental studies were the crucial point of this research. Experimental results are compared with the analytical and FEM results. The solutions for experimental and analytical Tsai-Wu were found to be very similar. Both for first-ply and burst failure pressures, the optimum winding angle is obtained as 55˚ for internal pressure loading composite pressure vessels.

Figure 7.6 to Figure 7.9 show different failure mechanisms.

Figure 7.6 Fiber breakage damage mechanism

Figure 7.7 Fiber breakage damage mechanism

Figure 7.8 Fiber breakage damage mechanism

Figure 7.9 Fiber breakage damage mechanism

CHAPTER EIGHT
CONCLUSION

This thesis is subdivided into two major parts: The theoretical studies for composite pressure vessels were covered in Chapter 4 and Chapter 5, and experimental investigations of composite pressure vessels were presented in Chapter 6.

The analytical Tsai-Wu studies include a simplified elastic solution to analyze the burst pressure of multi-layered composite pressure vessels with a plastic liner under internal pressure and hygrothermal force. The temperatures influence has shown significant change especially for 55˚ winding angle orientation for both first-ply and burst failure pressure values. For other orientations, some change has been observed, but they are not as significant as 55˚ orientation.

FEM Max Stress method was an advantage to determine first-ply failure pressure easily. Considering an orthotropic material and its progressive failure, stress analysis on composite pressure vessels becomes very complex. In this study, two different finite element analysis approaches are employed. It is significant to integrate the composite material and composite failure into a finite element analysis geared towards the design of composite pressure vessels. Two different FEA analysis on one E-glass-epoxy composite pressure vessel, for which experimental data is available, is carried out. Comparisons of these results have shown that FEA is an assistant tool for the prediction of first-ply failure pressure when coupled with an appropriate failure criterion.

Composite material failure has been extensively studied. The thesis also focuses on the failure analysis of composite pressure vessels by Tsai-Wu failure criteria both with FEM and analytical solutions..

For experimental failure pressures of the composite pressure vessels, there are significant differences between different fiber orientations, which concludes us the

most efficient fiber orientation is 55˚. But, when observing the temperature effects on different fiber oriented composite pressure vessels, it is clearly seen that the most significant changes in failure pressures with different temperatures occur at composite pressure vessels of 55˚ fiber orientation. The cause for this biggest change in 55˚ orientation may be, as mentioned before, due to the full structural capacity usage of the fibers along the composite pressure vessel, which represents the existence of maximum total strain energy stored in the fibers of the vessel. This maximum value of strain energy may cause the most significant changes with different temperatures. Finally, the most appropriate application temperature seems to be 25˚C for the mentioned procedure of these composite pressure vessels with the relevant geometry of the liner plastic materials.

In this work, only internal pressure, temperature effect and internal plastic liner effect were studied. Other loads such that impact, external pressure and their combinations are possible. Fatigue analysis is also extremely important, since typically 15000-20000 cycles are the medium cycles in qualification tests for commercial service approvals.

Voids within the composites should have an effect on material properties. Production of these vessels including the void effects should be considered. Hence, improvement of composite pressure vessel production processes may contribute to better results in future.

REFERENCES

Azzam, B. S., Muhammad, M. A. A., & Mokhtar, M. O. A. (1996). Comparison between Analytical and Experimental Failure Behaviour of a Proposed Design for the Filament-wound Composite Pressure Vessels, *Current Advances in Mechanical Design & Production, Sixth Cario University International MDP Conference, June 2-4, 1996*.

Adali, S., Verijenko, V. E. etc. al(1995). Optimization of multilayered composite pressure vessels using exact elasticity solution, *Composites for the Pressure Vessels Industry, PVP-V302, ASME,* 203-312.

Akdemir, A., Tarakcioglu, N. & Avci, A. (2000). Stress Corrosion Crack Growth in Glass-Polyester Composites with Surface Crack, *Composites, Part B, 32*: 123-129.

Babu, M., S., Srikanth, G. & Biswas, S. (2006). *Composite Fabrication by Filament Winding - An Insight.* Retrived December 4, 2006, from http://www.tifac.org.in/news/acfil.htm.

Chang, R. R. (2000). Experimental and Theoretical Analyses of First-Ply Failure of Laminated, Composite Pressure Vessels, *Composite Structures, 49*, 237-243.

Chen , Z. (2004). Nonlinear Stres Analysis and Design Optimization of Ultra-High Pressure Composite Vessels, Master of Science thesis. Ontario:Faculty of *Graduate School of Natural and Applied Sciences of Windsor University.*

Cohen, D., Mantell, S. C. & Zhao, L. (2001). The Effect of Fiber Volume Fraction on Filament Wound Composite Pressure Vessel Strength, *Composites: Part B, 32*, 413-429.

Crawford R. J. (1998). *Plastics Engineering* (3rd ed.). Oxford: Butterworth Heinemann

Doğan, T. (2006). Predection of Composite Vessels Under Various Loadings, Master of Science thesis. İzmir: *Graduate School of Natural and Applied Sciences of Dokuz Eylül University.*

Hwang, T. K., Hong, C. S., & Kim, C. G. (2003). Size Effect on the Fiber Strength of Composite Pressure Vessels, *Composite Structures, 59*, 489-498.

Jacquemin, F. & Vautrin, A. (2002). A Closed-Form Solution for the Internal Stresses in Thick Composite Cylinders Induced by Cyclical Environmental Conditions, *Composite Structures, 58*, 1-9.

Jacquemin, F. & Vautrin, A. (2002). The Effect of Cyclic Hygrothermal Conditions on the Stresses near the Surface of a Thick Composite Pipe, *Composite Science and Technology, 62*, 567-570.

Jones, R. M. (1998). Mechanics of Composite Material (2nd ed.). Philadelphia: Taylor & Francis.

Kabir, M. Z. (2000). Finite Element Analysis of Composite Pressure Vessels with a Load Sharing Metallic Liner, *Composite Structures, 49*, 247-255.

Kam, T. Y., Liu, Y.W., & Lee, F.T. (1997). First-ply Failure Strength of Laminated Composite Pressure Vessels, *Composite Structures, 38*, 65-70.

Lekhnitskii, S. G. (1981). Theory of Elasticity of an Anisotropic Body, Mir Publishers, Moscow.

Liang, C. C., Chen, H.W., Wang, C.H. (2002). Optimum Design of Dome Contour for Filament-Wound Composite Pressure Vessels Based on a Shape Factor, *Composite Structures*, *58*, 469-482

Mackerle, J. (2002). Finite Elements in the Analysis of Pressure Vessels and Piping, an Addendum: a Bibliography (1998-2001), *International Journal of Pressure Vessels and Piping, 79*, 1-26.

Mazumdar, S. K. (2001). *Composite Manufacturing* :*Materials, Product, and Process Engineering*. London: Crc Press.

Mirza, S., Bryan, A., Noori, M. (2001). Fiber-Reinforced Composite Cylindrical Vessel with Lugs, *Composite Structures, 53*, 143-151.

Ochoa, O. O. & Reddy, J. N. (1992). *Finite Element Analysis of Composite Laminates.* Netherland: Kluwer Academic Publishers.

Önder, A., Sayman, O., Doğan, T., & Tarakçıoglu, N. (2007). Burst Failure Load of Composite Pressure Vessels, *Composite Structures, 89*, 159-166.

Parnas, L. & Katırcı, N. (2002). Design of Fiber-Reinforced Composite Pressure Vessels under Various Loading Conditions, Composite Structures, 58, 83-95.

Rao, V. V. S. & Sinha, P. K. (2004). Dynamic Response of Multidirectional Composites in Hygrothermal Environments, *Composite Structures, 64*, 329-338.

Roy, A. K., Massard, T. N.(1992). A Design Study of Multilayered Composite Spherical Pressure Vessels, *Journal of Reinforced Plastic and Composites, VII*, 479-493

Sayman, O. (2005). Analysis of Multi-Layered Composite Cylinders Under Hygrothermal Loading, *Composites Part A*, 1-11.

Soden, P. D., Kitching, R., Tse, P. C., Hinton, M. J. & Tsavalas, Y. (1993). Influence of Winding Angle on the Strength and Deformation of Filament-Wound

Composite Tubes Subjected to Uniaxial and Biaxial Loads, *Composites Science and Technology, 46(4)*, 363-378.

Sonnen M., Laval C. & Seifert A. (2004). Computerized Calculation of Composite Laminates and Structures: Theory and Reality, Material S.A.

Sun, X. K., Du, S. Y. & Wang, G. D. (1999). Bursting Problem of Filament Wound Composite Pressure Vessels, *International Journal of Pressure Vessels and Piping, 76,* 55-59.

Tabakov, P.Y. (2001). Multi-Dimensional Design Optimization of Laminated Structures Using an Improved Genetic Algorithm, *Composite Structures, 54*, 349-354.

Tsai, S. W. & Roy A. K. (1988). Design of Thick Composite Cylinders, *Journal of Pressure Vessel Technology.*

Vasiliev, V.V., Krikanov, A.A., & Razin, A.F. (2003). New Generation of Filament - Wound Composite Pressure Vessels for Commercial Applications, *Composite Structures, 62*, 449-459.

Vasilev, V. V. & Morozov, E. V. (2001). *Mechanics and Analysis of Composite Materials*.Oxford: Elseiver.

Wild, P. M. & Vickers, G. W. (1997). Analysis of Filament-Wound Cylindrical Shells under Combined Centrifugal, Pressure and Axial Loading, *Composites: Part A*, 28A, 47-55.

Xia, M., Takayanagi, H. & Kemmochi, K. (2001). Analysis of Multi-Layered Filament- Wound Composite Pipes under Internal Pressure, *Composite Structures, 53*, 483-491.

Xia, M., Takayanagi, H. & Kemmochi, K. (2001). Analysis of Transverse Loading for Laminated Cylindrical Pipes, *Composite Structures, 53*, 279-285.

Xia, M., Takayanagi, H. & Kemmochi, K. (2002). Bending Behaviour of Filament-Wound Fiber-Reinforced Sandwich Pipes, *Composite Structures, 56*, 201-210.